Title
Identification of New Trophic Factors that Prevent Photoreceptor Degeneration

Author
Deng, Jun

Publication Date
2014

Peer reviewed|Thesis/dissertation

UNIVERSITY OF CALIFORNIA

Los Angeles

Identification of New Trophic Factors that Prevent Photoreceptor Degeneration

A dissertation submitted in partial satisfaction of the requirements

for the degree Doctor of Philosophy in

Molecular, Cellular, and Integrative Physiology

by

Jun Deng

2014

ABSTRACT OF THE DISSERTATION

Identification of New Trophic Factors that Prevent Photoreceptor Degeneration

by

Jun Deng

Doctor of Philosophy in Molecular, Cellular, and Integrative Physiology

University of California, Los Angeles, 2014

Professor Hui Sun, Chair

Diseases that cause photoreceptor degeneration such as age-related macular degeneration (AMD) and retinitis pigmentosa (RP) affect millions of people and lead to blindness. The degeneration of photoreceptor cells in AMD or cone photoreceptors in RP is caused by stress in their environment and/or lack of trophic support, not by direct genetic mutation targeting of the photoreceptor cells. Therefore, providing effective trophic support can delay or prevent photoreceptor degeneration. It has been known for more than 20 years that natural trophic factors exist in the retina that protect photoreceptor cells, but these factors have never been identified. Recent gene therapy studies have revealed that targeting genetic mutations is not sufficient and that there is an urgent need to identify trophic factors that can maintain photoreceptor survival in the treatment of photoreceptor degeneration. Identification and

mechanistic study of trophic factors naturally present in the retina will lead to a better understanding of the photoreceptor protection mechanism and help to develop new therapeutic strategies. My thesis project aims to identify new natural trophic factors that protect photoreceptor cells and to test them using *in vitro* and *in vivo* models.

We found that natural trophic factors in the retina strongly protect photoreceptor cells from retinal-mediated light damage or chemically induced oxidative damage. Using classic techniques combined with advanced mass spectrometry and genome-wide database searching, we identified several candidate photoreceptor protective factors. These factors effectively protect primary cone photoreceptor cells from light damage and oxidative damage *in vitro*. We cloned candidate genes into lentiviral vectors and delivered them to the retina and RPE (retinal pigment epithelium) *in vivo* by subretinal injection. Using two mouse models of retinal degeneration: a light-induced retina degeneration model and a genetic retina degeneration model, we found that one factor almost completely protect retina from light-induced damage *in vivo*. In summary, we have identified a novel factor that can prevent photoreceptor cell degeneration *in vitro* and *in vivo*. This factor has potential therapeutic values in treating retina degenerative diseases.

The dissertation of Jun Deng is approved.

Gordon L. Fain

Yousang Gwack

Xianjie Yang

Hui Sun, Committee Chair

University of California, Los Angeles

2014

DEDICATION

THIS DISSERTATION IS DEDICATED TO MY PARENTS AND FAMILIES FOR THEIR LOVE, SUPPORT, INSPIRATION AND ENCOURAGEMENT

谨以此论文献给我的父母和家人

TABLE OF CONTENTS

LIST OF FIGURES

LIST OF TABLES

ACKNOWLEDGEMENTS

I would like to give my sincere thanks to my mentor Prof. Hui Sun for his support and guidance for the past few years. From him, I learned what are essential to become a scientist, persistence and original thinking. I am also extremely grateful for everyone who has helped on this project. Dr. Xian-Jie Yang and Dr. Kun Do Rhee provided countless support and guidance on the animal studies. Dr. Riki Kawaguchi taught me all the useful techniques from protein purification, mass spectrometry to data analysis. Ms. Ly Nguyen, Ms. Thao Nguyen, Dr. Ming Zhong, Dr. Miki Kassai, Ms. Guo Cheng, Ms. Mariam Ter-Stephanie, Dr. Haodong Chen, Dr. Yanjie Wang, and Dr. Xiangmei Zhang have been directly involved in this study.

In addition, I would like to thank the members of my dissertation committee: Dr. Xian-Jie Yang, Dr. Gordon L Fain, Dr. Yousang Gwack. I would also like to thank Dr. Steve Nusinowitz, Dr. Roxana Radu, Dr. Sophie Deng, Mr. Tongzhou Xu for their useful discussions, Dr. Jim Tidball for being a wonderful MCIP/IDP PhD program chair, Dr. Ren Sun for initiating and organizing the exceptional CSST (corss-disciplinary scholars in science and technology) program, and Dr. Arthur P Arnold for being the first person introducing me to the scientific world and his exceptional kindness.

I would also like to thank my husband Dr. Haodong Chen for always being supportive and inspirational. His expertise and knowledgeable suggestions have helped my project moving forward quickly.

Last but not least, I would like to acknowledge the China Scholarship Council (CSC) scholarship and Jennifer S. Buchwald Graduate Fellowship in Physiology for the scholarship award. The research in Sun lab was supported by National Eye Institute and Howard Hughes Medical Institute.

Biographical Sketch

EDUCATION

- **University of California, Los Angeles,** USA. Cross-disciplinary Scholars in Science and Technology (CSST), Summer Program and Winter Program, 2008 – 2009
- **Nankai University**, Tianjin, China. B.S., Biology, 2005 – 2009

PROFESSIONAL EXPERIENCE

- **Graduate Student Researcher,** David Geffen School of Medicine, University of California, Los Angeles. August 2010 – Present
    - Identified two novel trophic factors that can prevent photoreceptor cell degeneration *in vitro* and *in vivo*.
    - Specifically, through classic biochemistry techniques combined with advanced mass spectrometry and genome-wide database searching, we have identified two novel factors from the retina that could strongly protect photoreceptor cells from retinal-mediated light damage and chemically induced oxidative damage.
    - We cloned candidate genes into the lentiviral vector and delivered them to the subretinal area through subretinal injection. We found that one factor almost completely protected retina degeneration in the light-induced retina degeneration mouse model.
    - This factor has potential therapeutic values in treating retinal degenerative diseases.
    - This work has been presented at Howard Hughes Medical Institute Science Meeting in 2013.
- **Invited Attendee,** Howard Hughes Medical Institute Science Meeting, Washington D.C. November 2013
- **Judge,** STEM Essay Competition, Chinese-American Engineers and Scientists Association of Southern California. March 2013
- **Teaching Assistant**, Life Science Core Curriculums, UCLA. 2011 – 2012
- **Organizing Committee Member and Abstract Reviewer,** Jules Stein Eye Institute 16th Annual Vision Science Conference, UCLA. June 2010 – October 2010

AWARDS & PROFESSIONAL HONORS

- **Best Oral Presentation Award**, Jules Stein Eye Institute 20th Annual Vision Science Retreat, 2014

- **Best Oral Presentation Award**, Jules Stein Eye Institute 19th Annual Vision Science Retreat, 2013
- **China Scholarship Council (CSC) Scholarship**, 2009 – 2013
- **Student Scholarship, Chinese-American Engineers and Scientists Association of Southern California (CESASC) Scholarship**, 2012
- **Jennifer S. Buchwald Graduate Fellowship in Physiology**, UCLA, 2010 – 2011
- **Student Representative,** selected to give a closing remark, Cross-disciplinary Scholars in Science and Technology (CSST), 2008
- **Excellent Research Project Award**, 'A Hundred Projects' of the Creative Research, Nankai University, 2008
- **Baosteel Scholarship**, Nankai University, 2007 (Top5%; awarded to excellent student leaders)
- **Excellent Student Leader**, Nankai University, 2006

INVITED PRESENTATIONS

- **Identification of Novel Neurotrophic Factors and Their in Vivo Applications.** Jules Stein Eye Institute 20th Annual Vision Science Retreat, UCLA, 2014 Oct 11.
- **Identification of Novel Neurotrophic Factors and Their in Vivo Applications.** MCIP Student Seminar, UCLA, 2014 Aug 12.
- **Mechanism of Trophic Factor-Mediated Cell Survival.** JSEI Clinical and Research Seminar, UCLA, 2014 Jun 13.
- **Mechanism of Trophic Factor-Mediated Cell Survival.** Jules Stein Eye Institute 19th Annual Vision Science Retreat, UCLA, 2013 Oct 25.

Chapter 1: Introduction

1.1 Anatomy of the Eye

The eye is the sensory organ we use to see the world. Human eyes sit in the orbital cavities of the frontal bones of the skull (Caranci et al., 2012). Each part of the eye is an extremely specialized structure. Externally, the eyes are surrounded by layers of soft and adipose tissue, which protects and lubricates the eye. The motion of the eyes is regulated by six extra ocular muscles. Internally, the eye is divided into three chambers, the anterior chamber, the posterior chamber and the vitreous chamber. The anterior and posterior chambers are filled with aqueous humor and the vitreous chamber is filled with vitreous humor, both of which are transparent and allow light to pass through. The eyeball has three layers. From the outermost to the innermost are: the sclera and cornea layer, the uvea and the retina (Fig 1.1).

The sclera and cornea compose the protective layer of the eyeball. The cornea is the outermost layer and is a perfectly transparent membrane. The sclera is the white, dense tissue that coats the sides and back of the eye, often referred to as the white of the eye.

The uvea refers to the choroid, the ciliary body and the iris. The iris controls the size of the pupil. The choroid, located between the sclera and the retina, is a highly vascularized layer of the eye. The choroid provides oxygen and nutrients to the photoreceptors of the retina via the retinal pigmented epithelium (RPE).

The retina is a multilayered structure. It covers the back two-thirds of the inner eye. The main function of the retina is to convert light signals into neural signals that we interpret as images in our world.

Mice, as a useful animal model in biomedical research, share similarities in retinal anatomy and physiology with humans. There are, however, important differences, such as a larger lens and the lack of a cone-rich macula in mice. Cones in mice are rare and distributed over the whole retina (Samardzija Marijana, 2014).

1.1.1 The Retina

The retina is the photon absorption and signal transmission tissue lining on the back of the vertebrate eye. The retina pigmented epithelium, a monolayer of highly pigmented hexagonal cells, is commonly included in the retina but is not involved in the light signal transmission. It caters nutrients from the choroid to the photoreceptors (Shichi, 1983).

The neural retina consists of six types of neuronal cells: rod photoreceptors, cone photoreceptors, bipolar cells, horizontal cells, amacrine cells and ganglion cells. There is also a type of glial cell called Müller cell. The retina has a multilayered structure, from the RPE side towards the vitreous side, which is composed of the photoreceptor outer segment (OS) layer, the photoreceptor inner segment (IS) layer, the outer nuclear layer (ONL), the outer plexiform layer (OPL), the inner nuclear layer (INL), the inner plexiform layer (IPL) and the ganglion cell layer (GCL).

OS layer are the outer segments of the photoreceptors. The cell bodies of the photoreceptors consist of the ONL. The synapses between dendrites of horizontal cells and photoreceptor cells form the OPL. The INL contains the cell bodies of amacrine cells, horizontal cells, and bipolar cells. The INL is thinner than the ONL. The IPL is another layer where synaptic interaction forms. The RGCs send theirs axons to the optic disk to make up the optic nerve that travel all the way to the lateral geniculate nucleus (LGN).

1.1.2 Photoreceptors

Photoreceptors were first described by Treviranus in around 1835 upon the development of the microscope. We now know that there are two kinds of light receptor cells: rods and cones, which are given their name by the shape of their outer segments (Fig 1.2) (Gregory, 1966). In the human eye, rods are primarily distributed in the peripheral region of the retina and function under dim light (night). In contrast, cones are concentrated in the macular (central) region of the retina and function in the interpretation of color. Humans normally have three different types of cones which respond to light of short, medium, and long wavelengths. The human eye contains approximately 120 million rods and 6.5 million cones (Goldstein, 2007). The fovea is the region where cones are packed exceedingly close together.

Both rods and cones consist of the outer segment, inner segment, cell body and the synaptic terminus. The inner segment contains mitochondria and other subcellular organelles. The outer segments of the photoreceptors are composed of a large stack of disks encased in a sack of plasma membrane where the visual pigments are located. The visual pigment opsins are inserted into the lipid bilayer membranes of these disks. Each outer segment disc contains thousands of visual pigment molecules.

1.1.3 The Retinal Chromopheres

Opsins are seven trans-membrane proteins that belong to the G-protein coupled receptor (GPCR) family. Photoreactive chromophore is a cofactor that is reversibly covalently bound to the opsin. Retinal, also called vitamin A aldehyde, was firstly identified by Morton as the chromophore of visual pigment (Morton, 1972). Vitamin A is transported to RPE cells through RBP (retinol

binding protein) cell surface receptor, STRA6 (stimulated by retinoic acid 6) (Kawaguchi et al., 2007). Later, it was known that the 11-cis isomer is the chromophore for rhodopsin in terrestrial vertebrates (human, pig, cow, mouse, chicken, frog, etc.) and some marine fishes. Porphyropsin, found in the eye of freshwater fishes, was identified as another type of chromophore derived from vitamin A (Hitoshi, 1983). Isomerization of 11-cis-retinal into all-trans-retinal by light induces a conformational change in opsin, which triggers phototransduction (Fain et al., 2010; Shichida and Matsuyama, 2009). Humans have the following types of opsins in photoreceptors: rhodopsin, which is expressed in rod cells and used in night vision, long (red) -, medium (green) - and short (blue) - wavelength cone opsins, which are expressed in cones and used in color vision.

1.1.4 Visual Cycle

Once the chromophore captures a photon, it converts 11-cis retinal to all-trans-retinal (atRAL). The atRAL is reduced to all-trans-retinol (atROL), which diffuses to the RPE and is further esterified to all-trans-retinyl-ester by retinol acyltransferase (LRAT). The isomerization from all-trans-retinyl-ester to 11-cis-retinol (11cROL) is catalyzed by RPE-specific-65kDa protein (RPE65). 11cROL is then oxidized by 11-cis retinol dehydrogenase to 11-cis-retinal, which diffuses back to photoreceptors to reform visual pigment (Wang et al., 2012) (Fig 1.3).

The visual cycle, also called phototransduction, is the process by which light is converted into an electrical signal. The visual cycle is mediated by opsins located on the OS and initiated by the capture of a photon by the chromophore. In the dark, cGMP levels are high in photoreceptors and keep cGMP-gated sodium channels open, leading to an inward current, called the dark current. Once phototransduction is initiated by retinal isomerization, opsin changes its

conformation and activates the G-protein transducin. Transducin dissociates from its bound GDP and binds to GTP, causing α-subunit dissociation from the β and γ subunits of transducin. The α-subunit –GTP complex activates cGMP-phosphodiesterase (PDE) which then breaks down cGMP to 5'GMP. The lowered concentration of cGMP leads to closure of sodium channels and causes hyperpolarization of the cell. This then leads to voltage-gated calcium channel closure and a subsequent drop in intracellular calcium concentration. This drop in calcium concentration leads to a further drop in the release of neurotransmitter glutamate, causing depolarization of ON-bipolar cells and hyperpolarization of OFF-bipolar cells. Thereby, a light signal is transmitted into an electrical signal and transmitted to the bipolar cells and further to the brain (Jin et al., 2005).

1.1.5 The Interphotoreceptor Matrix

In vertebrates, the extracellular material located between the photoreceptors and the RPE is referred to as the interphotoreceptor matrix (IPM). Major functions of IPM include providing adhesion between photoreceptors and RPE, phagocytosis, maintaining outer segment stability, facilitating nutrient exchange, development, and vitamin A trafficking in the visual cycle. The IPM is composed of diffusible soluble molecules and an insoluble network of proteoglycans and lyco-conjugates (Hageman, 1998). Elegant studies have demonstrated light-induced changes in the conformation of the IPM (Wolfensberger, 1998). IPM is most likely assembled with components synthesized by all of the surrounding cell types including the photoreceptor cells, the RPE cells, and the Müller cells (Mieziewska, 1996).

The most common way of collecting the soluble part of IPM is to separate the retina from the RPE and rinse the apical surface of the retina with various buffers (Adler and Martin, 1982).

The predominant parts of the soluble IPM consist of proteins, glycoproteins and glycosaminoglycans. The major soluble glycoprotein is known as interphotoreceptor retinoid-binding protein (IRBP). Others components include enzymes, mucins, carbohydrates, growth and neurotrophic factors, survival –promoting factor(s), glucose, lactate and miscellaneous proteins (Hageman, 1998). A number of neurotrophic factors have been characterized in the IPM, including basic fibroblast growth factor (bFGF), pigment-epithelium-derived factor (PEDF) , insulin like growth factor (IGF-I), and neuron-specific enolase. "Photoreceptor-survival –promoting activity" and other uncharacterized IPM components have been documented in the literature as unsolved puzzles until today (Hewitt et al., 1990; Lemmon, 1988; Mieziewska et al., 1994).

1.2 Retinal Degeneration

Vision loss significantly affects people's daily activity and their quality of life. According to data available on the National Eye Institute's website, the leading causes of blindness in the US are cataracts (17.2%) and various forms of retinal degeneration, including aged-related macular degeneration (AMD; 7.6%), diabetic retinopathy (DR; 3.4%), glaucoma (1.9%) and retinitis pigmentosa (RP; 0.34%). Most retinal degenerations are characterized by the progressive loss of photoreceptor cells initially affecting rods (Gaillard and Sauve, 2007).

The underlying pathophysiology of photoreceptor degeneration can be classified into several groups. These include defects in disc morphogenesis and protein routing, phototransduction cascade mutations that create the equivalent of chronic photicactivation, loss of trophic support, prolonged low calcium concentration, metabolic overload and toxicity and development defects (Chaum, 2003; Fain, 2006).

1.2.1 Age-related Macular Degeneration

Age-related Macular Degeneration (AMD) is the leading cause of blindness in individuals over 50 years old in developed countries. AMD can be divided into two groups, 'wet' and 'dry' and these groups are also known as the neovascular and nonneovascular form. Signs of developing AMD include: drusen accumulation between the retina and choroid, pigmentary alterations, a decrease in visual acuity, central scotomas and so on.

Exposure to intense light has been suggested to be one of the causing factors of AMD. Multiple animal studies and case reports have supported light as a causative factor in the development of AMD (Augustin et al., 2002; Borges et al., 1990; Provis, 2005a; Roberts, 2001; Winkler et al., 1999). An epidemiologic study showed only a weak association between light exposure and AMD (Mitchell et al., 1998). However, this may have been due to the limitation of using a questionnaire method to obtain information on life behavior.

1.2.2 Retinitis Pigmentosa

Retinitis pigmentosa (RP) is a leading cause of inherited and incurable blindness in the developed world, affecting about 1 in 3500 individuals world wide (Chaum, 2003; Francis, 2006; Weleber, 2005; Wright et al., 2010). RP typically starts with poor night vision (due to rods dysfunction), progressing to loss of the mid-peripheral field of vision, and gradually extending to small central vision (due to loss of macular cones). Therefore, RP is defined as rod-cone degeneration (Kannabiran et al., 2011; Wright et al., 2010). RP is known to be remarkably genetically heterogeneous with over 150 mapped chromosomal loci and one hundred genes responsible for the phenotype, rendering gene therapy difficult to generalize (Chaum, 2003;

Francis, 2006; Wright et al., 2010). In fact, more human genes have been identified that cause blindness than genes for any other disease. It is also considered a final common clinical pathway that arises from a number of insults that lead to rod-degeneration through apoptosis (Francis, 2006). Most RP mutations affect rods selectively, but it is the secondary wave of cone loss that accounts for the ultimate vision handicaps seen in humans (Chaum, 2003; Francis, 2006; Shichida and Matsuyama, 2009). There is no clear evidence regarding what triggers the ultimate cone death in RP, but elevated oxidative stress due to retinal hyperoxia after rods die has been a leading hypothesis for this secondary cone loss (Stone et al., 1999). Numerous treatments and therapies including dietary supplements, growth factor treatments, and silicon based devices are under investigation (Francis, 2006).

1.3 Photooxidative Damage

Visible light is the cue for visual perception, but excessive light can cause damage to the retina. Light has been known to cause photooxidative damage to photoreceptors and RPE for five decades (Noell et al., 1966) .

1.3.1 Photooxidative Damage and Retinal Degenerative Diseases

Photooxidative damage has long been suggested to play critical roles in the progression of retina degeneration diseases such as AMD and RP (Chang et al., 2008; Komeima et al., 2006; Shen et al., 2005). Photoreceptors have an extremely high metabolic rate and are exposed to a highly oxidative environment. They are exposed to a combination of sunlight, high oxygen, and high concentrations of polyunsaturated fatty acids. It’s proposed that reactive oxygen species, such as hydrogen peroxide, superoxide anion, hydroxyl radicals and singlet oxygen are

constantly generated in this environment (Chang et al., 2008; Provis, 2005). Oxidative stress can induce mitochondiral dysfunction, which is an important apoptotic signal. In fact, during RPE ingestion of rod outer segment, there is generation of H_2O_2 (Tate et al., 1995). It's shown that reactive oxygen species (ROS) concentrations dramatically increased in RP disease progression (Shen et al., 2005). Research showed that treating the retina with antioxidants could effectively slow down the cone death (Komeima et al., 2006; Usui et al., 2009). Overall, oxidative stress is believed to play an important role in RPE apoptosis and in the development of many retinal degeneration diseases (Winkler et al., 1999).

An increase of oxidative stress is associated with an increase of cellular catalase and glutathione S transferase, which protects against ROS. However, this protective mechanism decreases with age and therefore, RPE is more susceptible to oxidative damage in elder eyes. One of the unsolved mysteries in RP is that cones die after the primary loss of rods. Although mutations specifically target rod photoreceptors, the cones will inevitably undergo degeneration after loss of rods. There are several theories regarding why cones die after rods, such as the release of toxins by rods or other parts of the retina, or loss of survival signal released by rods. However, these are hard to explain given the long progression and high individual difference of the cone degeneration (Shen et al., 2005). Another hypothesis is that the secondary wave of cone loss is due to oxidative damage derived from the loss of rods. In fact, it has been shown that the oxidative stress on cones increases dramatically upon rod degeneration in pig. In a normal retina, photoreceptors consume large amount of oxygen and nutrition provided from the choroidal vessels. Once the majority of the rods degenerate, the cones can no longer consume the same huge amount of oxygen and will suffer from hyperemia induced damage.

1.3.2 Photooxidative Damage Mechanism

Light inducing photooxidative damage needs two players, oxygen and all-trans-retinal. Free all-trans-retinal is toxic as a reactive aldehyde and a source of free radicals, and is a potent photosensitizer. Photoexcitation of all-trans-retinal with light is followed by formation of an excited triplet state, which contains energy high enough to enable energy transfer to molecular oxygen resulting in the formation of reactive oxygen species (ROS), including singlet oxygen, peroxides and radical anion (Fig 1.4). Normal cells use antioxidants, enzymes, catalase, and glutathione peroxidase to counter act against the ROS and keep it at a safe level. However, if the cells are not able to produce enough anti-ROS species, excessive amounts of ROS will oxidize nucleotides, amino acids, and unsaturated lipids. This unfavorable oxidation may damage various cellular components which can lead to cell dysfunction and cell death may occur (Lascaratos et al., 2007).

1.3.3 The Strategies the Retina Uses to Fight against Photooxidative Damage

There are many natural ways to protect photoreceptors against photo oxidative damage. The primary method is to reduce the amount of light exposure. Humans developed eyelids to block light entering through the pupil. Also, the amount of light traversing the lens is controlled by the iris contraction of the iris and pupil size during the opening of the eyes. So far, wearing sunglasses is still known as the most effective way for slowing down the progression of certain types of retinal degeneration. A second way is the eyes ability to adapt to its environment after long-term exposure. The concentration of rhodopsin can be down-regulated when animals are exposed to strong light.

Furthermore, high concentrations of antioxidants, such as vitamin C and vitamin E can protect macro-molecules from photo oxidative damage. In general, the outer retina exhibits high concentrations of antioxidant enzymes as a natural protectant against light-induced damage.

1.4 Neurotrophic Protection

The structure and functions of the cell are frequently modulated by signaling molecules. A major type of such signaling molecules is growth factors (Yang, 2004). Growth factors have been shown to provide neuroprotection to retinal neurons *in vivo* and *in vitro*. The two major families are ligands of receptor tyrosine kinases (RTKs) and the Trk neurotrophin receptor family (LaVail et al., 1992). Such factors include the basic fibroblast growth factor (bFGF), neurotrophic cytokines, nerve growth factor (NGF) and brain-derived neurotrophic factor (BDNF), pigment-epithelium-derived factor (PEDF), and the neuropoietic cytokine ciliary neurotrophic factor (CNTF) (Chaum, 2003). Factors, such as BNDF, bFGF, CNTF, PEDF and RdCVF, have been suggested to delay retina degeneration (Lavail, 2005; Leveillard et al., 2004).

Fibroblast growth factor (FGF) is known to have many members. Acidic and basic fibroblast growth factors are demonstrated to protect photoreceptors in rats with retinal dystrophy and rats exposed to constant light (Faktorovich et al., 1990; Wolfensberger, 1998). Basic fibroblast growth factor (bFGF) has been identified biochemically in the IPM of adult monkeys, humans and mice. However, FGF cannot be used in retinal degeneration due to its property of triggering neovascularization (Usui et al., 2009).

Ciliary neurotrophic factor (CNTF) is known to rescue photoreceptors and retinal ganglion cells from genetic and environmental insult and is one of the most studied neurotrophic factors for neuroprotection of the retina (LaVail et al., 1992; Wen et al., 2012). It belongs to the

IL-6 family of neuropoietic cytokines. AAV-mediated gene delivery of CNTF has been shown to offer long-term protection of photoreceptors in various rodent models of retinal degeneration, despite no significant functional protection (Rhee et al., 2004; Rhee et al., 2013; Schlichtenbrede et al., 2003; Smith et al., 2003; Wen et al., 2012).

Rod-derived cone viability factor (RdCVF) was discovered by Léveillard et al. in 2004 (Leveillard et al., 2004). RdCVF was shown to promote cones survival as well as preserve their function (Leveillard et al., 2004; Sahel, 2005). We were trying to search for the cell surface receptors that mediate RdCVF's protective effect; however, we had difficulties reproducing the RdCVF protective effect in the embryonic chicken culture system

Pigment-epithelium-derived factor (PEDF) has been isolated from cultured fetal human RPE cells (Tombran-Tink et al., 1991). This factor has shown neuronal differentiation effects *in vitro* (Steele et al., 1993).

1.5 Urgency of Identifying New Trophic Factors

Retina degenerative diseases are commonly treated by gene therapy, cell replacement therapy and growth factor therapy (Leveillard and Sahel, 2010). In 2001, the Leber congenital amaurosis (LCA) was successfully cured by RPE65 gene therapy in dog models. However, LCA caused by a RPE65 mutation accounts for only 2% of the LCA patients, which renders the application of this therapy limited. Similarly, due to the high heterogeneic nature of the Retinitis Pigmentosa (RP), it is not practical to perform individual specific gene therapy for all the RP patients. Recent gene therapy studies have shown that neurotrophic support is necessary to prevent long term degeneration in retina diseases (Beltran et al., 2012). Moreover, gene therapy is not easy for rod photoreceptor cells, which is sensitive and may degenerate due to over-

expressing proteins involved in phototransduction. Cell replacement therapy has been limited by the hurdle of forming correct synaptic connections between implanted photoreceptors, progenitor cells, engineered stem cells and inner neurons (Leveillard and Sahel, 2010) .

In both cases of AMD and RP, the loss of vision is not a direct result of genetic mutations in cone photoreceptor cells. The causal reasons for AMD are complex and have not been clearly elucidated so far. Age and a family history are the only two factors consistently found to be associated with AMD. Life behavior, such as smoking, and environmental factors, such as light, have been suggested to play a role in some studies (Provis, 2005). The term RP, on the other hand, encompasses a large number of retinal diseases caused by mutations in rods followed by gradual loss of cones (Anasagasti et al., 2012). The secondary cone loss leads to the ultimate visual handicap and has been suggested caused by loss of trophic support or excessive oxidative stress after majority of rods are gone. Therefore, effective trophic support that delays or prevents photoreceptor, especially cone, degeneration in these diseases may lead to the discovery of effective treatment.

With the advance of modern light systems, rods are less essential to human life. Saving cones is the priority in treating retina degenerations. Neurotrophic factor support, in theory, could save the photoreceptors as a whole. Delay of rods loss will ultimately delay the loss of cones. Therefore, we hope to search for factors that could directly or indirectly keep cone cells alive in the retina degenerative diseases. The fact that the IPM contains unidentified photoreceptor-survival proteins and the limitations of using the known factors to treat retina degeneration diseases reveals the urgency of identifying new trophic factors that naturally exist in the retina.

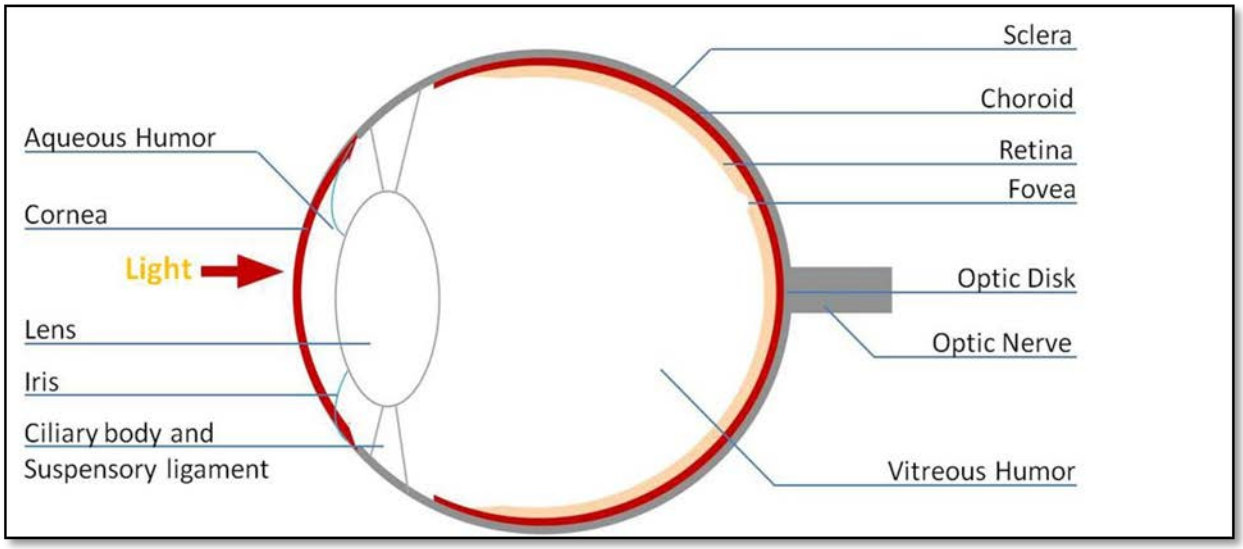

Figure 1.1 Anatomy of the Human Eye

The human eye is divided into two chambers by the lens, the anterior chamber and vitreous chamber. These chambers are filled with aqueous humor and vitreous humor respectively. In the front of the eye, the structures are the cornea, iris, lens, ciliary body and suspensory ligament. In the back of the eye, from the outermost to the innermost, the structures are the sclera, choroid and the retina. Fovea is 1.5 mm wide retinal region where the photoreceptors are entirely cones.

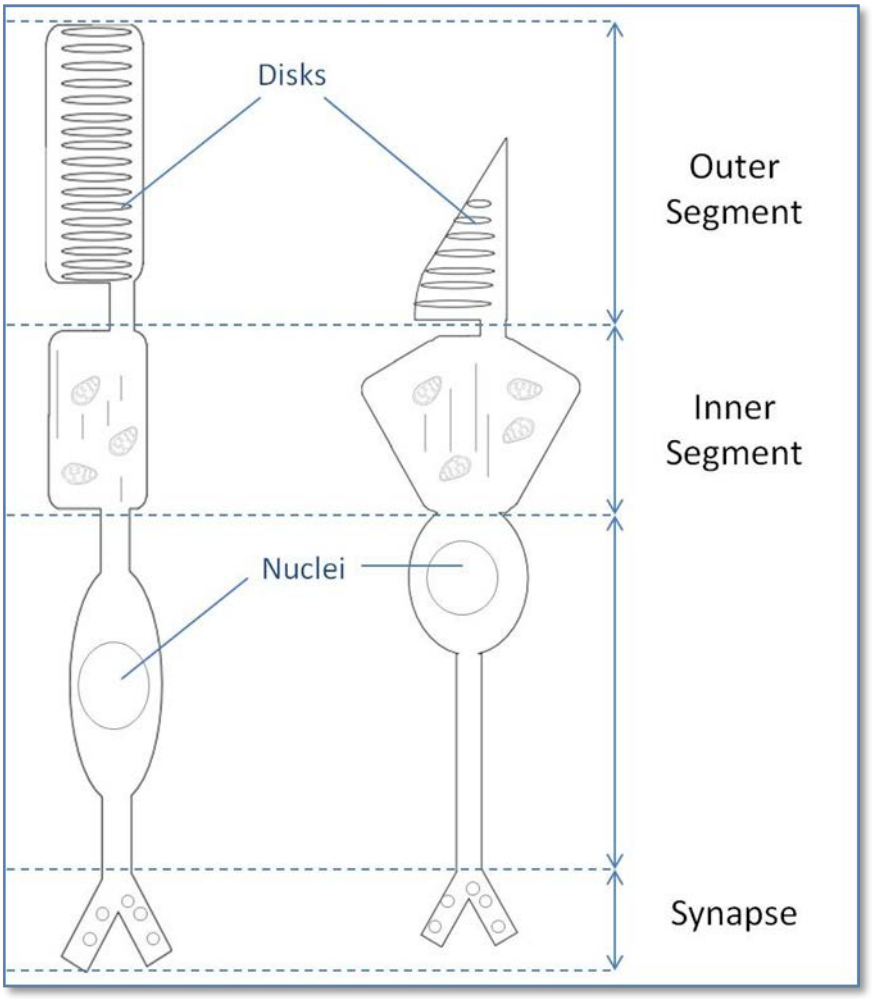

Figure 1.2 The Photoreceptors

Both rods and cones consist of the outer segment, inner segment, cell body and the synaptic terminus, but are distinguished by the shape of their outer segments.

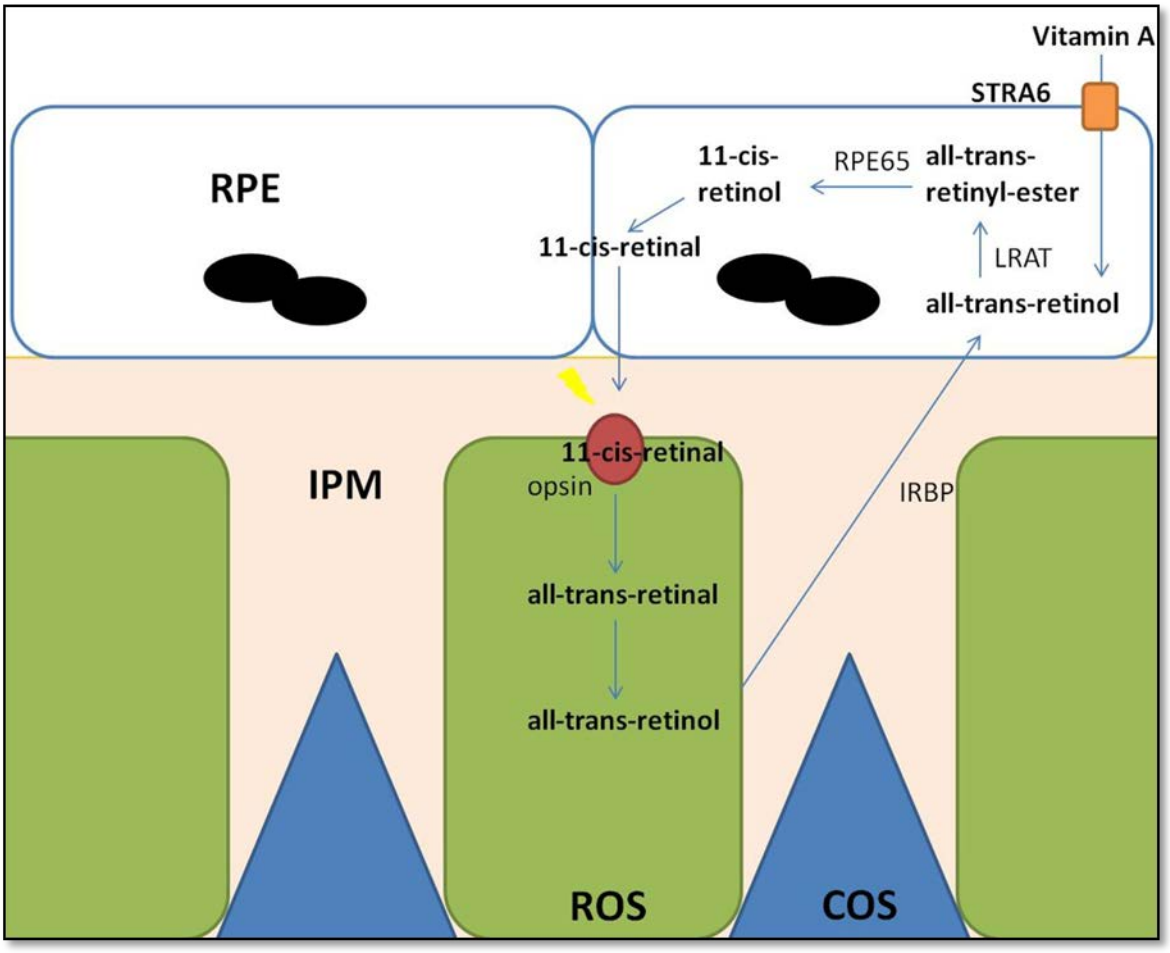

Figure 1.3 The Visual Cycle in Vertebrate Vision

Upon absorption of a photon by chromophore 11-cis-retinal, it converts to all-trans-retinal, which is further reduced to all-trans-retinol via catalysis by NADPH-dependent all-trans-retinal-specific dehydrogenase. All-trans-retinol diffuses to the RPE though IPM and is esterified to all-trans-retinyl-ester via catalysis by lecithin retinol acyltransferase (LRAT). The isomerization from all-trans-retinyl-ester to 11-cis-retinol is catalyzed by RPE-specific-65kDa protein (RPE65). 11-cis-retinol is then oxidized to 11-cis-retinal via catalysis by retinal-dehydrogenase. 11-cis-retinal diffuses back to photoreceptor cells where it combines opsins to regenerate visual pigment. Vitamin A (all-trans-retinol) is transported into the RPE through RBP receptor STRA6. RPE, retinal pigment epithelium; IPM, interphotoreceptor matrix; ROS, rod outer segment; COS, cone outer segment; RBP, retinol binding protein; STRA6, stimulated by retinoic acid 6.

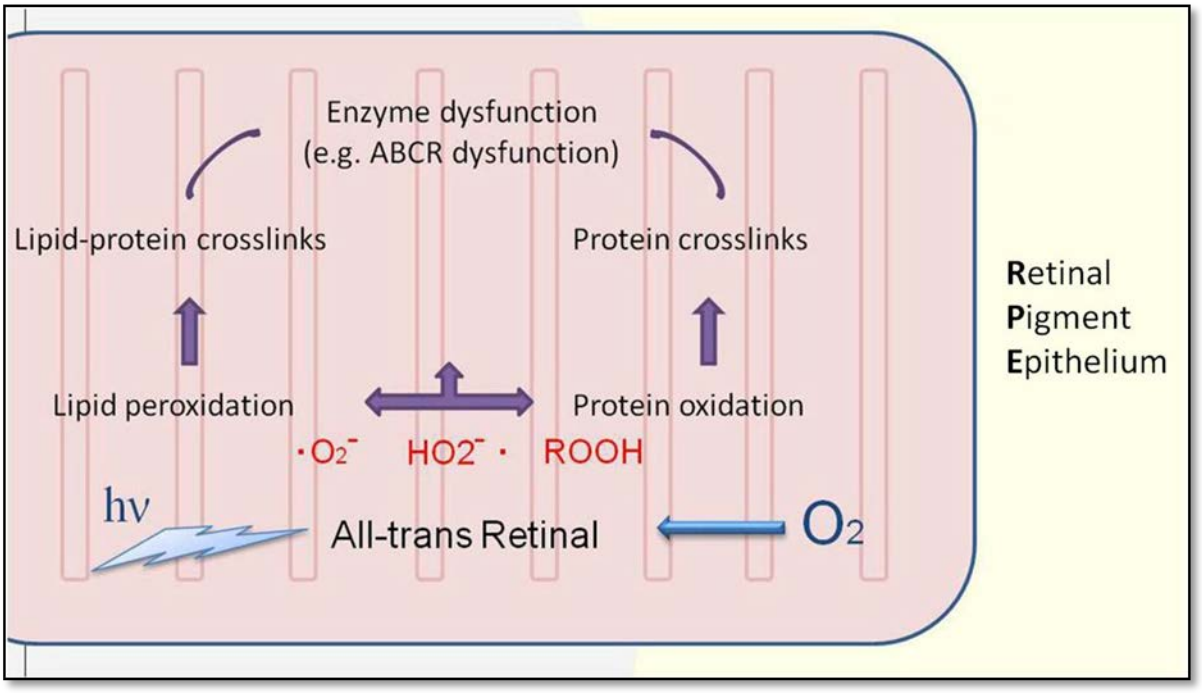

Figure 1.4 Photooxidative Damage in Photoreceptor Cells

Light induces photoxidative damage though oxygen and all-trans-retinal. Photoexcitation of all-trans-retinal by light is followed by the formation of an excited, high energy, triplet state. This state contains high enough energy to enable energy transfer to molecular oxygen, resulting in a reactive oxygen species (ROS), which oxidizes proteins and lipids, and leads to misfunction of functional enzymes. In the absence of sufficient antioxidant, cell apoptosis will occur.

Reference

Adler, A.J., and Martin, K.J. (1982). Retinol-binding proteins in bovine interphotoreceptor matrix. Biochem Biophys Res Commun *108*, 1601-1608.

Anasagasti, A., Irigoyen, C., Barandika, O., Lopez de Munain, A., and Ruiz-Ederra, J. (2012). Current mutation discovery approaches in Retinitis Pigmentosa. Vision Res *75*, 117-129.

Augustin, A.J., Dick, H.B., Offermann, I., and Schmidt-Erfurth, U. (2002). [The significance of oxidative mechanisms in diseases of the retina]. Klin Monbl Augenheilkd *219*, 631-643.

Beltran, W.A., Cideciyan, A.V., Lewin, A.S., Iwabe, S., Khanna, H., Sumaroka, A., Chiodo, V.A., Fajardo, D.S., Roman, A.J., Deng, W.T., *et al.* (2012). Gene therapy rescues photoreceptor blindness in dogs and paves the way for treating human X-linked retinitis pigmentosa. Proc Natl Acad Sci U S A *109*, 2132-2137.

Borges, J., Li, Z.Y., and Tso, M.O. (1990). Effects of repeated photic exposures on the monkey macula. Arch Ophthalmol *108*, 727-733.

Caranci, F., Cicala, D., Cappabianca, S., Briganti, F., Brunese, L., and Fonio, P. (2012). Orbital fractures: role of imaging. Semin Ultrasound CT MR *33*, 385-391.

Chang, J.Y., Bora, P.S., and Bora, N.S. (2008). Prevention of Oxidative Stress-Induced Retinal Pigment Epithelial Cell Death by the PPARgamma Agonists, 15-Deoxy-Delta 12, 14-Prostaglandin J(2). PPAR Res *2008*, 720163.

Chaum, E. (2003). Retinal neuroprotection by growth factors: a mechanistic perspective. J Cell Biochem *88*, 57-75.

Fain, G.L. (2006). Why photoreceptors die (and why they don't). Bioessays *28*, 344-354.

Fain, G.L., Hardie, R., and Laughlin, S.B. (2010). Phototransduction and the evolution of photoreceptors. Curr Biol *20*, R114-124.

Faktorovich, E.G., Steinberg, R.H., Yasumura, D., Matthes, M.T., and LaVail, M.M. (1990). Photoreceptor degeneration in inherited retinal dystrophy delayed by basic fibroblast growth factor. Nature *347*, 83-86.

Francis, P.J. (2006). Genetics of inherited retinal disease. J R Soc Med *99*, 189-191.
Gaillard, F., and Sauve, Y. (2007). Cell-based therapy for retina degeneration: the promise of a cure. Vision Res *47*, 2815-2824.

Goldstein, E.B. (2007). Sensation and perception

Gregory, R.L. (1966). Eye and Brain : The Psychology of Seeing

Hageman, G.S. (1998). The Retinal Pigment Epithelium 30.

Hewitt, A.T., Lindsey, J.D., Carbott, D., and Adler, R. (1990). Photoreceptor survival-promoting activity in interphotoreceptor matrix preparations: characterization and partial purification. Exp Eye Res *50*, 79-88.

Hitoshi, S. (1983). Biochemistry of vision

Jin, M., Li, S., Moghrabi, W.N., Sun, H., and Travis, G.H. (2005). Rpe65 is the retinoid isomerase in bovine retinal pigment epithelium. Cell *122*, 449-459.

Kannabiran, C., Singh, H.P., and Jalali, S. (2011). Mapping of locus for autosomal dominant retinitis pigmentosa on chromosome 6q23. Hum Genet *131*, 717-723.

Kawaguchi, R., Zhong, M., Kassai, M., Ter-Stepanian, M., and Sun, H. (2007). STRA6-catalyzed vitamin A influx, efflux, and exchange. J Membr Biol *245*, 731-745.

Komeima, K., Rogers, B.S., Lu, L., and Campochiaro, P.A. (2006). Antioxidants reduce cone cell death in a model of retinitis pigmentosa. Proc Natl Acad Sci U S A *103*, 11300-11305.

Lascaratos, G., Ji, D., Wood, J.P., and Osborne, N.N. (2007). Visible light affects mitochondrial function and induces neuronal death in retinal cell cultures. Vision Res *47*, 1191-1201.

Lavail, M.M. (2005). Survival factors for treatment of retinal degenerative disorders: preclinical gains and issues for translation into clinical studies. Retina *25*, S25-S26.

LaVail, M.M., Unoki, K., Yasumura, D., Matthes, M.T., Yancopoulos, G.D., and Steinberg, R.H. (1992). Multiple growth factors, cytokines, and neurotrophins rescue photoreceptors from the damaging effects of constant light. Proc Natl Acad Sci U S A *89*, 11249-11253.

Lemmon, V. (1988). A monoclonal antibody that binds to the surface of photoreceptors. Brain Res *467*, 117-123.

Leveillard, T., Mohand-Said, S., Lorentz, O., Hicks, D., Fintz, A.C., Clerin, E., Simonutti, M., Forster, V., Cavusoglu, N., Chalmel, F., *et al.* (2004). Identification and characterization of rod-derived cone viability factor. Nat Genet *36*, 755-759.

Leveillard, T., and Sahel, J.A. (2010). Rod-derived cone viability factor for treating blinding diseases: from clinic to redox signaling. Sci Transl Med *2*, 26ps16.

Mieziewska, K. (1996). The interphotoreceptor matrix, a space in sight. Microsc Res Tech *35*, 463-471.

Mieziewska, K., Szel, A., Van Veen, T., Aguirre, G.D., and Philp, N. (1994). Redistribution of insoluble interphotoreceptor matrix components during photoreceptor differentiation in the mouse retina. J Comp Neurol *345*, 115-124.

Mitchell, P., Smith, W., and Wang, J.J. (1998). Iris color, skin sun sensitivity, and age-related maculopathy. The Blue Mountains Eye Study. Ophthalmology *105*, 1359-1363.

Morton, R.A. (1972). The chemistry of the visual piments Handbook of Sensory Physiology *7*, 35.

Noell, W.K., Walker, V.S., Kang, B.S., and Berman, S. (1966). Retinal damage by light in rats. Invest Ophthalmol *5*, 450-473.

Provis, P.L.a.J.M. (2005a). Macular Degeneration

Rhee, K.D., Goureau, O., Chen, S., and Yang, X.J. (2004). Cytokine-induced activation of signal transducer and activator of transcription in photoreceptor precursors regulates rod differentiation in the developing mouse retina. J Neurosci *24*, 9779-9788.

Rhee, K.D., Nusinowitz, S., Chao, K., Yu, F., Bok, D., and Yang, X.J. (2013). CNTF-mediated protection of photoreceptors requires initial activation of the cytokine receptor gp130 in Muller glial cells. Proc Natl Acad Sci U S A *110*, E4520-4529.

Roberts, J.E. (2001). Ocular phototoxicity. J Photochem Photobiol B *64*, 136-143.

Sahel, J.A. (2005). Saving cone cells in hereditary rod diseases: a possible role for rod-derived cone viability factor (RdCVF) therapy. Retina *25*, S38-S39.

Samardzija Marijana, G.C. (2014). Retinal Degnerative Diseases : Advances in Experimental Medicine and Biology *801*, 7.

Schlichtenbrede, F.C., MacNeil, A., Bainbridge, J.W., Tschernutter, M., Thrasher, A.J., Smith, A.J., and Ali, R.R. (2003). Intraocular gene delivery of ciliary neurotrophic factor results in significant loss of retinal function in normal mice and in the Prph2Rd2/Rd2 model of retinal degeneration. Gene Ther *10*, 523-527.

Shen, J., Yang, X., Dong, A., Petters, R.M., Peng, Y.W., Wong, F., and Campochiaro, P.A. (2005). Oxidative damage is a potential cause of cone cell death in retinitis pigmentosa. J Cell Physiol *203*, 457-464.

Shichi, H. (1983). Biochemistry of Vision

Shichida, Y., and Matsuyama, T. (2009). Evolution of opsins and phototransduction. Philos Trans R Soc Lond B Biol Sci *364*, 2881-2895.

Smith, A.J., Schlichtenbrede, F.C., Tschernutter, M., Bainbridge, J.W., Thrasher, A.J., and Ali, R.R. (2003). AAV-Mediated gene transfer slows photoreceptor loss in the RCS rat model of retinitis pigmentosa. Mol Ther *8*, 188-195.

Steele, F.R., Chader, G.J., Johnson, L.V., and Tombran-Tink, J. (1993). Pigment epithelium-derived factor: neurotrophic activity and identification as a member of the serine protease inhibitor gene family. Proc Natl Acad Sci U S A *90*, 1526-1530.

Stone, J., Maslim, J., Valter-Kocsi, K., Mervin, K., Bowers, F., Chu, Y., Barnett, N., Provis, J., Lewis, G., Fisher, S.K., *et al.* (1999). Mechanisms of photoreceptor death and survival in mammalian retina. Prog Retin Eye Res *18*, 689-735.

Tate, D.J., Jr., Miceli, M.V., and Newsome, D.A. (1995). Phagocytosis and H2O2 induce catalase and metallothionein gene expression in human retinal pigment epithelial cells. Invest Ophthalmol Vis Sci *36*, 1271-1279.

Tombran-Tink, J., Chader, G.G., and Johnson, L.V. (1991). PEDF: a pigment epithelium-derived factor with potent neuronal differentiative activity. Exp Eye Res *53*, 411-414.

Usui, S., Komeima, K., Lee, S.Y., Jo, Y.J., Ueno, S., Rogers, B.S., Wu, Z., Shen, J., Lu, L., Oveson, B.C., *et al.* (2009). Increased expression of catalase and superoxide dismutase 2 reduces cone cell death in retinitis pigmentosa. Mol Ther *17*, 778-786.

Wang, H., Cui, X., Gu, Q., Chen, Y., Zhou, J., Kuang, Y., Wang, Z., and Xu, X. (2012). Retinol dehydrogenase 13 protects the mouse retina from acute light damage. Mol Vis *18*, 1021-1030.

Weleber, R.G. (2005). Inherited and orphan retinal diseases: phenotypes, genotypes, and probable treatment groups. Retina *25*, S4-S7.

Wen, R., Tao, W., Li, Y., and Sieving, P.A. (2012). CNTF and retina. Prog Retin Eye Res *31*, 136-151.

Winkler, B.S., Boulton, M.E., Gottsch, J.D., and Sternberg, P. (1999). Oxidative damage and age-related macular degeneration. Mol Vis *5*, 32.

Wolfensberger, M.F.M.a.T.J. (1998). The Retinal Pigment Epithelium

Wright, A.F., Chakarova, C.F., Abd El-Aziz, M.M., and Bhattacharya, S.S. (2010). Photoreceptor degeneration: genetic and mechanistic dissection of a complex trait. Nat Rev Genet *11*, 273-284.

Yang, X.J. (2004). Roles of cell-extrinsic growth factors in vertebrate eye pattern formation and retinogenesis. Semin Cell Dev Biol *15*, 91-103.

Chapter 2: The Protective Effect of the Interphotoreceptor Matrix on Photoreceptor Cells

2.1 Introduction

In vertebrate vision, light induces the release of a chromophore from visual pigments in the retina. The released chromophore all-trans-retinal is known to be highly toxic. Retinal is a potent photo-oxidizer and can mediate photooxidative damage to photoreceptor cells. This may be because the interaction between light and oxygen with retinal generates reactive oxygen species, which oxidizes proteins and lipids, and leads to misfunction of functional enzymes (Lascaratos et al., 2007). An increasing amount of evidence suggests that the exposure to elevated light is an important cofactor in the development of retinal degeneration (Borges et al., 1990; Provis, 2005; Shen et al., 2005). In daylight, constant release of retinal by light can potentially cause damage to photoreceptor cells (Provis, 2005). However, how photoreceptors protect themselves from photooxidative damage is not well understood. Identification of new retina trophic factor(s) will lead to a better understanding of the mechanism of cone survival and will help to develop new therapeutic strategies to promote cone survival in patients.

Previously, several studies have suggested the essential role of IPM in photoreceptor function and survival (Wolfensberger, 1998). In the 1990s, Ruben Adler's group first described the photoreceptor survival promoting activities (PSPA) of the IPM. They found that crude extracts of IPM increased photoreceptor survival in an embryonic chicken culture system (Hewitt 1989). However due to the technique limitations, the exact identity of PSPA has not been discovered.

In our study, we found that the soluble fraction of the interphotoreceptor matrix (IPM) from the retina potently protected photoreceptor cells from retinal-mediated light damage and oxidative damage *in vitro*. Inspired by Rita Levi Montalcini's Nobel Prize winning discovery of the nerve growth factor (NGF) from the conditioned media of mouse tumor explants, we tried to indentify the factors that accounts for the powerful protective effect of the IPM. Tandem purification methods were employed to fractionate the IPM. Mouse cone-derived cell 661W cells and primary cone cultures were prepared to screen for the protective fraction(s). Mass spectrometry was used to identify the protein candidates. Through the comparison of the protein identities generated by mass spectrometry, we were able to discover numerous candidate proteins and verify their protective effect in cell culture systems.

2.2 Methods

2.2.1 Material

The murine photoreceptor-derived 661W cell was a generous gift by Dr. Muayyad Al-Ubaidi of at the University of Oklahoma Health Sciences Center. These cells are cone photoreceptor cell lineage that could undergo light-induced apoptosis. 661W cells were grown in DMEM high glucose media (Thermo Scientific Inc) with 10% FBS, penicillin and streptomycin. Cells from passage 18 to 24 were incubated in a humidified atmosphere of 5% CO_2-95% air and subjected to a retinal-light damage assay and H_2O_2 oxidative damage assays.

Mouse polyclonal antibodies against chicken visinin (7G4) and against chicken actin (IgM) were purchased from Developmental Studies Hybridoma Bank. GAPDH antibody

(GA1R) was purchased from Thermo Scientific, Inc. The presence of visinin was detected with peroxidase-conjugated goat anti-mouse secondary antibodies (Southern Biotech, Inc) and visualized using Luminata Forte Western HRP substrate (Millipore, Inc).

2.2.2 Preparation of Chicken Cone Culture

Embryonic chicken retina culture was prepared according to the published paper (Hsieh and Yang, 2009). Fertilized white leghorn eggs were obtained from A A Lab Eggs Inc, and incubated in a humidified egg incubator at 37 ºC for 8 days. On Day 8, retinas were dissected free of pigment epithelium and placed in sterile phosphate-buffered saline (PBS; Mediatech, Inc). Retina pieces were rinsed once in PBS and rotated in 500 μl 0.25% trypsin (HyClone, Inc) at 37 ºC incubator for 10 minutes . The enzymatic reaction was stopped by adding an equal volume of medium Dulbecco's Modified eagle's medium/Ham's nutrient mixture F12 (1:1 DME/F12 modified) containing 1% fetal bovine serum, 0.2% chicken serum, penicillin and streptomycin. The retinas were spin down at 1,200 rpm for 5 min (Eppendorf centrifuge 5702R) and the supernatant was removed by suction. The resultant cells were gently mechanically dissociated with a pipette. Retinal cells were seeded either into poly-D-lysine (10 μg/ml)-coated 96-well plates at half retina per plate for the retinal-light damage experiment, or 12-well plates at one retina/plate for Western Blot. The cells were incubated with purified factors for up to 6 days in a humidified atmosphere of 5% CO_2-95% air.

2.2.3 Isolation of the Soluble Fraction of the Interphotoreceptor Matrix

Freshly dissected bovine retinas were washed in 10ml Tris-buffered saline (pH= 7.4) for 10 min at 4 ºC. Retinas were spun down at 4 ºC, 1000 G for 5 min. This step was repeated twice and the supernatant was combined for high-speed centrifugation at 25,000 G using Eppendorf SW28 spin bucket for 30 min, at 4 ºC. The supernatant was stored at 4 ºC with protease inhibitor. Before applying to cells, IPM was sterilized with a 20 nm filter to remove bacteria or debris.

2.2.4 Light Damage Assay

661W cells were seeded on a 96-well tissue culture plate (Olympus) and allowed to grow overnight. The next day, purified factors or IPM fractions were added to the wells according to the design. DMEM media containing 10% FBS, HEPES pH 7.0 and all-trans retinal (ATR) 100 µl were added to the wells. The culture dish was sealed with tape and exposed to 10,000 lux of light for the indicated time length. The plates were incubated overnight before cell survival assay.

2.2.5 IPM Fractionation through Ion Exchange Q Column

Q Sepharose High Performance beads from GE Healthcare were packed into Poly-Prep chromatography column (Bio-Rad), and equilibrated with the column buffer: 10 mM Tris, pH 7.5, 50 mM NaCl. On the day before the fractionation, 12 ml of IPM was dialyzed overnight in a 1L column equilibration buffer. 4 ml of the dialyzed IPM was applied to 2 ml Q Sepharose. The flow-through was collected for analysis. The column was washed with 500 µl equilibration

buffer and eluted in the elution buffers with increasing amount of NaCl concentration at 100 mM, 200 mM, 300 mM, 400 mM, 500 mM, 800 mM and 2 M in 10 mM Tris pH 7.5. The flow-through and each eluate were collected and concentrated to 500 µl.

2.2.6 Buffer Change and Sterilization Method

Centrifugal filters from Millipore Inc. were used to change the Tris-salt buffer to cell—friendly PBS buffer for cell assays. Semi-permeable cellulose at 3K cutoff allows proteins with molecular weights larger than 3 KDa be preserved in the filter device, and the solvent pass through. Each fraction is applied to a filter cassette and concentrated through centrifugation at 3000 G (rcf) at 4 ºC to 500 µl. PBS was added to fill up the upper filter chamber (~7.5 ml) and concentrate down to 50 0µl. The buffer changing step was repeated three times in total. Since the original salt concentration is diluted 15 times (7.5 ml / 0.5 ml) through each concentration. Repeating this step three times will generate a factor of 3375 times dilution (15^3). After the buffer changing step, the original salt concentration is negligible.

All the fractions were changed to PBS buffer through the method mentioned above and were sterilized through centrifugal filtration with a DURAPORE-PVDF membrane at 0.22 µm cutoff from (EMD Millipore Inc.) at 12,000 g for 1 min before being applied to the cell culture.

2.2.7 IPM Fractionation through Sequential Ammonium Sulfate

Ammonium sulfate 144 mg was slowly added to1 ml of IPM in an Eppendorf tube to reach 25% ammonium sulfate concentration (ammonium sulfate was added very slowly with a

vortex to ensure that local concentrations around the site of addition did not exceed the desired salt concentration). Rotate the Eppendorf tube at 4 ºC for 2 hours. The precipitate was collected though centrifugation at 16000 g for 10 minutes. The supernatant was transferred to another Eppendorf tube, 100 mg of ammonium sulfate was added to reach 40% ammonium sulfate concentration. After two hours of rotation, the precipitate was removed using the same method. To generate the 60% ammonium sulfate concentration in the IPM, 150 mg of ammonium sulfate was added to the transferred supernatant. All the precipitates were inverted and drained on a piece of tissue wiper and re-dissolved in 1 ml PBS. To reach optimal solublization of the precipitates, the dissolved precipitates were rotated over night at 4 ºC. Insoluble components were removed by centrifugation at 16000 g for 10 min 4 ºC. The soluble, and re-solubles from 25%, 40%, 60% ammonium sulfate precipitates were changed to PBS buffer and sterilized using the method in 2.2.6 section.

2.2.8 IPM Fractionation through Phengl-Sepharase CL-4B column

Nine volumes of 1.6M ammonium sulfate were added to one volume of IPM to reach a final volume of 1.48 M ammonium sulfate concentration. Insoluble components were removed through centrifugation at 16,000 G for 10 min. Soluble proteins were applied to pre-equilibrated CL-4B column (GE HealthCare). Flow-though was collected and the column was washed with 5 ml of 1.48 M ammonium sulfate in Tris-buffered saline (TBS , column buffer). The column was eluted sequentially in elution buffer containing decreasing amounts of ammonium sulfate at the concentrations of 1.18 M, 0.89 M, 0.6 M, and 0.3 M in 20mM Tris pH7.5. Each of the eluates and the flow-through were collected and changed to PBS buffer according to the method

described in section 2.2.6. The column was regenerated though washing with 2 bed volumes of 30% isopropanol, followed by 3-5 bed volumes of distilled water and column buffer.

2.2.9 Fractionation of IPM by Heparin Column

4 ml of IPM was dialyzed in 1 L TBS buffer (pH 7.4) overnight and applied to a pre-equilibrated Heparin-agarose column (GE HealthCare). The flow-though was collected and the column was washed with 5 ml of TBS. The column was eluted sequentially in 7.5 ml of TBS containing increasing NaCl concentration at 0.25 M, 0.5 M, 0.75 M, 1 M and 2 M. Each eluate was collected directly in a 10 K filtering tube and then concentrated down to 500 µl by spinning at 4.4x1000 g for 20 min, 4 ºC. Both flow-though and elution fractions was changed to PBS buffer and sterilized for cell culture assays. Column is regenerated though washing with 2 bed volumes of 8 M urea, 1.5 M NaCl in PBS, following with 3-5 bed volumes of TBS.

2.2.10 Fractionation of IPM by ConA Sepharose 4B

ConA Sepharose 4B was packed in the Bio-Rad chromatography column and equilibrated with column buffer (20 mM Tri, pH 7.4 containing 0.5 M NaCl) at room temperature. Binding of glycoproteins and carbohydrate-containing proteins occurs at neutral pH. The binding to ConA Sepharose 4B requires the presence of both Manganese and Calcium. The IPM is dialyzed in the column buffer over night at 4 ºC, and applied to the equilibrated column. The IPM was allowed to incubate with the column beads for 30 min to promote binding and the flow-though was collected. Elution of bound substances is achieved using 0.1 M and 0.5 M α-D-methylmannoside

respectively. Each elution buffer was incubated with the beads for 2 hours to guarantee thorough elution. The flow-through and eluates were collected and changed to PBS buffer using the method mentioned in the method section 2.2.6.

2.2.11 IPM Fractionation through High Performance Liquid Chromatography (HPLC) Using Ion Exchange Column

We use the HPLC ion exchange column (EPROGEN CA 30125) with capacity for 10 μg of proteins for the fractionation. Due to the limited capacity of the HPLC column, we use it as the secondary fractionation method. Selected fractions were changed to HPLC filtered column buffer (25 mM Tris, pH8.4) using Amicon Ultra Centrifugal Filters (3K membrane) and applied to the column. Column was equilibrated with 25 mM Tris and 10 mM NaCl and continuous eluted from 10 mM NaCl to 1.8 M NaCl in Tris buffer. Fractions with an obvious protein peak were collected and changed to PBS buffer using the method mentioned in session 2.2.6.

2.2.12 MTT Assay

The survival of 661W cells upon light damage was analyzed by MTT assay. Briefly, cells were grown in 10% FBS in DMEM containing penicillin and streptomycin until confluency. Cell death was induced by light damage. After overnight incubation, MTT assay was done by incubating cells with 100 g/ml MTT reagent (3-(4,5-dimethylthiazol-2-yl)-2,5-diphenyltetrazolium bromide) in SFM for 2 hours at 37°C. Dimethyl sulfoxide (DMSO) was added to each well after MTT was removed. The absorbance of the purple color from the

formazan formed was measured and quantified using POLARstar Omega (BMG Labtech) at 540 nm. All assays were performed in 96-well plates in triplicate.

2.2.13 P.I and FDA Co-Staining

Fluorescein diacetate (FDA) and propidium iodide (PI) stain viable cells and dead cells, respectively. The general mechanism is that FDA is taken up by cells which convert the non-fluorescent FDA into the green fluorescent metabolite fluorescein, which is an indicator for viable cells. In contrast, the nuclei staining by PI cannot pass through a viable cell membrane. It reaches the nucleus of dead cells, and serves as a dead cell indicator.

FDA stock was prepared by dissolving 5mg of FDA in 1ml of acetone. PI stock solution was prepared by dissolving 2 mg of PI in 1ml PBS. 661W cells 24 hours post light damage experiment were replaced with the staining solution at 8 μg/ml of FDA and 20 μg/ml of PI. Cells were incubated at room temperature for 5 min in the dark. The staining solution was removed and replaced with PBS.

2.2.14 Sample Preparation for Mass Spectrometry Analysis

The same volume of the fractions used to treat the cells was used to do in-solution digestion. The amount of protein in each of the fractions varied from 0.5 μg to 5 μg. Volume was filled to 10μl. 1.1 μl 100mM DTT (EMD Millipore Inc.) in 100 mM ammonium bicarbonate (Fisher Scientific) was added to the each sample and incubated at 37 ºC for 30 min to reduce the

bisulfate-bond. 1.2 µl 400 mM iodoacetaminde (Sigma-Aldrich) in 100 mM ammonium bicarbonate was added to each sample and was incubated at 37 ºC for 30 min. 100 ng of trypsin (Thermo Scientific) was added to each tube and incubated at 37 ºC for 2 hrs. We then placed the samples (on float) in 500 ml of water in a beaker and applied microwaves at 20% power for 8 min Tryptic digestion was terminated with 1 µl 15% formic acid (Fisher Scientific) in water. Each fraction was cleaned up with C18 ZipTip (Thermo Scientific) following the protocol from Millipore Inc. Acetonitrile (HPLC grade, Fisher Scientific) was used to elute the peptides from the C18 ZipTip tips (Pierce C18 Tips, Thermo Scientifics). The elution was dried using a Speedvac condensation trap without a complete dry. Samples were filled up with HPLC grade water (Fisher Scientific) to 20 µl and analyzed by mass spectrometer.

2.2.15 Peptide Identification by LC-MS/MS

Protein samples were subjected to in-solution trypsinization as previously described. Digestions were carried out at 37 ºC for two hours. Peptides were purified by zip-tip brought to a final volume of 20 µl with formic acid. Analysis was done by LC-MS/MS. Easy nLCII (Thermo Scientific) was performed using an ultimate HPLC system with a capillary column using water/ACN/formic acid gradients. The LC effluent was electrosprayed into the sampling orifice of a LTQ-Velos mass spectrometer (Thermo Scientific) operated to collect MS/MS spectra. The MS/MS data was searched using three software, X! tandem, MSGF and MyriMatch, and was matched to two bovine databases, Uniport database and NCBI database.

2.3 Results

2.3.1 IPM Protects Cone-Like 661W Cells from Retinal-mediated Light Damage

Mouse cone-derived 661W cells were used in this study to test IPM's effect. 661W is a cone-like cell line that could undergoes light-induced cell death. This feature resembles photoreceptor cell death. Addition of all-trans retinal (ATR) was included to mediate the photooxidative damage to the cells. Light damage was induced by white light at an intensity of 10,000 lux. We found that IPM protects 661W cells against retinal-mediated light damage, as shown in Fig 2.1. With pretreatment of 30 μl of ATR, 661W cells were completely protected from the damage. On the other hand, without IPM (PBS control), retinal and light induced severe damage to the cells, as the cells were observed to be detached from the culture dish. Both conditions were done in triplicate and treated under the exact same conditions.

To test if light induced apoptosis is inhibited by IPM, we performed the fluorescein dictate (FDA) and propidium iodide (PI) co-staining, which distinguishes dead cells (red) from live cells (green). With IPM addition (Fig 2.1C), many green cells were preserved in the wells but few red cells left. In the control group, very few green cells were left in culture dish, yet many more red cells were present (Fig 2.1D). Pictures were taken one day after the light damage assay. Similar results were seen after 48 hours (data not shown).

MTT is a commonly used to measure the cell survival rate. Live cells convert yellow MTT substrate into purple formazan. Therefore, the more purplish the color is, the more remaining live cells are, and the degree of protection is determined. Throughout the study, we use MTT assay to quantify the 661W cell survival rate upon various treatment. We found that the

protective activity in IPM is sensitive to freeze-thaw, indicating the protective substrate in the IPM is most likely a protein molecule.

2.3.2 IPM Protects Primary Cones from Retinal-mediated Light Damage

To test if IPM protects primary cone photoreceptors from light damage, we generated primary chicken cone culture from embryonic day-8 chicken retina. Cells were allowed to settle for 2 days before the IPM treatment (same amount of PBS was added to the control group) followed by the light damage experiment. Anti-visinin staining was employed to highlight the cone photoreceptors. Similarly, we found that IPM protects primary cones from retinal-mediated light damage (Fig 2.1 E and F).

2.3.3 Fractionation by Q Sepharose

To identify which factor (factors) accounted for the protective activity in the IPM, we performed IPM fractionation to narrow down the number of proteins for mass spectrometer identification. Here we show the total gel picture of the proteins fractionated by the strong anion exchange Q column in Figure 2.2 A. Increasing concentration of sodium chloride in Tris-buffered saline was used to elute different proteins off the column. The separation was effective since the protein pattern of each lane on the gel looks different from the other (Fig 2.2 A). We tested each fraction on the primary cone culture in the light damage assay and we showed that Q-300 mM NaCl elution is the most protective fraction while Q-200 mM NaCl partially protects the cones (Fig 2.2 B-G). The flow-through and the other fractions do not show a protective effect.

2.3.4 Fractionation by Sequential Ammonium Sulfate Precipitation

Another effective fractionation method is sequential ammonium sulfate precipitation. IPM was precipitated by 25%, 40%, 60% ammonium sulfate sequentially, and resolublized in PBS buffer. Each resolublized precipitate was tested on the primary chicken culture to assay their protective effect against light damage. The ammonium sulfate precipitation method effectively separated proteins as shown in Figure 2.3A. In Figs 2.3 B-D, we show that 25% ammonium sulfate preserves the protective effect of IPM, however, not the 40%, 60% or the unprecipitable proteins (ammonium sulfate soluble) of the IPM. Figs 2.3 E-G shows the total cell number of cones staining by DAPI and PNA stains.

2.3.5 Tandem Purification by HPLC

Although Q Sepharose is a powerful tool to separate IPM protein and preserve the protective activity, the proteins in each of the Q fraction were still too complex to be resolved by mass spectrometer. As we took this to mean that, the minor proteins were less likely to be discovered, a secondary fractionation was needed to further resolve the complexity left over from the primary fractionation method.

We further fractionated protective Q-300 (300 mM NaCl elution) fraction with ion-exchange HPLC. Finer fractionation was achieved as evidenced by the decrease amount of protein in each fraction, and protective effect being preserved in the Q300-HPLC7, which was the high salt elution as shown in Fig 2.4. Other combinations of the fractionation methods were

employed in this study, such as 25% Ammonium Sulfate precipitate followed by Q fractionation and vise versa.

2.3.6 Mass Spectrometry Identification for Candidate Proteins

After persistent exploration of different fractionation methods and their combinations, together with the help of mass spectrometry and large-scale data analysis, we have identified nearly forty candidates. Table 2.1 lists all the identified candidate proteins and their synonyms. Other fractionation methods include size exclusion chromatography, WGA affinity column, Heparin affinity column, ConA affinity column, DEAE anion exchange column, CL4B hydrophobic interaction column, and CHT cation exchange column.

The criteria that we have been following when making decisions regarding which gene is the cone protective candidate is that we have picked proteins that basically match the activity profile, in other words, those that were high in all active fractions but low or absent in inactive fractions. Among all the candidate genes, some are secreted proteins and others are currently known intracellular proteins. We have cloned all the genes into our expression vectors so that these genes are expressed through mammalian cell lines (Cos-1 or 293T). Since all the genes are identified though an unbiased comparison and search, we decided to test these genes in an unbiased way. For all the known intracellular proteins, we added a secretion signal in front of the gene, harvested the secretion and tested them on the cone cultures.

We commonly used three kinds of expression vectors to express our protein: pRK5-His-HA (N terminus, no secretion signal), pRK5-APSS-His-HA (N terminus, with secretion signal),

pRK5- His Rim (C terminus, no secretion signal). pRK5 is a vector designed to use the CMV promoter for mammalian expression. The first and the third vectors are used to clone secreted factor (s). Tagging on the C or N terminus mostly depends if the same restriction endonuclease site is inside of the gene. The 6xHis tag is added to help purify the factor through Nickel beads. HA- and Rim- tags are included for detection purposes.

Among all of the tested clones, UBB has shown consistent cone-protective effect. UBB was identified through tandem purification of sequential ammonium sulfate precipitation followed by anion exchange Q Sepharose methods. Fig 2.5 A shows that 3 distinct peptides were identified in the protective AS25-Q500 fraction, and 1distinct peptide was identified in the AS25-Q200 fraction showing a weaker protection. Nothing was identified anywhere else. Three distinct peptides identified for UBB are listed in Fig 2.5 B, which do not show up in the gene ubiquitin. Ubiquitin is known to be present in extracellular medium and is a signal for tissue repair (Majetschak, 2010). In addition, natural ubiquitin is presented in multiple forms and is highly heterogeneous, which can perfectly explain why the factor activity was easily lost when we tried further purification methods. A high degree of purification is impossible for a highly heterogeneous factor because further purification can only get rid of different active forms (e.g., due to different MW or charges). This may explain why it is impossible to see a peak after a third round of fractionation.

2.4 Discussion

In this study, we showed that IPM protects cone photoreceptors against acute light damage. The combination of tandem purification and mass spectrometry techniques allows us to search for the factor(s) accounting for the protective effect. Proteins enriched in the protective

fractions but not in the control fractions were selected as candidates. During this study, more than 30 candidates have been cloned and tested for verification of protective effects in cone cultures. We have confirmed the protective effect of one factor UBB, whose protective effect will be illustrated in detail in the following chapters.

Early Evidence for the Existence of Endogenous Photoreceptor Protective Factors in the Retina

Several studies have produced evidence suggesting that the IPM may play a significant role in photoreceptor degeneration (Wolfensberger, 1998). Two decades ago, Ruben Adler's group first described the photoreceptor survival promoting activities (PSPA) of the IPM. They found that crude extracts of IPM increased photoreceptor survival in a 10-day culture of embryonic chicken neurons and photoreceptors. They also found that this PSPA was heat labile, sensitive to freeze-thawing, and stable only within a narrow pH (Hewitt 1989). This group has partially purified a fraction with PSPA activity through heparin-affinity chromatography and hydrophobic chromatography (Hewitt 1989). However, due to technique limitations at that time, the exact identity of PSPA was not elucidated.

Similarities and Differences of Our Study and Adler's Research

Although this study was originally inspired by Ruben Adler's study and the Nobel Prize winning work of Rita Levi Montalcini (introduction), we believe that our purified factors may not be equal to the 'PSPA' (Hewitt et al., 1990). The similarities and the differences of the two studies are compared in the following aspects:

Culture system: Comparing the cell culture used in Hewitt's and my study, there are similarities and differences. Both cultures use embryonic day 8 chicken retina and are dissociated by 0.25% Trypsin. However, in Hewitt's study, poly-L-ornithine hydrobromide was used to coat the dish, and the culture media was medium 199 supplemented with 10% fetal bovine serum and 110 ug/ml of linoleic acid-BSA preparation. In contrast, our study uses poly-D-Lysine to coat the dish, and the cells were cultured in Dulbecco's Modified eagle's medium/Ham's nutrient mixture F12 (1:1 DME/F12 modified) containing 1% fetal bovine serum, 0.2% chicken serum, penicillin and streptomycin.

Damaging methods: In our study, we applied extracellular all-trans-retinal and strong light (10,000 lux) to induce acute damage. Cell apoptosis was usually observed within a few hours and became very obvious in samples allowed to incubate overnight. In Hewitt's study, naturally occurring cell death after culturing for 7-10 days without further medium changes was used as the cell death model.

Nature of the factors: In the Hewitt's publication, PSPA was found bind to a heparin column and hydrophobic interaction chromatography (CL-4B column). However, our identified factors were purified by an anion-exchange column and sequential ammonium sulfate purification methods. The activity of IPM was lost in our study when purified with CL-4B column.

Innovation and Significance

In this study, we invented a novel and quick screening method to search for the neurotrophic factors in the IPM. Avoiding long term culture (as mentioned in Adler's study), we

are able to perform large scale screening tests. More than ten fractionation methods based on distinct separation principles are used as a single or combined method to look for the protective fraction(s). The advancement of modern protein detection tool and mass spectrometry makes it possible to separate and detect hundreds to thousands of proteins in each fraction. Through proteomics study, we were able to identify the candidate proteins enriched in the protective fraction and verify the candidates.

Due to the limitation of the gene therapy method and the difficulties in the cell replacement method, neurotrophic factor therapy is promising in its application as a method to improve photoreceptor survival in a more general way. In theory, neurotrophic factors that naturally exist in the retina would provide natural protection to the photoreceptor cells at both morphological and functional levels. Further identification of its signaling mechanism and cell surface receptor could lead to new drug discovery to treat retina diseases.

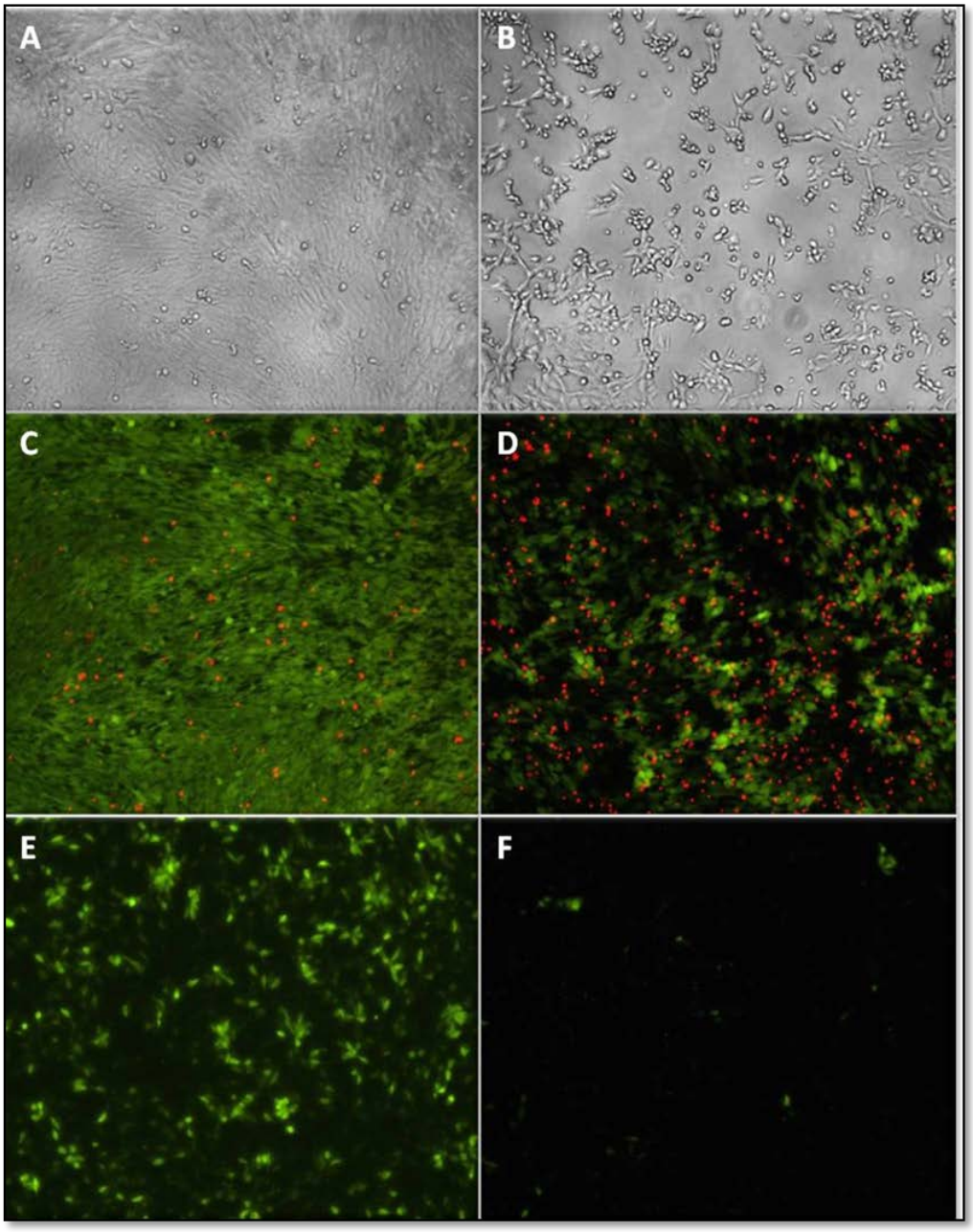

Figure 2.1 IPM Protects 661W Cells and Primary Cones from Retinal-mediated Light Damage

The morphology of 661W cells post light damage, with (A) and without (B) IPM addition. FDA (Green) and PI (Red) co-staining for 661W cells after retinal-mediated light damage with (C) and without (D) IPM protection. The morphology of primary cones post light damage, with (F) and without (G) IPM addition. Cones were shown by anti-visinin staining.

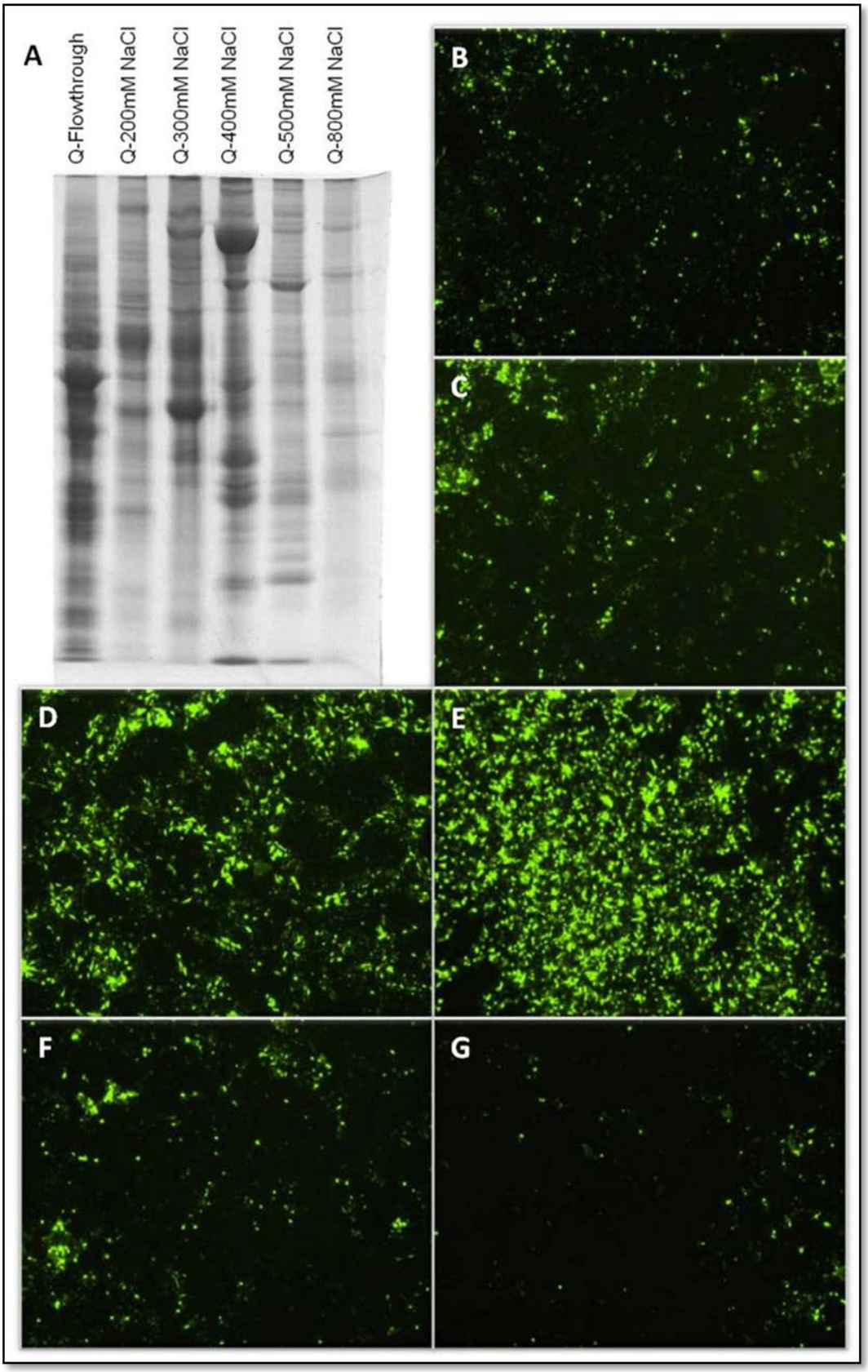
A
Q-Flowthrough
Q-200mM NaCl
Q-300mM NaCl
Q-400mM NaCl
Q-500mM NaCl
Q-800mM NaCl
B
C
D
E
F
G

Figure 2.2 Cone Protection by Q Anion Exchange Column Fractions from IPM

A. The total gel picture showing the protein pattern of the flow-through and the eluates. B-G, The protective effect of the flow-though and different eluates by Q Sepharose fractionation on chicken cones. (B. flowthrough, C. NaCl 100mM Elution, D. NaCl 200mM Elution, E. NaCl 300mM Elution, F. NaCl 400mM Elution, G. NaCl 800mM Elution) . Green is anti-visinin staining. The pictures were taken at 40 times magnification.

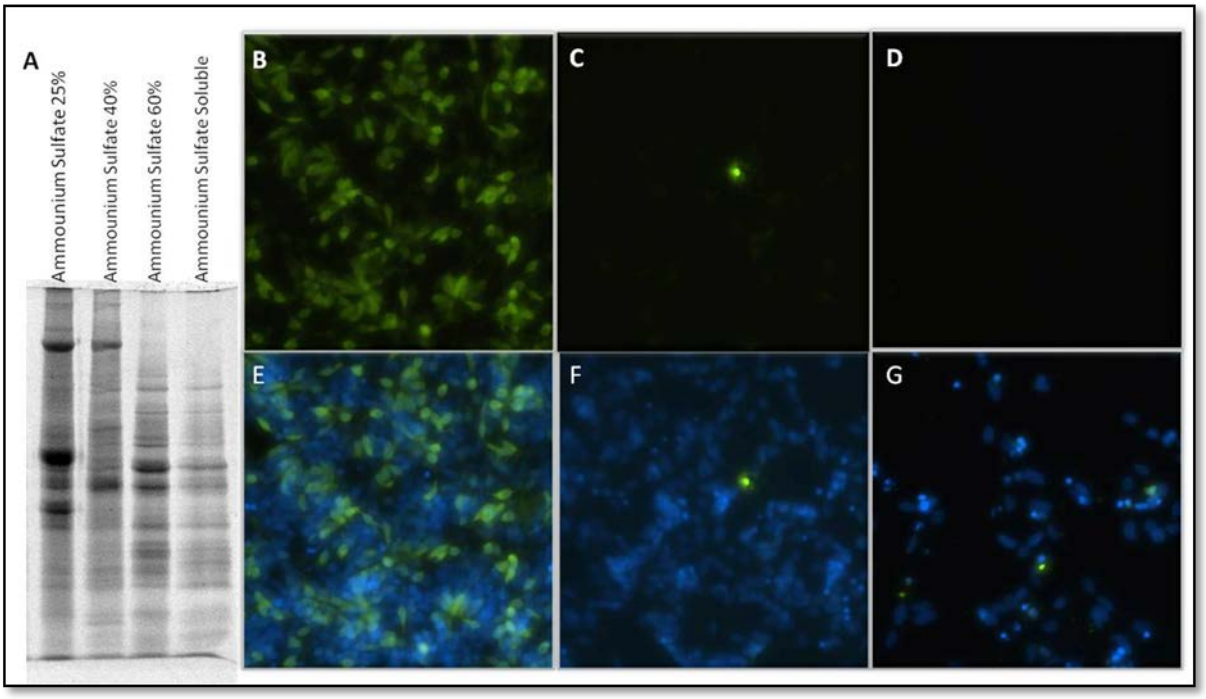

Figure 2.3 Cone Protection by Sequential Ammonium Sulfate Precipitation Fractions

A. The total gel picture showing the protein pattern of each of the fractions from the ammonium sulfate fractionation method. B-G, The protective effect of each fraction on chicken cones. (B and E. 25% ammonium sulfate precipitates resolublized solution; C and F. 40% ammonium sulfate precipitates resolublized solution ; D and G. 60% ammonium sulfate precipitates resolublized solution). B-D. Anti-visinin staining, green. E-G. DAPI (blue) and anti-visinin (green) co-staining. The pictures were taken at 200 times magnification.

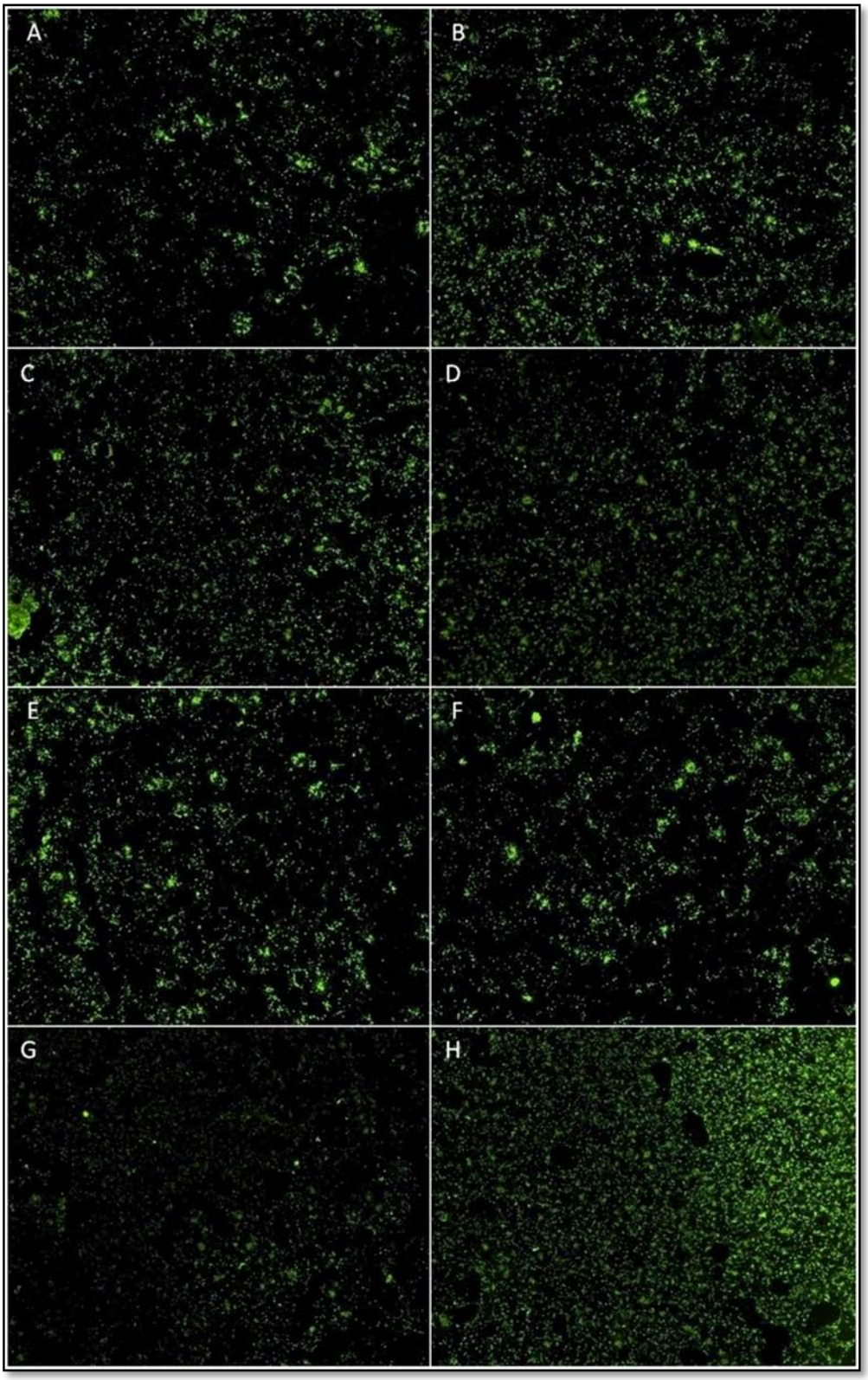
A
B
C
D
E
F
G
H

Figure 2.4 Cone Protection by HPLC Fractions

The protective effect on cones by fractions separated by ion-exchange HPLC column. A. PBS treated; B-H. Q-300 further fractionated by ion-exchange HPLC, fraction 1 to fraction 7. Green, anti-visinin staining. The pictures were taken at 40 times magnification.

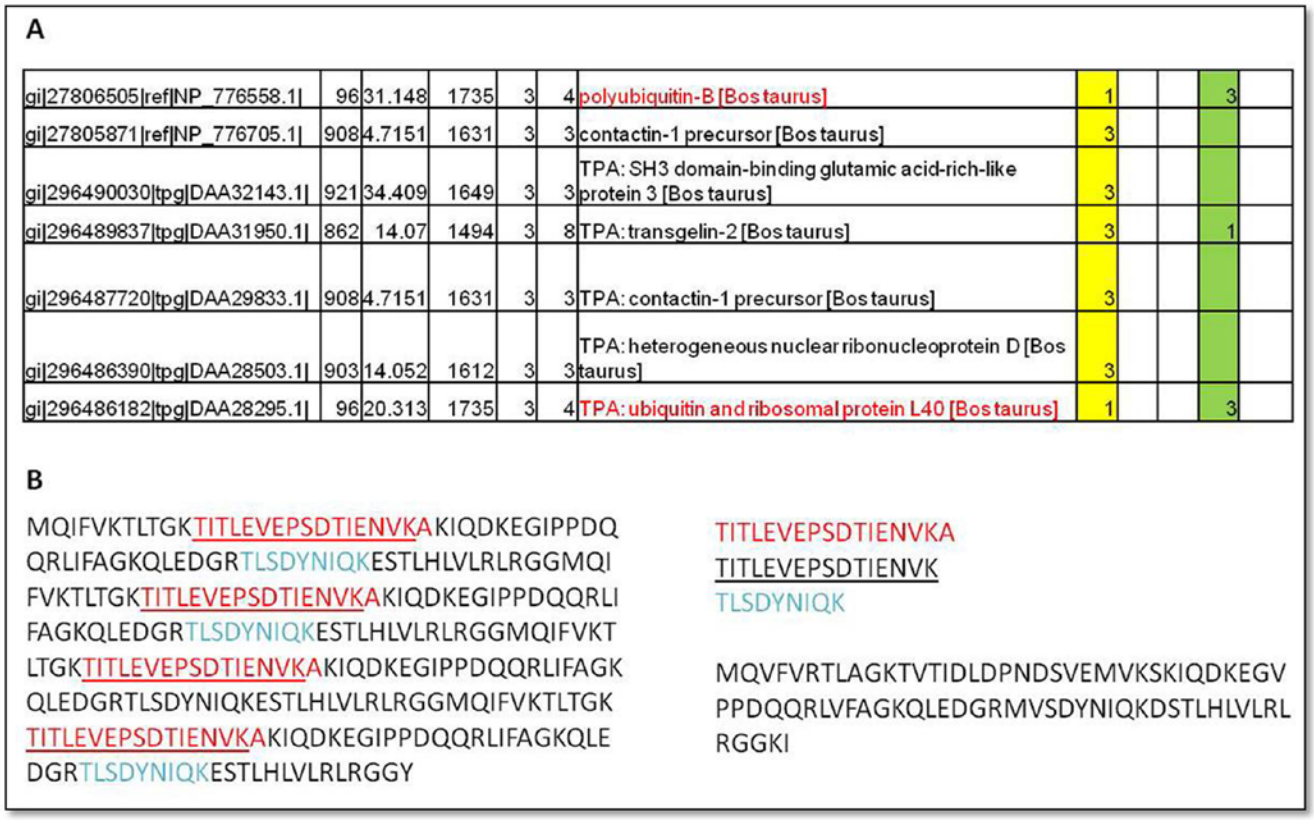

A

gi|27806505|ref|NP_776558.1|	96	31.148	1735	3	4	polyubiquitin-B [Bos taurus]	1			3		
gi|27805871|ref|NP_776705.1|	908	4.7151	1631	3	3	contactin-1 precursor [Bos taurus]	3					
gi|296490030|tpg|DAA32143.1|	921	34.409	1649	3	3	TPA: SH3 domain-binding glutamic acid-rich-like protein 3 [Bos taurus]	3					
gi|296489837|tpg|DAA31950.1|	862	14.07	1494	3	8	TPA: transgelin-2 [Bos taurus]	3			1		
gi|296487720|tpg|DAA29833.1|	908	4.7151	1631	3	3	TPA: contactin-1 precursor [Bos taurus]	3					
gi|296486390|tpg|DAA28503.1|	903	14.052	1612	3	3	TPA: heterogeneous nuclear ribonucleoprotein D [Bos taurus]	3					
gi|296486182|tpg|DAA28295.1|	96	20.313	1735	3	4	TPA: ubiquitin and ribosomal protein L40 [Bos taurus]	1			3		

B

MQIFVKTLTGKTITLEVEPSDTIENVKAKIQDKEGIPPDQ
QRLIFAGKQLEDGRTLSDYNIQKESTLHLVLRLRGGMQI
FVKTLTGKTITLEVEPSDTIENVKAKIQDKEGIPPDQQRLI
FAGKQLEDGRTLSDYNIQKESTLHLVLRLRGGMQIFVKT
LTGKTITLEVEPSDTIENVKAKIQDKEGIPPDQQRLIFAGK
QLEDGRTLSDYNIQKESTLHLVLRLRGGMQIFVKTLTGK
TITLEVEPSDTIENVKAKIQDKEGIPPDQQRLIFAGKQLE
DGRTLSDYNIQKESTLHLVLRLRGGY

TITLEVEPSDTIENVKA
TITLEVEPSDTIENVK
TLSDYNIQK

MQVFVRTLAGKTVTIDLDPNDSVEMVKSKIQDKEGV
PPDQQRLVFAGKQLEDGRMVSDYNIQKDSTLHLVLRL
RGGKI

Figure 2.5 Identification of UBB through Mass Spec Search and the Distinct Peptides for UBB

A. Identification of UBB. 3 distinct peptides were identified in the protective AS25-Q500 fraction, and 1distinct peptide was identified in the AS25-Q200 fraction showing a weaker protection. Nothing was identified anywhere else. (fractions' name not shown). B. The three distinct peptides identified for UBB, which are not in the ubiquitin sequence.

Synonym	Definition	Synonym	Definition
Anxa2	annexin a2	HSPA2	heatshock protein 5
Anxa5	annexin a5	HSPA5	heatshock protein 5
Anxa6	annexin a6	HSP90α	heat shock protein 90 alpha
ARF5	ADP-ribosylation factor 5	HSP90β	heat shock protein 90 beta
AspAT	aspartate aminotransferase	IMPG1	interphotoreceptor matrix proteoglycan 1
AP3	adaptor-related protein complex 3	Ltbp1	latent transforming growth factor beta binding protein 1
C3	complement 3	OPTC	opticin
C5a	complement 5 a	P4hb	prolyl 4-hydroxylase, beta polypeptide
CALR	calreticulin	Rplp1	ribosomal protein, large, p1
Copg1	human coatomer subunit gamma-1	RPLP0	60s acidic ribosomal protein p0
Dpysl4	dihydropyrimidinase-like 4	Sfrp2	frizzled-related protein 2
Dpysl5	dihydropyrimidinase-like5	Sfrp3	frizzled-related protein 3
EIF4G2	mouse eukaryotic translation initiation factor 4 gamma 2	Stc2	stanniocalcin 2
Eno1	enolase 1, alpha non-neuron	SOD2	superoxide dismutase 2
Eno3	enolase 3, beta muscle	Spon-1	spondin-1
Eno2	enolase 2, gamma neuronal	SRC	src proto-oncogene, non-receptor tyrosine kinase
Got2	glutamatic-oxaloacetic transaminase 2, mitochondrial	UBB	poly-ubiquitin b
Grn	granulin	UBC	poly-ubiquitin c
Hdgf	hepatoma-derived growth factor	USO1	general vesicular transport factor p115

Table 2.1 All the Identified Protein Candidates and Their Full Name

Reference

Borges, J., Li, Z.Y., and Tso, M.O. (1990). Effects of repeated photic exposures on the monkey macula. Arch Ophthalmol *108*, 727-733.

Hewitt, A.T., Lindsey, J.D., Carbott, D., and Adler, R. (1990). Photoreceptor survival-promoting activity in interphotoreceptor matrix preparations: characterization and partial purification. Exp Eye Res *50*, 79-88.

Hsieh, Y.W., and Yang, X.J. (2009). Dynamic Pax6 expression during the neurogenic cell cycle influences proliferation and cell fate choices of retinal progenitors. Neural Dev *4*, 32.

Lascaratos, G., Ji, D., Wood, J.P., and Osborne, N.N. (2007). Visible light affects mitochondrial function and induces neuronal death in retinal cell cultures. Vision Res *47*, 1191-1201.

Majetschak, M. (2010). Extracellular ubiquitin: immune modulator and endogenous opponent of damage-associated molecular pattern molecules. J Leukoc Biol *89*, 205-219.

Provis, P.L.P.a.J.M. (2005). Machlar Degeneration.

Shen, J., Yang, X., Dong, A., Petters, R.M., Peng, Y.W., Wong, F., and Campochiaro, P.A. (2005). Oxidative damage is a potential cause of cone cell death in retinitis pigmentosa. J Cell Physiol *203*, 457-464.

Wolfensberger, M.F.M.a.T.J. (1998). The Retinal Pigment Epithelium.

Chapter 3: UBB Protects Photoreceptors against Retinal-Mediated Light Damage and Oxidative Damage

3.1 Introduction

In the previous chapter, through unbiased tandem purification and mass spectrometry, we have identified more than 30 candidate proteins that exhibit cone protection. In the present study, we demonstrated that UBB functions as a cone-survival factor that protects against photooxidative damage. Specifically, UBB effectively protects cone-like 661W cells and primary cones against acute retinal-light damage and hydrogen peroxide induced oxidative damage. The half maximal concentration of UBB's protective effect against light damage is around 10 nano molar (nM). Furthermore, the fact that 661W secretion of UBB can be induced by mild light damage or oxidative damage and that UBB binds to the 661W cell surface indicates an autocrine rescuing effect on cone photoreceptor cells.

The newly identified neurotrophic function of UBB has opened up a new field as to how a well-known intracellular protein plays a completely different role extracellularly. The identification of UBB's cone protective function could lead to the invention of a new treatment for retina degeneration diseases.

3.2 Methods

2.2.1 Material

The murine photoreceptor-derived 661W cells are cone-lineage. 661W cells were grown in DMEM high glucose media (Thermo Scientific Inc) with 10% FBS, penicillin and

streptomycin. Cells from passage 18 to 24 were incubated in a humidified atmosphere of 5% CO_2-95% air and subjected to a retinal-light damage assay and H_2O_2 oxidative damage assays.

Mouse polyclonal antibodies against chicken visinin (7G4) and against chicken actin (IgM) were purchased from Developmental Studies Hybridoma Bank. GAPDH antibody (GA1R) was purchased from Thermo Scientific, Inc. The presence of visinin was detected with peroxidase-conjugated goat anti-mouse secondary antibodies (Southern Biotech, Inc) and visualized using Luminata Forte Western HRP substrate (Millipore, Inc).

2.2.2 Preparation of Chicken Cone Culture

Embryonic chicken retina culture was prepared according to the published paper (Hsieh and Yang, 2009). Fertilized brown chicken eggs were obtained from A A Lab Eggs Inc, and incubated in a humidified egg incubator at 37 ºC for 8 days. On Day 8, retinas were dissected free of pigment epithelium and placed in sterile phosphate-buffered saline (PBS; Mediatech, Inc). Retina pieces were rinsed once in PBS and rotated in 500 µl 0.25% trypsin (HyClone, Inc) at 37 ºC incubator for 10 min . The enzymatic reaction was stopped by adding an equal volume of medium Dulbecco's Modified eagle's medium/Ham's nutrient mixture F12 (1:1 DME/F12 modified) containing 1% fetal bovine serum, 0.2% chicken serum, penicillin and streptomycin. The retinas were spin down at 1,200 rpm for 5 min (Eppendorf centrifuge 5702R) and the supernatant was removed by suction. The resultant cells were gently mechanically dissociated with a pipette. Retinal cells were seeded either into poly-D-lysine (10 µg/ml)-coated 96-well plates at half retina per plate concentration for the retinal-light damage experiment, or 12-well plates at one retina per plate concentration for Western Blot.

3.2.3 Light Damage Assay

661W cells or primary cone culture were inoculated on a 96-well plate and pretreated with factors for two days. DMEM media containing 10% FBS, HEPES pH 7.0 and all-trans retinal (ATR) 100 µl were added to the cells. Cells in absence or presence of ATR were exposed to white light at intensity of 10,000 lux for 1 hour. Plates were sealed with tape during the light damage. The media was changed to normal media after light damage. The plates were then incubated overnight before fixation with 4% paraformaldehyde (PFA) and staining with anti-visinin antibody and DAPI.

3.2.4 Hydrogen Peroxide Damage on Cones

661W cells or primary cone culture were inoculated on a 96-well plate and pretreated with factors for two days. DMEM media containing 10% FBS, HEPES pH 7.0 and H_2O_2 was added to the wells. Cell were incubated at different concentration of H_2O_2 for 2 hours in 37 ºC incubator, and changed to normal media to terminate the damage. The plates were incubated overnight before they were fixed with 4% PFA for staining assay or harvested for Western Blot (WB).

3.2.5 Fluorescent Measurement for Quantification

Cultured retina cells were fixed for 15 minutes in 4% PFA in HBSS and washed three times with PBS plus 10 mM magnesium (PBS+) to enhance cell attachment. The cells were incubated in the PBS blocking buffer containing 5% normal goat serum (NGS) and 0.3% Triton at room temperature for 1 hour. The cells were then incubated with the blocking buffer containing visinin antibodies (1:1000) at room temperature for 1 hour. The plates were washed

three times in PBS+ and followed by incubation with the blocking buffer containing goat anti-mouse IgG and 4',6-diamidino-2-phenylindole (DAPI) at room temperature for 1 hour. The cells were washed thoroughly with PBS+ and observed under a fluorescence microscope (Nikon).

Fluorescent images were taken at 100x or 200x magnifications. To quantify the total number of cone photoreceptors in each well, the total green fluorescent signal or DAPI signal was measured at the magnification of 40x. Average intensity was recorded for quantification. Background signal from empty wells was subtracted from the recorded signal.

3.2.6 Western Blot Analysis and Quantification

Primary chicken cones were inoculated on a 12-well plate for WB. One day after the oxidative damage assay, all the cells were harvested from the plate using PBS with 5 mM EDTA (ethylenediaminetetraacetic acid). Harvested cells were spun down at 1000 g at room temperature for 5 min. The cells were lysed by PBS containing 1% Triton and a cocktail of protease inhibitors on ice for 15 min. The nuclei was harvested by centrifugation at 3000 g at 4 ºC for 5 min. Supernatant containing cytosolic proteins was loaded on a 10% SDS-polyacrylamide gel and transferred to polyvinylidene difluoride (PVDF) membrane. Membranes were incubated in the blocking buffer, 5% milk in TBST (Tris- buffered saline with 0.1% Tween-20), at room temperature for 1 hour. The membrane was then incubated with the blocking buffer containing anti-GAPDH antibody (GA1R; 1:10,000, Thermo Scientific Inc) and anti-visinin antibody (7G4; 1: 1000, Developmental Studies Hybridoma Bank). The presence of visinin and GAPDH were detected with peroxidase-conjugated goat anti-mouse secondary antibodies (Southern Biotech). The membrane was visualized using Luminata Forte Western

HRP substrate (Millipore, Inc) and Western blot detection system (Fujifilm, LAS-3000) according to the manufacturer's instruction.

3.2.7 Binding Assay

UBB and control factors (PEDF and ubiquitin) were biotinylated using sulfo-NHS-SS-biotin (Pierce) after overnight dialysis in PBS at 4 ^{o}C. After biotinylation, free biotin was removed by further overnight dialysis in PBS at 4 ^{o}C and the degree of biotinylation was assessed by visualizing the shifting of molecular weight in SDS-PAGE gels after incubation with streptavidin. Biotinylated factors were added to 661W or 3T3 cells in HBSS with 10 mM HEPES, pH 7.5 and 2 mg/ml BSA at room temperature for 1 hour. After two continuous washes with HBSS, 10 mM HEPES, pH 7.5, the cells were fixed using freshly made 4 % paraformaldehyde in HBSS, pH 7.5 for 20 min. The cells were heated in HBSS at 65 ^{o}C for 1 hour to inactive endogenous alkaline phosphatase (AP) activity. After blocking in 5 mg/ml BSA in PBS for 1 hour, the cells were incubated with streptavidin-AP diluted in 5 mg/ml BSA in PBS. After four washes using PBS, AP activity was visualized using NBT/BCIP (Thermo Scientific).

3.2.8 Statistical Analysis

Significant levels were obtained from the unpaired Student's *t*-test. The level of significance was set at $p < 0.05$.

3. 3 Results

3.3.1 UBB Cloning and Expression

We performed PCR and cloned UBB into the expression vector pRK5-APSS-His-HA and purified the protein through the interaction between Nickel Affinity column and 6xHis tag. APSS is an external secretion signal, alkaline phosphatase secretion signal. Fig 3.1 shows that UBB is secreted by 293T cells and purified via His-tag.

3.3.2 UBB Protects Cone Photoreceptors against Retinal-light Damage

To test UBB's protective effect, we applied the purified His-HA-UBB to the primary chicken cone culture for a two-day incubation, and performed retinal-mediated light damage. As shown in Fig3.2, we found that the addition of UBB could significantly protect primary cones against this acute light damage. Anti-visinin staining (green) highlights the cone photoreceptors from other retina neurons. There are significantly more visinin-positive cones in the UBB treated group than those in the control groups. HH-Enolase-β is another candidate cloned into the pRK5-APSS-His-HA- construct. Since the cloning and purification procedures are similar for all the candidate proteins, they serve nicely as controls for HH-UBB treatment. Total cell number was shown by DAPI staining. No significant changes were observed in the total cell number of the UBB treated group and other control groups. This indicates that the UBB's protective effect is specific to cone photoreceptors.

The UBB's protective effect has also been confirmed on the cone-like 661W cells. We found that addition of UBB for 2 days or 24 hours could protect 661W cells from retinal-mediated light damage. One day after the damage, the cell number in the control group was

much less than that in the UBB treated group. MTT assay was performed to measure the survival rate. The quantification of the MTT assay is shown in Fig 3.2 G. We observed a significant protective effect by HH-UBB but not by HH-Opticin, which was another candidate in the study. IPM served as the positive control.

3.3.3 Concentration Curve for the Protective Effect of UBB

To understand more regarding UBB's protective effect, we pretreated the chicken cones with different concentrations of UBB, and tested the protective effect of each concentration. Purified UBB was added to the cone culture at different concentrations, ranging from 0 nM to 200 nM. After two days of incubation, cells were subjected to light damage. 24 hours later, cells were fixed on the plate by 4% PFA and stained with anti-visinin antibody and DAPI. During this step, the dead cells were washed off, and everything that remained on the dish was the retaining cells. Total visinin (green) fluorescent signal was read from each well to quantify the survival cell number. By combining three independent assays, we were able to draw a UBB-protection concentration curve. Fig 3.3 E shows that UBB's protective effect saturates at 15 nM and the half maximum concentration is 7.5 nM.

3.3.4 Oxidative Damage is Protected by UBB

To test if UBB could protect against other kinds of oxidative damage, we tested the protection of UBB against hydrogen peroxide damage. We pretreated the primary cones with UBB and monomer ubiquitin for various amounts of time, 12 hours vs. 2 days. The protective effect was analyzed by anti-visinin antibody staining of the harvested cones by Western Blot

(WB). By both fluorescent staining and WB, we showed that 2 days of UBB treatment was able to prevent cells from dying under oxidative stress (Fig 3.4).

In addition to UBB's protective effect, we found extracellular addition of monomer ubiquitin and incubation for 2 days could also significantly protect the cells from oxidative damage. This protective effect was not seen in the retinal-light damage assays. It would be interesting to know if the extracellular UBB and ubiquitin protects the cones from oxidative stress through the same pathway.

3.3.5 UBB Secretion Increases upon Damage

To test if the secretion of UBB increases upon damage in the eye, we applied damage at different levels to the 661W cells as well as bovine RPE cells After 24 hours, we harvested the supernatant and measured the UBB secretion by anti-polyubiquitin antibody. We found that the release of polyubiquitin from photoreceptors increased with increasing damage. This was not observed in RPE cells (Fig 3.5).

3.3.6 UBB Binds to 661W Cells

Through a binding assay, we found that UBB, but not ubiquitin nor PEDF, another known neurotrophic factor, bound to the 661W cell surface. UBB bound strongly to the 661W cells. A weaker binding was identified between the UBB and fibroblast cell 3T3 cell line (Fig 3.6).

3.4 Discussion

In this chapter, we have demonstrated that UBB is a cone-protective factor using both immortalized photoreceptor cell culture and primary cone culture. Our experiments show that UBB can effectively protect chicken cone photoreceptors against light damage at the half maximum concentration of 10 nM. We also show that UBB protects chicken cones against hydrogen peroxide induced damage. UBB's secretion can be induced by mild light damage or oxidative damage. In addition, UBB strongly binds to the 661W cell surface, indicating the presence of a cell surface receptor for UBB.

Extracellular Ubiquitin

Our discovery of the role of extracellular UBB in photoreceptor protection is, in a sense, both surprising and not surprising. It is surprising because UBB is the precursor to ubiquitin, which is well known for its role in protein degradation. Ubiquitin is a small, heat-stable and highly conserved peptide that is known for playing essential roles as a post-translational protein modifier and cell signaling modulator (Dennissen et al., 2012; Goldstein et al., 1975). The discovery of a ubiquitin-mediated protein degradation mechanism has been awarded the Nobel Prize in 2004. It is not entirely surprising because ubiquitin was first known as a secreted protein before the Nobel Prize winning discovery. It was originally identified from bovine thymus as a T cell differentiation signal via β-adrenergic receptors (Goldstein et al., 1975). Ubiquitin naturally exists in human plasma and serum. The concentration varies from 9 ng/ml to 100 ng/ml as reported in the literature (Majetschak et al., 2003; Okada et al., 1993; Takada et al., 1997; Takagi et al., 1999). Multiple diseases are related to the increased concentration of ubiquitin in the extracellular fluid (Majetschak et al., 2003; Okada et al., 1993; Savas et al., 2003). Both passive release from damaged tissue and active secretion of ubiquitin are implied as the release

mechanism, however, the exact mechanism of how ubiquitin is released outside of the cell remains to be determined (Majetschak, 2011). So far, several pieces of evidence suggest that the extracellular roles of ubiquitin include the involvement in the immune system and host defenses. A proposed role of extracellular ubiquitin is seen during tissue damage, where ubiquitin is released to the outside of the cell and activates the immune system, producing proinflammaotry responses (Majetschak, 2011). One suggested cell surface receptor of extracellular ubiquitin is chemokine receptor type 4 (CXCR4) which mediates the endocytosis of the ubiquitin-receptor complex and inflammatory responses (Saini et al., 2010).

UBB

While UBB is known to encode the precursor protein of ubiquitin, its other functions have not been reported. This is the first time that we reported the extracellular role of UBB. In the history of science, it is not uncommon that a change of cellular location leads to profound differences on cellular behaviors. One such example is the dual-function of Cytochrome c. Cytochrome c is widely known to be localized in the mitochondrial intermembrane space as a central component of the electron transport chain and transfers electrons to complex IV. However, it was also identified as initiating cell apoptosis once being released from mitochondria to the cytosol, where it activates the caspase family of proteases (Kroemer et al., 1998; Liu et al., 1996).

Our evidence that UBB is secreted by photoreceptors in culture under mild damage conditions indicates an autocrine model for this protein. A possible model for UBB's protection on cones is that, upon light damage, UBB is released by the photoreceptor cells and binds to their cell surface receptors to initiate the cell signaling pathways.

Innovation and Significance

This discovery is highly innovative in that this is the first time that UBB has been reported to have an extracellular function other than being the ubiquitin precursor. Although knockout UBB mouse models have been well characterized and studied by the Kopito group at Stanford, demonstrating that the loss of UBB leads to fundamental changes in development and homeostatic regulations, such as neurodegeneration, stress regulation, energy balance, adult-onset obesity, sterility and sleep disruption, all these phenotypes were credited to the secondary loss of ubiquitin instead of a primary role of UBB (Ryu et al., 2010; Ryu et al., 2008a; Ryu et al., 2008b; Sinnar et al., 2011). In this study, purified UBB protein was added directly to the cell culture dish, without any additional truncation or processing of the protein, thereby demonstrating the direct role of UBB's protective effects. This finding will contribute to the current understanding of the cell survival mechanism and have the potential to impact current retina degeneration disease treatment.

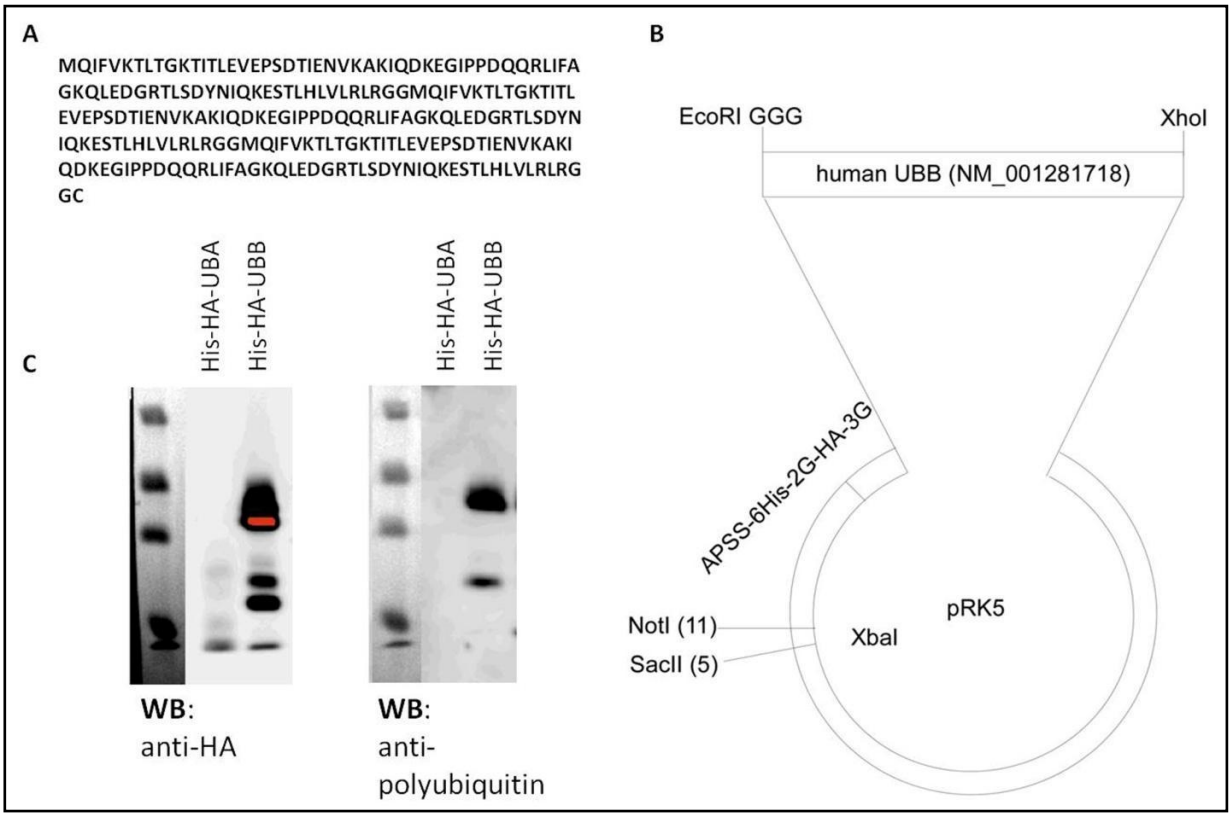

Figure 3.1 UBB Sequence, Cloning, Expression and Purification

A. UBB sequence for molecular cloning. B. the vector construct pRK5-APSS-His-HA-human UBB; C. Western Blot of purified His-HA-UBB detected by anti-HA antibody and anti-polyubiquitin antibody.

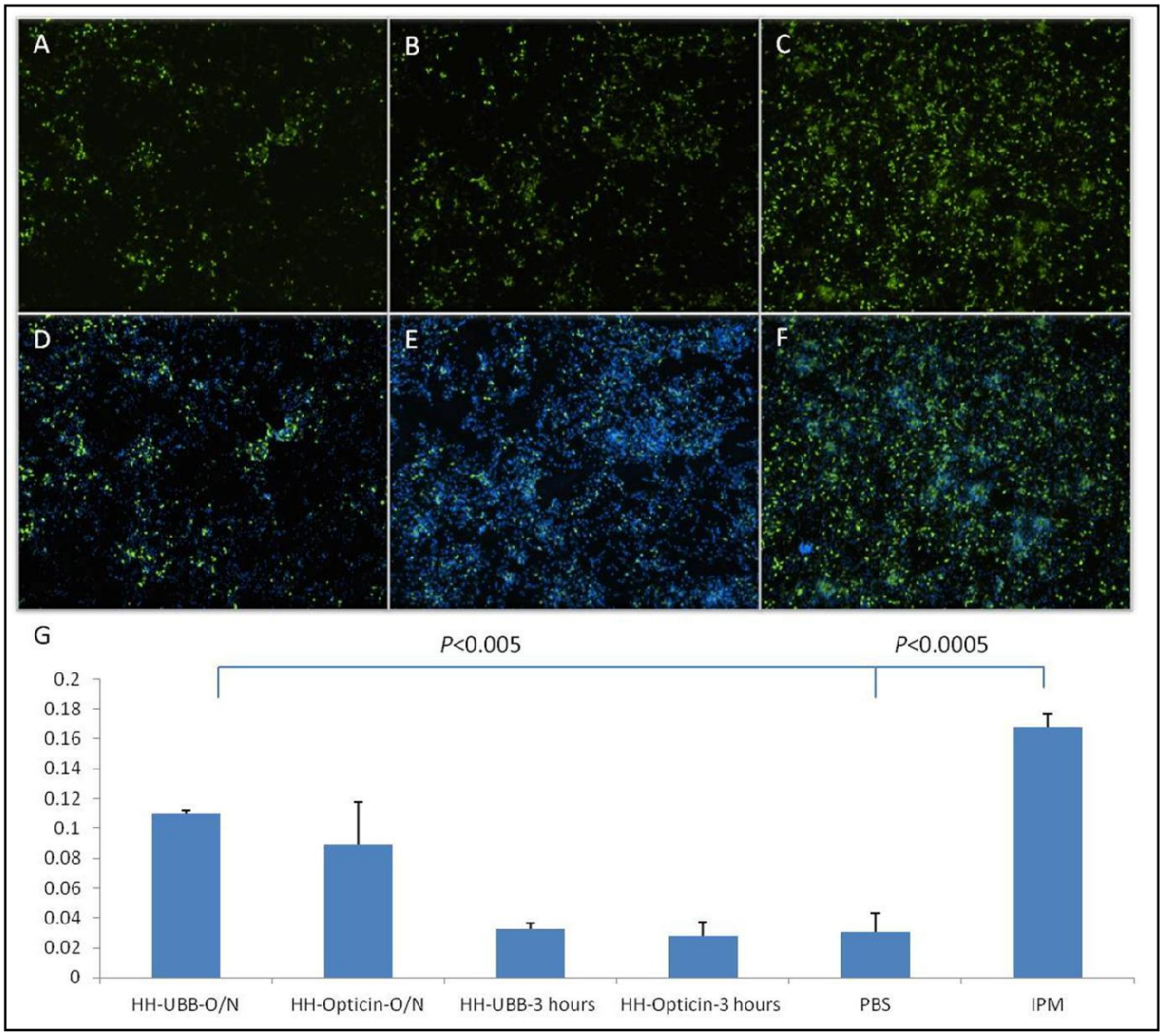

Figure 3.2 Purified His-HA-UBB Protects Cones against Retinal-mediated Light Damage

The remaining number of cones after retinal-light damage is shown by anti-visinin staining. A and D. PBS control, B and E. His-HA-Enolase-β incubated group, C and F. His-HA-UBB treated group. A-C. anti-visinin staining, green, D-F. DAPI (blue) and visinin (green) co-staining. G. The quantification of MTT assay on 661W protection by UBB and control factors.

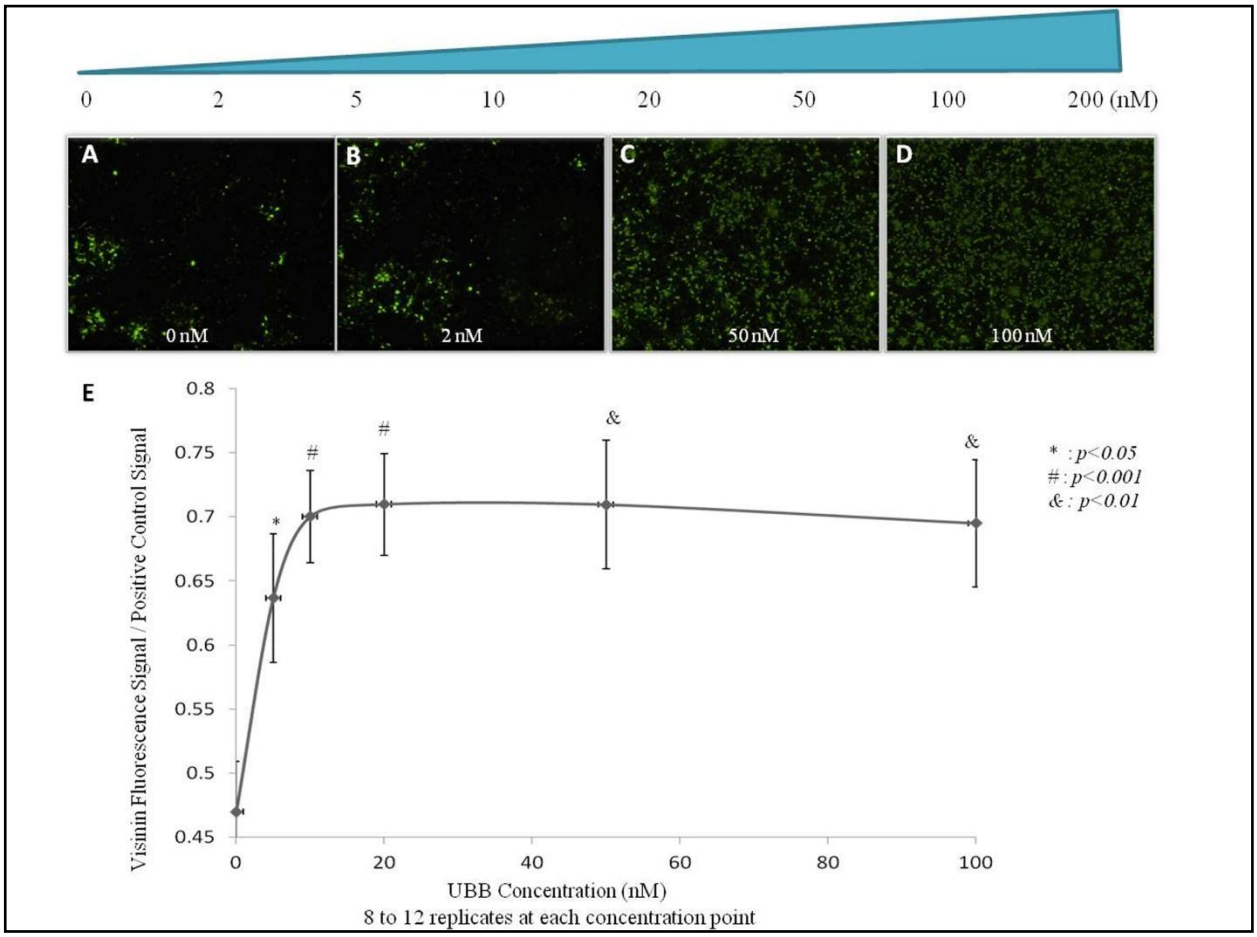

Figure 3.3 UBB's Concentration Curve in Light Damage Assay

Different concentrations of UBB, ranging from 0 to 200 nM, were added to the primary cones. Representative pictures were taken at 100 times magnification and revealed the different survival rates among different treatments. A. 0 nM UBB, B. 2 nM UBB, C. 50 nM UBB, D. 100 nM UBB. E. Concentration curve generated from the visinin fluorescent readout of the remaining (surviving) cones.

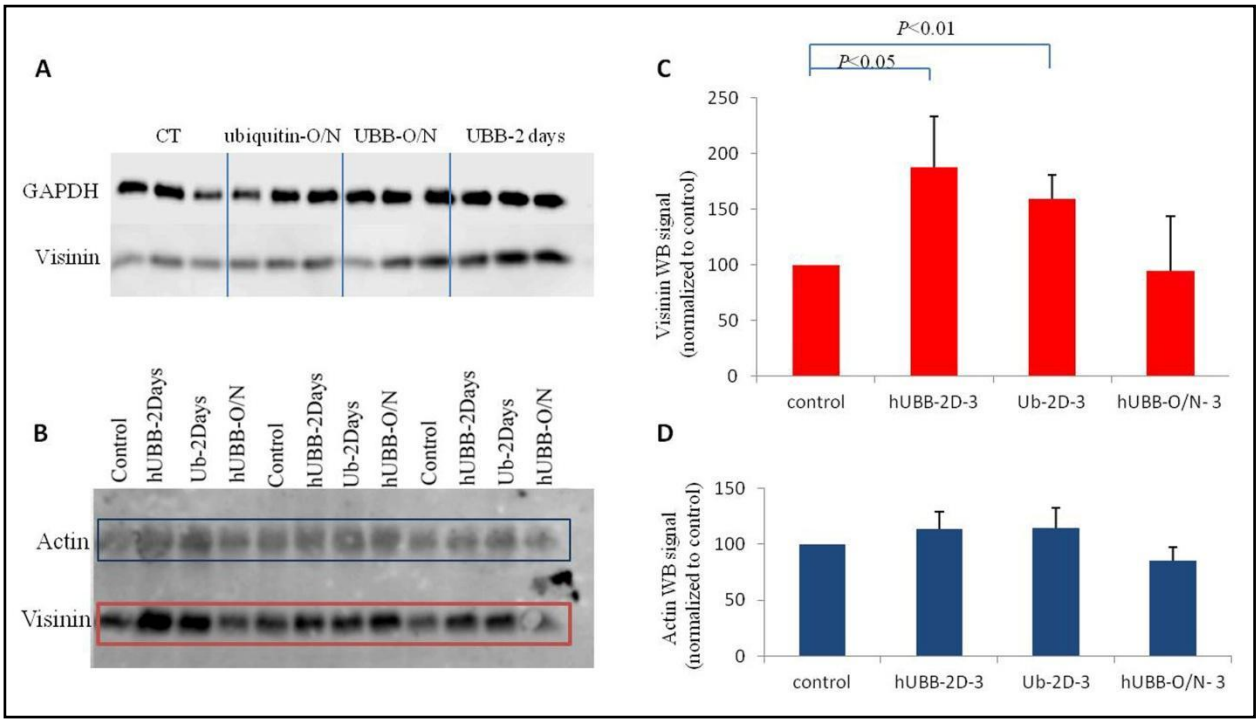

Figure 3.4 UBB Protects Primary Cones against Hydrogen Peroxide Damage

A and B. Primary cones pretreated with UBB or ubiquitin were protected against oxidative damage. C. Quantification of visinin signal in the Western Blot B. D. quantification of the actin signal in the Western Blot B. The protective effect is significant and specific in cone protection.

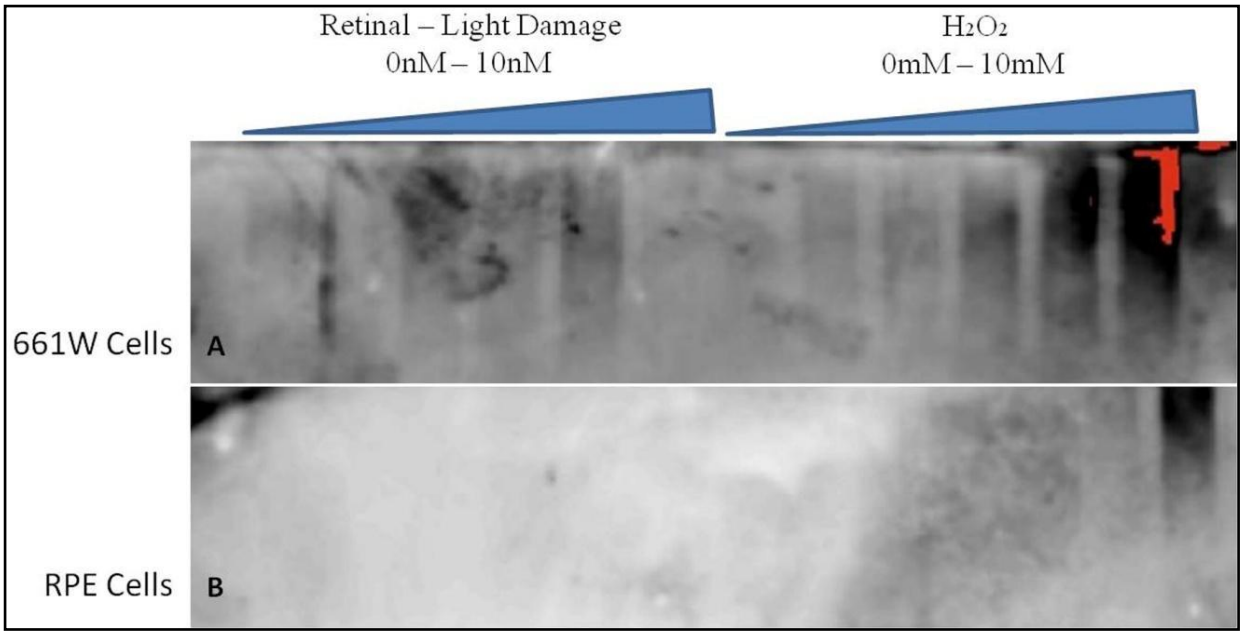

Figure 3.5 UBB's Release Increases upon Damage

Increasing amount of light damage or H_2O_2 damage has induced UBB release from 661W cells (A), but not from bovine RPE cells (B).

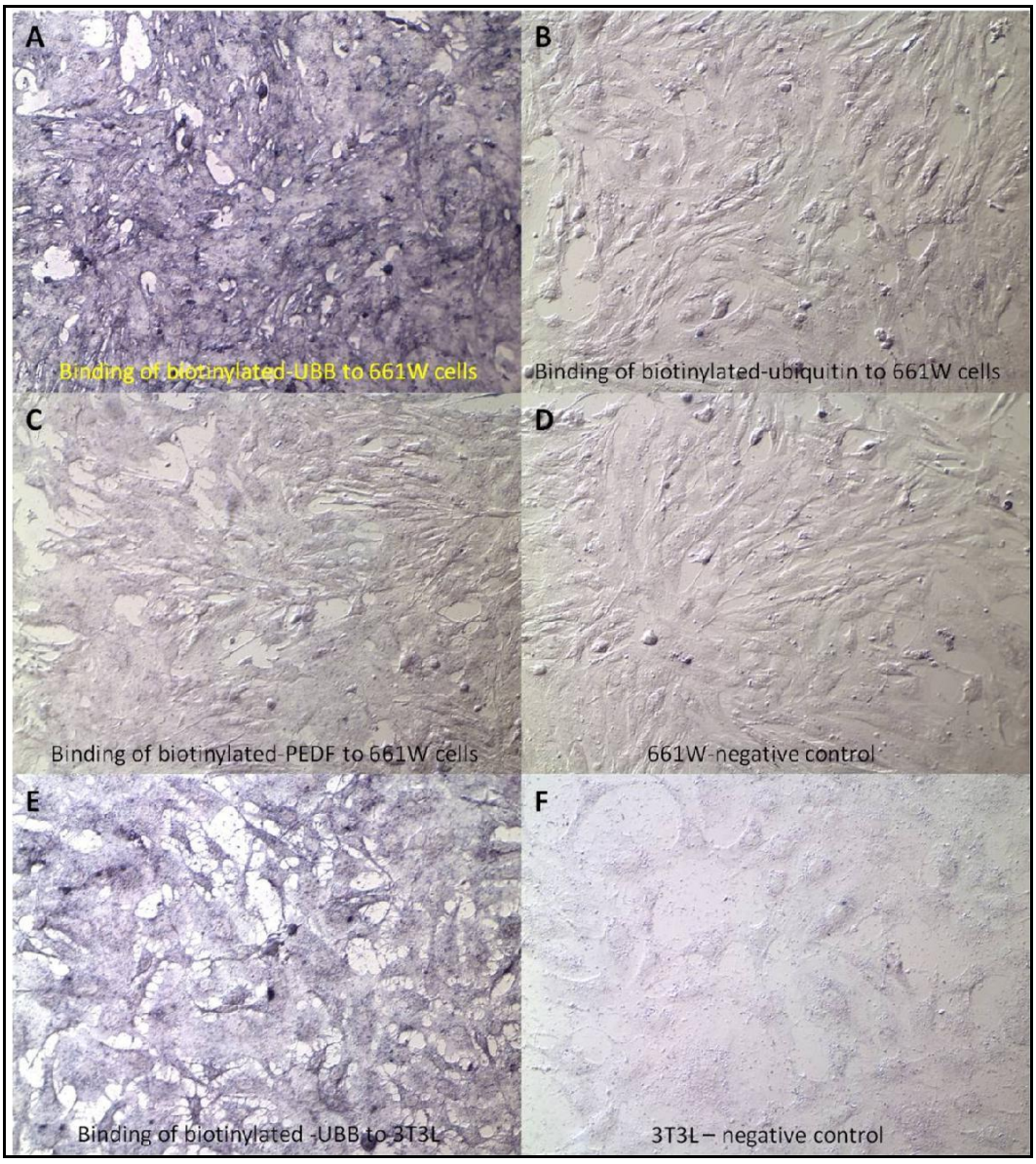

Figure 3.6 UBB Binds to 661W Cell Surface

Biotinylated-UBB strongly binds to 661W cells (A), but not other factors, such as biotinylated-ubiquitin (B) and biotinylated-PEDF (C). Weaker binding was detected between UBB and fibroblast cell 3T3 cells (E). D and F are the negative control stains of the 661W and 3T3L cells.

Reference

Dennissen, F.J., Kholod, N., and van Leeuwen, F.W. (2012). The ubiquitin proteasome system in neurodegenerative diseases: culprit, accomplice or victim? Prog Neurobiol *96*, 190-207.

Goldstein, G., Scheid, M., Hammerling, U., Schlesinger, D.H., Niall, H.D., and Boyse, E.A. (1975). Isolation of a polypeptide that has lymphocyte-differentiating properties and is probably represented universally in living cells. Proc Natl Acad Sci U S A *72*, 11-15.

Hsieh, Y.W., and Yang, X.J. (2009). Dynamic Pax6 expression during the neurogenic cell cycle influences proliferation and cell fate choices of retinal progenitors. Neural Dev *4*, 32.

Kroemer, G., Dallaporta, B., and Resche-Rigon, M. (1998). The mitochondrial death/life regulator in apoptosis and necrosis. Annu Rev Physiol 60, 619-642.

Liu, X., Kim, C.N., Yang, J., Jemmerson, R., and Wang, X. (1996). Induction of apoptotic program in cell-free extracts: requirement for dATP and cytochrome c. Cell *86*, 147-157.

Majetschak, M. (2011). Extracellular ubiquitin: immune modulator and endogenous opponent of damage-associated molecular pattern molecules. J Leukoc Biol *89*, 205-219.

Majetschak, M., Krehmeier, U., Bardenheuer, M., Denz, C., Quintel, M., Voggenreiter, G., and Obertacke, U. (2003). Extracellular ubiquitin inhibits the TNF-alpha response to endotoxin in peripheral blood mononuclear cells and regulates endotoxin hyporesponsiveness in critical illness. Blood *101*, 1882-1890.

Okada, M., Miyazaki, S., and Hirasawa, Y. (1993). Increase in plasma concentration of ubiquitin in dialysis patients: possible involvement in beta 2-microglobulin amyloidosis. Clin Chim Acta *220*, 135-144.

Ryu, K.Y., Fujiki, N., Kazantzis, M., Garza, J.C., Bouley, D.M., Stahl, A., Lu, X.Y., Nishino, S., and Kopito, R.R. (2010). Loss of polyubiquitin gene Ubb leads to metabolic and sleep abnormalities in mice. Neuropathol Appl Neurobiol *36*, 285-299.

Ryu, K.Y., Garza, J.C., Lu, X.Y., Barsh, G.S., and Kopito, R.R. (2008a). Hypothalamic neurodegeneration and adult-onset obesity in mice lacking the Ubb polyubiquitin gene. Proc Natl Acad Sci U S A *105*, 4016-4021.

Ryu, K.Y., Sinnar, S.A., Reinholdt, L.G., Vaccari, S., Hall, S., Garcia, M.A., Zaitseva, T.S., Bouley, D.M., Boekelheide, K., Handel, M.A., *et al.* (2008b). The mouse polyubiquitin gene Ubb is essential for meiotic progression. Mol Cell Biol *28*, 1136-1146.

Saini, V., Marchese, A., and Majetschak, M. (2010). CXC chemokine receptor 4 is a cell surface receptor for extracellular ubiquitin. J Biol Chem *285*, 15566-15576.

Savas, M.C., Koruk, M., Pirim, I., Yilmaz, O., Karakok, M., Taysi, S., and Yilmaz, A. (2003). Serum ubiquitin levels in patients with nonalcoholic steatohepatitis. Hepatogastroenterology *50*, 738-741.

Sinnar, S.A., Small, C.L., Evanoff, R.M., Reinholdt, L.G., Griswold, M.D., Kopito, R.R., and Ryu, K.Y. (2011). Altered testicular gene expression patterns in mice lacking the polyubiquitin gene Ubb. Mol Reprod Dev *78*, 415-425.

Takada, K., Nasu, H., Hibi, N., Tsukada, Y., Shibasaki, T., Fujise, K., Fujimuro, M., Sawada, H., Yokosawa, H., and Ohkawa, K. (1997). Serum concentrations of free ubiquitin and multiubiquitin chains. Clin Chem *43*, 1188-1195.

Takagi, M., Yamauchi, M., Toda, G., Takada, K., Hirakawa, T., and Ohkawa, K. (1999). Serum ubiquitin levels in patients with alcoholic liver disease. Alcohol Clin Exp Res *23*, 76S-80S.

Chapter 4: Follistatin Like Protein -1 (FSTL1) Protects Photoreceptors against Photooxidative Damage

4.1 Introduction

Follistatin-like 1 (FSTL1) is a secreted protein with homology to both follistatin and the SPARC/BM40 family of matricellular proteins. This autocrine glycoprotein is expressed in nearly all tissues of higher animals. Dip2A and CD14 are suggested to be the receptors of FSTL1 which regulate different downstream signaling pathways and gene functions (Murakami et al., 2012; Ouchi et al., 2010). FSTL1 regulates inflammatory cytokine expression, including Il-1β, Il-6, and TNF-α (Adams et al., 2010; Chaly et al., 2011; Liu et al., 2010). In the meantime, studies show that FSTL1 functions as a stress signal inhibiting apoptosis under ischemia or hypoxic conditions (Liang et al., 2014; Ouchi et al., 2008).

In the present study, we identified FSTL1 as a cone protective factor through an unbiased discovery-based tandem purification and mass spectrometry search. FSTL1 was identified from 661W secretion. We showed that FSTL1 can effectively protect cone-like 661W cells and primary chicken cones against light damage and hydrogen peroxide-induced oxidative damage. The half maximum protective effect for FSTL1 against light damage is about 40 nM. The identification of FSTL1 as s photoreceptor protective factor will expand our knowledge on FSTL1's function in the eye and may provide a new treatment for retina degeneration diseases.

4.2 Methods

4.2.1 Material

The murine photoreceptor-derived 661W cells are cone-lineage. 661W cells were grown in DMEM high glucose media (Thermo Scientific Inc) with 10% FBS, penicillin and streptomycin. Cells from passage 18 to 24 were incubated in a humidified atmosphere of 5% CO_2-95% air and subjected to a retinal-light damage assay and H_2O_2 oxidative damage assays.

Mouse polyclonal antibodies against chicken visinin (7G4) and against chicken actin (IgM) were purchased from Developmental Studies Hybridoma Bank. GAPDH antibody (GA1R) was purchased from Thermo Scientific, Inc. The presence of visinin was detected with peroxidase-conjugated goat anti-mouse secondary antibodies (Southern Biotech, Inc) and visualized using Luminata Forte Western HRP substrate (Millipore, Inc).

4.2.2 Preparation of Chicken Cone Culture

Embryonic chicken retina culture was prepared according to the published paper (Hsieh and Yang, 2009). Fertilized brown chicken eggs were obtained from A A Lab Eggs Inc, and incubated in a humidified egg incubator at 37 ºC for 8 days. On Day 8, retinas were dissected free of pigment epithelium and placed in sterile phosphate-buffered saline (PBS; Mediatech, Inc). Retina pieces were rinsed once in PBS and rotated in 500 μl 0.25% trypsin (HyClone, Inc) at 37 ºC incubator for 10 min . The enzymatic reaction was stopped by adding an equal volume of medium Dulbecco's Modified eagle's medium/Ham's nutrient mixture F12 (1:1 DME/F12 modified) containing 1% fetal bovine serum, 0.2% chicken serum, penicillin and streptomycin. The retinas were spin down at 1,200 rpm for 5 min (Eppendorf centrifuge 5702R) and the

supernatant was removed by suction. The resultant cells were gently mechanically dissociated with a pipette. Retinal cells were seeded either into poly-D-lysine (10 μg/ml)-coated 96-well plates at half retina per plate concentration for the retinal-light damage experiment, or 12-well plates at one retina per plate concentration for Western Blot.

4.2.3 Light Damage Assay

661W cells or primary cone culture were inoculated on a 96-well plate and pretreated with factors for two days. DMEM media containing 10% FBS, HEPES pH 7.0 and all-trans retinal (ATR) 100 μl were added to the cells. Cells in absence or presence of ATR were exposed to white light at intensity of 10,000 lux for 1 hour. Plates were sealed with tape during the light damage. The media was changed to normal media after light damage. The plates were then incubated overnight before fixation with 4% paraformaldehyde (PFA) and staining with anti-visinin antibody and DAPI.

4.2.4 Hydrogen Peroxide Damage on Cones

661W cells or primary cone culture were inoculated on a 96-well plate and pretreated with factors for two days. DMEM media containing 10% FBS, HEPES pH 7.0 and H_2O_2 were added to the wells. Cell were incubated at different concentration of H_2O_2 for 2 hours in 37 ºC incubator, and changed to normal media to terminate the damage. The plates were incubated overnight before they were fixed with 4% PFA for staining assay or harvested for Western Blot (WB).

4.2.5 Fluorescent Measurement for Quantification

Cultured retina cells were fixed for 15 minutes in 4% PFA in HBSS and washed three times with PBS plus 10 mM magnesium (PBS+) to enhance cell attachment. The cells were incubated in the PBS blocking buffer containing 5% normal goat serum (NGS) and 0.3% Triton at room temperature for 1 hour. The cells were then incubated with the blocking buffer containing visinin antibodies (1:1000) at room temperature for 1 hour. The plates were washed three times in PBS+ and followed by incubation with the blocking buffer containing goat anti-mouse IgG and 4',6-diamidino-2-phenylindole (DAPI) at room temperature for 1 hour. The cells were washed thoroughly with PBS+ and observed under a fluorescence microscope (Nikon).

Fluorescent images were taken at 100x or 200x magnifications. To quantify the total number of cone photoreceptors in each well, the total green fluorescent signal or DAPI signal was measured at the magnification of 40x. Average intensity was recorded for quantification. Background signal from empty wells was subtracted from the recorded signal.

4.2.6 Western Blot Analysis and Quantification

Primary chicken cones were inoculated on a 12-well plate for WB. One day after the oxidative damage assay, all the cells were harvested from the plate using PBS with 5 mM EDTA (ethylenediaminetetraacetic acid). Harvested cells were spun down at 1000 g at room temperature for 5 min. The cells were lysed by PBS containing 1% Triton and a cocktail of protease inhibitors on ice for 15 min. The nuclei was harvested by centrifugation at 3000 g at 4 ^{o}C for 5 min. Supernatant containing cytosolic proteins was loaded on a 10% SDS-polyacrylamide gel and transferred to polyvinylidene difluoride (PVDF) membrane. Membranes were incubated in the blocking buffer, 5% milk in TBST (Tris- buffered saline with 0.1%

Tween-20), at room temperature for 1 hour. The membrane was then incubated with the blocking buffer containing anti-GAPDH antibody (GA1R; 1:10,000, Thermo Scientific Inc) and anti-visinin antibody (7G4; 1: 1000, Developmental Studies Hybridoma Bank). The presence of visinin and GAPDH were detected with peroxidase-conjugated goat anti-mouse secondary antibodies (Southern Biotech). The membrane was visualized using Luminata Forte Western HRP substrate (Millipore, Inc) and Western blot detection system (Fujifilm, LAS-3000) according to the manufacturer's instruction.

4.2.7 Statistical Analysis

Significant levels were obtained from the unpaired Student's *t*-test. The level of significance was set at $p < 0.05$.

4. 3 Results

4.3.1 Identification of FSTL1 from 661W Cell Secretion

Inspired by the fact that UBB secretion increases upon damage, we tested if 661W secretes protective factors under stressed conditions. Serum free media containing mildly damaged 661W secretion was tested on the 661W cells using either light damage or H_2O_2-induced damage method. FSTL1 was identified through the combination of Q anion-exchange column and HPLC ion-exchange column together with mass spectrometry (Fig 4.1 A). Serum free media was harvested from 293T cells expressing untagged-FSTL1. Compared to media only condition, media containing FSTL1 showed a protective effect on the 661W cells and the primary cones against the retinal-light damage test (Fig 4.1).

4.3.2 FSTL1 Protects Cone Photoreceptors against Retinal-mediated Light Damage

We further cloned FSTL1 into pRK5-His-HA- (N-terminus-tag) and pRK5- -His-Rim (C-terminus tag) expression vectors. FSTL1 was purified through a Nickel affinity column. Purified factors showed a significant protective effect against the retinal-light damage assay on chicken cones (Fig 4.2). Similar to generating the UBB concentration curve, a wide range of FSTL1-His Rim factors, ranging from 0 nM to 100 nM, was added to the cone culture and pre-incubated for two days before the light damage assay. One day after the damage assay, cells were fixed on a plate by 4% PFA and stained with anti-visinin antibody to highlight the surviving cones. Total fluorescent signals were read from each well to measure the surviving cells. Fig 4.2 D shows a concentration – survival curve for FSTL1.

4.3.2 FSTL1 Protects Cone Photoreceptors against Oxidative Damage

FSTL1 was identified through the H_2O_2 oxidative damage assay. Therefore, we tested if FSTL1 could protect primary cones against H_2O_2 damage. We pretreated the primary cones with purified FSTL1-His-Rim or His-HA-FSTL1 for various amounts of time, 12 hours vs. 2 days. The protective effect was analyzed by harvesting the cones and performing anti-visinin WB. We showed that the purified FSTL1 could effectively protect primary cones from oxidative damage (Fig 4.3).

4.3.4 No Additional Effect by FSTL1 and UBB

Since both UBB and FSTL1 protect primary cones from photooxidative damage and H_2O_2 damage, we were interested to see if the two factors had an additional protective effect

when they were combined. Thus, we applied the factors together to the culture and incubated for 2 days before the damaging assay. However, the protective effect remained at a similar level as the protective effect from either one of the factors (Fig 4.4). No additional protection was observed by the combination of the two factors, which indicates they signal through the same survival pathway.

4.4 Discussion

In this chapter, we described how FSTL1 is identified as a protective factor from the 661W secretion. We have confirmed that FSTL1 protects 661W cells and primary chicken cones from acute light damage and hydrogen peroxide induced oxidative damage. We determined the half maximal concentration of FSTL1's protective effect in the light damage assay at 40 nM. Furthermore, we tested if the combination of FSTL1 and UBB exhibits a superimposed protective effect *in vitro*. We found that combining the two factors results in a similar level of protection when compared to each of the factors alone. This result indicates that the two proteins may share the same signaling pathway regarding cone protection.

FSTL1

Follistatin-like 1 (FSTL1) is an extracelluar glycoprotein grouped into the follistatin family. It was originally identified as a heparin-binding protein in rat C_6 glioma-conditioned media (Zwijsen et al., 1994). FSTL1 is highly conserved among different species (>92% sequence identity in mouse, rat and human) (Zwijsen et al., 1994). Since the discovery of this gene, more than a hundred papers have been published on its function and signaling pathways over the past 20 years. FSTL1 has been shown to play roles in various disease models including

rheumatoid arthritis, cancer development, cardiovascular diseases, and ischemic stroke, etc (Adams et al., 2010; Kudo-Saito, ; Liang et al., 2014; Ogura et al., 2012; Ouchi et al., 2008; Sylva et al., 2013). FSTL1's role in immunological conditions is controversial. Some publications claim FSTL1 is a proinflammatory factor while others shows it is an anti-inflammatory protein (Fan et al., ; Liang et al., 2014; Miyamae et al., 2006; Ogura et al., 2012; Rainer et al., 2014). The completely opposing roles of FSTL1 might be mediated through distinct signaling pathways. FSTL1 is known to interact with and regulate numerous genes (Sylva et al., 2013). In cardiovascular and neuronal systems, FSTL1 seems to protect the cells through a cell surface receptor DIP2A (Disco-interacting protein 2 homolog A) to activate the PI3K/Akt (Phosphatidylinositol-4,5-bisphosphate 3-kinase/ Protein kinase B) pathway (Liu et al., 2010; Murakami et al., ; Ouchi et al., 2010; Walsh, 2009). Its proinflammatory properties are suggested to be mediated through the interaction with CD14 (cluster of differentiation 14) and TLR4 (tall-like receptor 4) (Murakami et al., 2012; Tanaka et al., 2010). In addition, FSTL1 is known to regulate embryonic development of many organs, including the skeletal, lung, and ureter systems (Sylva et al., 2013; Xu et al., 2012).

Innovation and Significance

In our study, we found FSTL1 as a cone photoreceptor protective factor through a discovery-based method. Multiple assays demonstrated that addition of FSTL1 could save cones from strong light damage and oxidative damage *in vitro*. Numerous studies have shown FSTL1's anti-apoptosis function (Liang et al., 2014). FSTL1 has been reported to inhibit apoptosis in many organs under ischemia-reperfusion conditions, including the heart (heart failure), skeletal muscles, and brain (ischemic stroke) (Liang et al., 2014; Walsh, 2009). Identification of FSTL1

as a cone protective factor would greatly improve the knowledge of FSTL1 in the nervous system. Confounding studies have been published on FSTL1's function in regulating inflammatory systems. More study should be done on the signaling pathways of FSTL1 in retina protection to reveal how this factor protects photoreceptors from environmental damage.

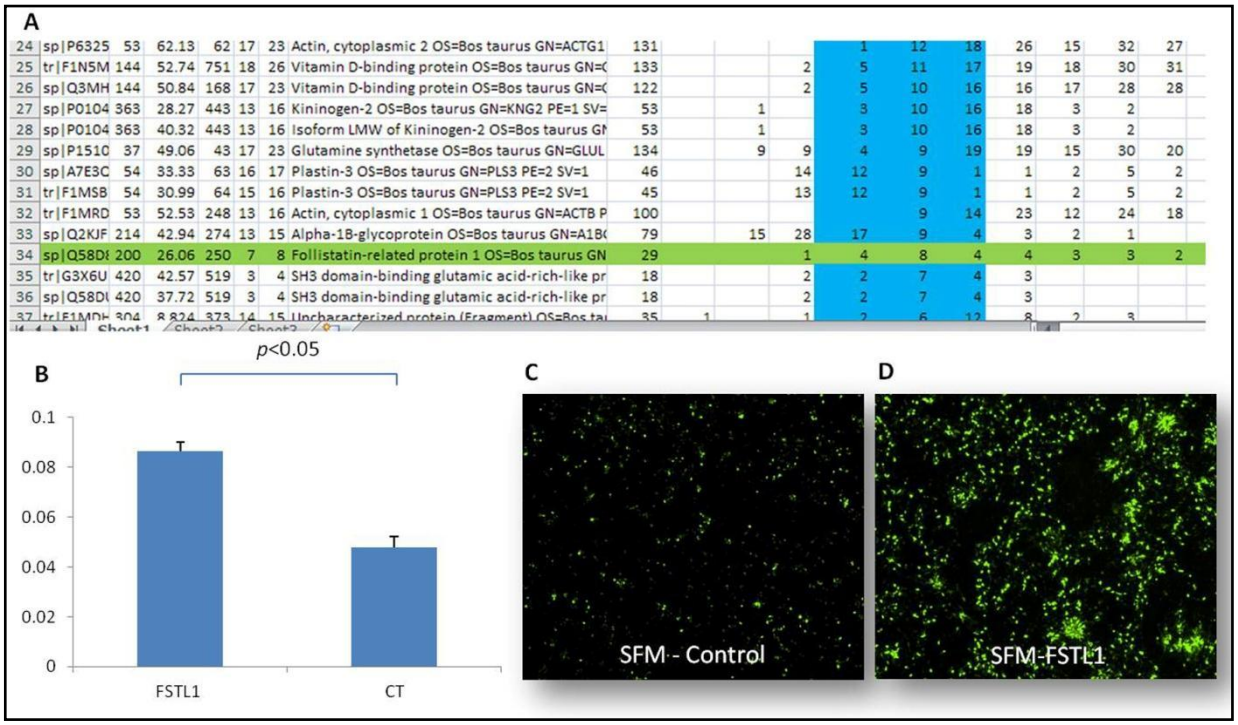

Figure 4.1 FSTL1 Identification and Protection

A. Identification of FSTL1. More distinct peptides were identified in the protective Q300-HPLC 4-7 fractions. Less peptides were identified in other fractions. B. Serum free media containing untagged-FSTL1 protects 661W cells in the H_2O_2 damage assay. Primary cones were protected against light damage with the serum free media containing FSTL1 (D) compared to the serum free media only (C). SFM, serum free medium. Green is anti-visinin staining.

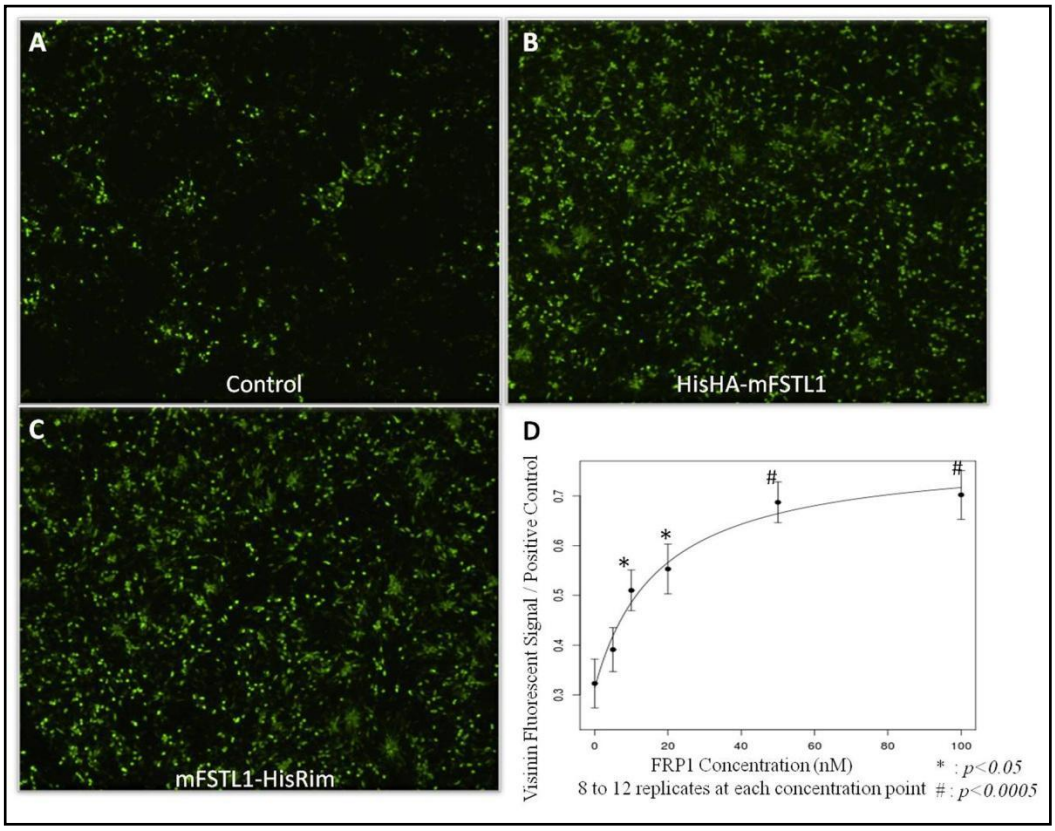

Figure 4.2 FSTL1's Concentration Curve in Light Damage Assay

A-C. Purified FSTL1 factors effectively protect primary chicken culture against light damage. A. Cone culture treated with PBS control; B. Cone culture treated with His-HA-FSTL1 (N-terminal tag); C. Cone culture treated with FSTL1-His-Rim (C-terminal tag). D. The FSTL1 concentration-protection curve generated using FSTL1-His-Rim. Each concentration contains 8 to 12 replicates. Green is the anti-visinin fluorescent staining.

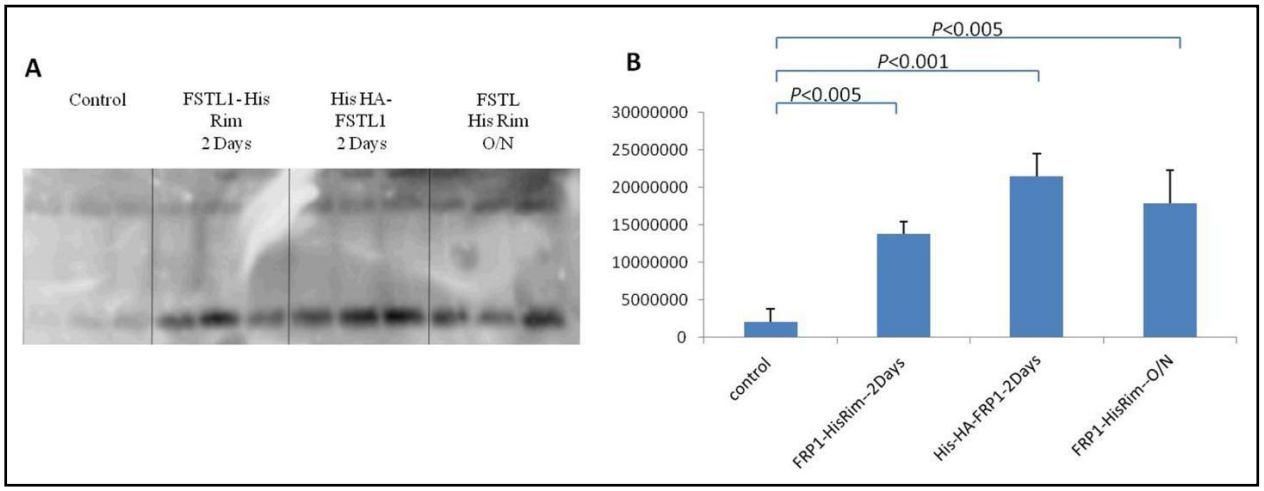

Figure 4.3 FSTL1 Protects Primary Cones against Hydrogen Peroxide Damage

A. Western Blot showing purified FSTL1 with tagging on the –C or –N terminus protects the primary chicken cones against oxidative damage. B. The quantification of the visinin signal from the Western Blot.

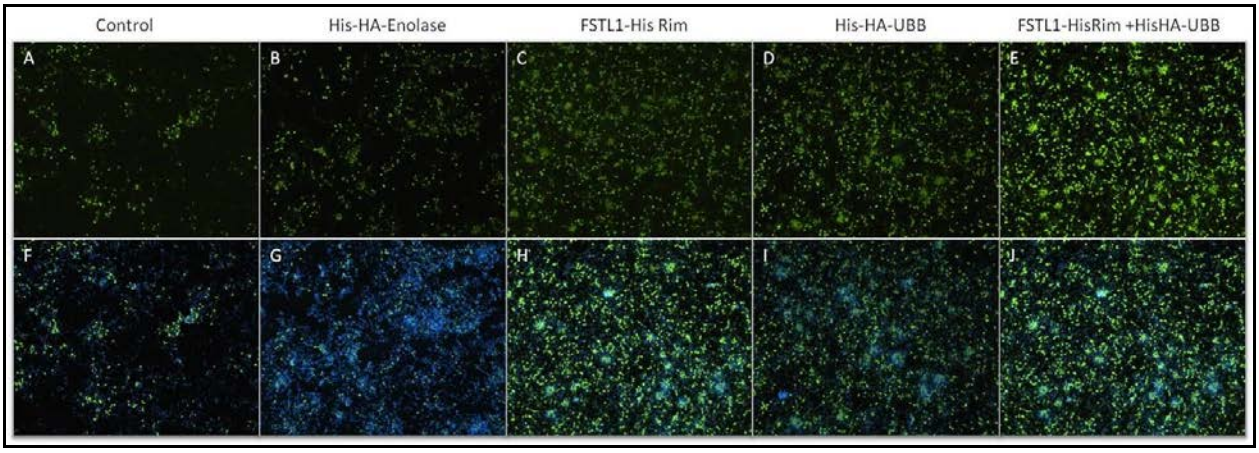

Figure 4.4 No Additional Protective Effect by UBB and FSTL1 *in vitro*

PBS (A and F), His-HA Enolase β (B and G), FSTL1-His Rim (C and H), His-HA-UBB (D and I), and the combination of FSTL1 and UBB (E and J) were applied to the primary cones and tested for the protective effect in light damage assays. A-E, Anti-visinin staining, green. F-J, anti-visinin and DAPI co-staining. Pictures were taken at 100 times magnification.

Reference

Adams, D.C., Karolak, M.J., Larman, B.W., Liaw, L., Nolin, J.D., and Oxburgh, L. (2010). Follistatin-like 1 regulates renal IL-1beta expression in cisplatin nephrotoxicity. Am J Physiol Renal Physiol *299*, F1320-1327.

Chaly, Y., Marinov, A.D., Oxburgh, L., Bushnell, D.S., and Hirsch, R. (2011). FSTL1 promotes arthritis in mice by enhancing inflammatory cytokine/chemokine expression. Arthritis Rheum *64*, 1082-1088.

Fan, N., Sun, H., Wang, Y., Zhang, L., Xia, Z., Peng, L., Hou, Y., Shen, W., Liu, R., Yin, J., *et al.* Follistatin-like 1: a potential mediator of inflammation in obesity. Mediators Inflamm *2013*, 752519.

Hsieh, Y.W., and Yang, X.J. (2009). Dynamic Pax6 expression during the neurogenic cell cycle influences proliferation and cell fate choices of retinal progenitors. Neural Dev *4*, 32.

Kudo-Saito, C. FSTL1 promotes bone metastasis by causing immune dysfunction. Oncoimmunology *2*, e26528.

Liang, X., Hu, Q., Li, B., McBride, D., Bian, H., Spagnoli, P., Chen, D., Tang, J., and Zhang, J.H. (2014). Follistatin-Like 1 Attenuates Apoptosis via Disco-Interacting Protein 2 Homolog A/Akt Pathway After Middle Cerebral Artery Occlusion in Rats. Stroke *45*, 3048-3054.

Liu, S., Shen, H., Xu, M., Liu, O., Zhao, L., Guo, Z., and Du, J. (2010). FRP inhibits ox-LDL-induced endothelial cell apoptosis through an Akt-NF-{kappa}B-Bcl-2 pathway and inhibits endothelial cell apoptosis in an apoE-knockout mouse model. Am J Physiol Endocrinol Metab *299*, E351-363.

Miyamae, T., Marinov, A.D., Sowders, D., Wilson, D.C., Devlin, J., Boudreau, R., Robbins, P., and Hirsch, R. (2006). Follistatin-like protein-1 is a novel proinflammatory molecule. J Immunol *177*, 4758-4762.

Murakami, K., Tanaka, M., Usui, T., Kawabata, D., Shiomi, A., Iguchi-Hashimoto, M., Shimizu, M., Yukawa, N., Yoshifuji, H., Nojima, T., *et al.* Follistatin-related protein/follistatin-like 1 evokes an innate immune response via CD14 and toll-like receptor 4. FEBS Lett *586*, 319-324.

Murakami, K., Tanaka, M., Usui, T., Kawabata, D., Shiomi, A., Iguchi-Hashimoto, M., Shimizu, M., Yukawa, N., Yoshifuji, H., Nojima, T., *et al.* (2012). Follistatin-related protein/follistatin-like 1 evokes an innate immune response via CD14 and toll-like receptor 4. FEBS Lett *586*, 319-324.

Ogura, Y., Ouchi, N., Ohashi, K., Shibata, R., Kataoka, Y., Kambara, T., Kito, T., Maruyama, S., Yuasa, D., Matsuo, K., *et al.* (2012). Therapeutic impact of follistatin-like 1 on myocardial ischemic injury in preclinical models. Circulation *126*, 1728-1738.

Ouchi, N., Asaumi, Y., Ohashi, K., Higuchi, A., Sono-Romanelli, S., Oshima, Y., and Walsh, K. (2010). DIP2A functions as a FSTL1 receptor. J Biol Chem *285*, 7127-7134.

Ouchi, N., Oshima, Y., Ohashi, K., Higuchi, A., Ikegami, C., Izumiya, Y., and Walsh, K. (2008). Follistatin-like 1, a secreted muscle protein, promotes endothelial cell function and revascularization in ischemic tissue through a nitric-oxide synthase-dependent mechanism. J Biol Chem *283*, 32802-32811.

Rainer, P.P., Hao, S., Vanhoutte, D., Lee, D.I., Koitabashi, N., Molkentin, J.D., and Kass, D.A. (2014). Cardiomyocyte-specific transforming growth factor beta suppression blocks neutrophil infiltration, augments multiple cytoprotective cascades, and reduces early mortality after myocardial infarction. Circ Res *114*, 1246-1257.

Sylva, M., Moorman, A.F., and van den Hoff, M.J. (2013). Follistatin-like 1 in vertebrate development. Birth Defects Res C Embryo Today *99*, 61-69.

Tanaka, M., Murakami, K., Ozaki, S., Imura, Y., Tong, X.P., Watanabe, T., Sawaki, T., Kawanami, T., Kawabata, D., Fujii, T., *et al.* (2010). DIP2 disco-interacting protein 2 homolog A (Drosophila) is a candidate receptor for follistatin-related protein/follistatin-like 1--analysis of their binding with TGF-beta superfamily proteins. FEBS J *277*, 4278-4289.

Walsh, K. (2009). Adipokines, myokines and cardiovascular disease. Circ J *73*, 13-18.
Xu, J., Qi, X., Gong, J., Yu, M., Zhang, F., Sha, H., and Gao, X. (2012). Fstl1 antagonizes BMP signaling and regulates ureter development. PLoS One *7*, e32554.

Zwijsen, A., Blockx, H., Van Arnhem, W., Willems, J., Fransen, L., Devos, K., Raymackers, J., Van de Voorde, A., and Slegers, H. (1994). Characterization of a rat C6 glioma-secreted follistatin-related protein (FRP). Cloning and sequence of the human homologue. Eur J Biochem *225*, 937-946.

Chapter 5: Verification of the Protective Factors *in vivo*

5.1 Introduction

We depend on photoreceptor cells to see the world because they sense light in vision. Diseases that cause photoreceptor degeneration such as age-related macular degeneration (AMD) and retinitis pigmentosa (RP) affect millions of people and lead to blindness (Seiler and Aramant, 2012; Weleber, 2005; Wood-Gush, 1989). The degeneration of photoreceptor cells in AMD or cone photoreceptors in RP is due to stress in their environment and or a lack of trophic support, and is not due to direct genetic mutation targeting the photoreceptor cells. Therefore, providing effective trophic support can delay or prevent photoreceptor degeneration. Recent gene therapy studies revealed that targeting genetic mutations is not sufficient and that there is an urgent need to identify trophic factors to maintain photoreceptor survival in the treatment of photoreceptor degeneration. Identification and mechanistic study of trophic factors naturally present in the retina will lead to a better understanding of the mechanism of photoreceptor protection and help to develop new therapeutic strategies to prevent photoreceptor degeneration. As shown in the previous chapters, we have identified two novel trophic factors that protect cone photoreceptors from retinal-mediated light damage and oxidative damage *in vitro*.

In this study, we will further explore the UBB and FSTL1's function *in vivo.* We will address the following questions: 1) Do these factors protect the retina from light induced degeneration *in vivo*? 2) Do the factors delay retinal degeneration in the RP animal models? 3) Which kind(s) of photoreceptors are protected in the retina? To answer these questions, two mouse models were used in this study, the albino mouse line BABL/cJ and a rapid retina degeneration mouse model, NMF137. We found that UBB protects both rods and cones in the

light damage model, which is consistent with our *in vitro* result. Furthermore, UBB partially delayed the rod degeneration in the eyes of the NMF137 mouse model. Both results strongly support the therapeutic value of UBB as a potent treatment in retinal degeneration diseases.

5.2 Methods

5.2.1 Animal models

Two types of animal models were used in this study including NMF137 (*C57BL/6J-Pde6b^{2J}/J*) and albino BALB/cJ mice from the Jackson Laboratory. All mice were maintained in a temperature-controlled 68 °F-79 °F and humidity-controlled 30%-70% room with a 12 hour: 12 hour light-dark (ON 6:00 am/OFF 6:00 pm) photoperiod. All procedures involving the use of mice were in accordance with the guidelines of the University of California, Los Angeles.

Mice homozygous for the allele of *Pde6b* mutation have an early onset, severe retinal degeneration. A viral insert and a second nonsense mutation in exon 7 of the beta-subunit of cGMP-PDE (*Pde6b*) gene exists in all mouse strains with NMF137 mutation.

5.2.2 Lentivirus constructs

The exact constructs used in the *in vitro* study were cloned into the lentiviral vector to create LV-CIG-APSS-His-HA-UBB and LV-CIG-FSTL1-His-Rim vectors. For LV-CIG-APSS-His-HA-UBB, the vector carries the cytomegalovirus (CMV) immediate-early promoter followed by a human UBB cDNA encoding a secreted and tagged UBB. For LV-CIG-FSTL1-His-Rim, the vector carries the cytomegalovirus (CMV) immediate-early promoter followed by a

mouse FSTL1 cDNA encoding a C-terminus tagged FSTL1. The control lentivirus (LV-CIG-CT) encodes only the internal ribosomal entry site and GFP downstream of the CMV promoter.

5.2.3 Lentivirus Transfection

293T cells were split one day before the experiment at a 1:3 ratio in DMEM/10% FBS with 1% penicillin- streptomycin. Before transfection, cells should be 95-99% confluent. 15 dishes of 75 ml of unconcentrated virus were collected to generate high-titer virus. For each 10 cm petri dish, media was first switched to 5 ml fresh medium. 1:2 DNA to jetPRIMETM reagent ratio (w/v) was used for transfection. 3 μg of each helper DNA (3 plasmids) and 3 μg of viral vector DNA was mixed with 500 μl of jetPRIMETM buffer, and vortexed for 10 sec. 20 μl of reagent was added into the mixture and mixed by vortexing for 10 sec. Mixture was spun down and incubated at room temperature for 10 min. DNA –lipo mixture was added to the cells in a drop-wise manner. The culture was incubated at 37 ºC incubator for 6 hours before the media was changed to 5 ml fresh DMEM/10% FBS with 1% penicillin- streptomycin.

5.2.4 Lentivirus Concentration

24 hours after transfection, media was replaced with 5 ml of CD293 serum (Gibco by lifetechnologies, defined medium). Replaced medium was collected and bleached. At the 48 hour time point, the viral production reached its peak. Media containing virus was collected on ice and filtered through 0.45 μm Durapore filter unit. Freeze and thaw was avoided to reach high viral concentration. Dishes and the filter units were bleached for 10 min and autoclaved afterwards.

Lentivirus was concentrated using ultracentrifugation. Beckman SW28 swing bucket rotor and tubes were sterilized with 70% ethanol followed by 100% ethanol, and air dried in the tissue culture hood. Each tube was loaded with up to 37.5 ml sterilized virus solution. The bucket was capped tightly and carefully transferred into the centrifuge. Virus was concentrated at 4 ºC for 2 hours and 15 min at 20,000 rpm. After removing majority of the supernatant, 200 µl media containing virus was left in the bottom of each tube. Each tube was capped and packed tightly on ice and shaked at 1000 rpm for 1 hour. After 1 hour, viral particles were resuspended by pipetting, and aliquoted as 10 µl into tubes with rubber O-ring caps. Bubbles should be avoided during this step. The buckets and caps were completely cleaned with Envirocide and then rinsed with 70% ethanol. Viral supernatant were collected and bleached with 10% CLOROX bleach for overnight before flashed through the sewer.

5.2.5 Determine Virus Titer

293T cells were split at 1:3 ratio to a 24-well plate the day before infection. Cells should reach 95-99% confluence before tittering. For each kind of virus, 6 ml of fresh 293T media (DMEM/10% FBS with 1% penicillin- streptomycin) containing 10 µg/ml polybrene in 6 sterile Eppendorf tubes were prepared. Concentrated lentivirus was thawed on ice, and serial diluted to the concentration of 10xe-3, 10xe-4, 10xe-5, 10xe-6, 10xe-7, 10xe-8 using prepared media.

To infect 293T cells, 500 µl of medium was replaced with 500 µl of virus media. After 48 hours, cells were fixed with 4% PFA at room temperature for 5 min. Immnofluorescence staining was used to stain for transgene GFP to determine the viral titer. Titer was determined at the

dilution factor where the lowest number of the GFP-positive cells was observed. Titer of 10xe7 or 10xe8 is needed for effective infection during the subretinal injection.

5.2.6 Subretinal Injection

Tools and equipment prepared before injection include: dissecting microscope, light source, micro manipulator, tweezers, micro scissors (Integra™ Miltex™), Hamilton syringe (80308 Hamilton 701SN 32GA), 8 Eppendorf tubes with de-ionized H2O, balance, pipette tip container, Ketamine & Xylazine solution, Povidone –iodiene (Aplicare) , 70% ethanol, viralcide, antibiotics , 60mm cell culture dish, cover slips, cotton applicators, sleeves, N99 mask, ice bucket filled with ice, virus, polybrene (Sigma) , Fast Green dye (CI42053, Food Green 3, Sigma), 10 µl pipette, 30 gauge needles (VWR), syringe, Neomycin & polymyxin B ointment (FALCON) , cage card, "Investor will change the cage" card, small black bags, bleach tube, Sulfamethoxazole (Pharmacal) and 1% Tropicamide Ophthalmic Solution (AKORN). Hamilton syringe should be washed with 70% ethanol for at least10 min, and rinsed with de-ionized H2O twice before use.

Ketamine and Xylazine anesthetic was diluted in sterile water at concentration of 100 mg/ml and 20 mg/ml. Mouse was weighed by a balance. Ketamine and Xylazine was injected to the animal intraperitoneally (IP) at volume (µl) = 10 x body weight (g). (100 µl /10 g mouse body weight).

Virus was thawed on ice right before the injection. Polybrene was added to the virus to reach the final concentration at 4 μg/ml. Fast Green FCF dye was added to the virus to help visualization during the injection. 0.6 μl of viral mixture was used for each injection.

Aplicare Povidone –iodiene was applied to the mouse eye using cotton-tipped applicator. One drop of 1% Tropicamide Ophthalmic Solution was used to dilate mouse eye. Under the dissecting microscope, a hole was poked on the sclera outside of iris with a 30 gauge needle. Cautions should be paid to avoid blood vessels in this step. Syringe loaded with 0.6 μl virus was pushed through the hole. One drop of PBS was added to the center of the eye and a cover slip was put on top of that to assist visualization of the retina though pupil. Syringe was adjusted till a resistance was sensed from the back of eye. Virus was injected to the subretinal while a blurry blue color diffusion underneath the retina should be observed. The syringe needs to be retrived slowly after injection. Neomycin & Polymyxin B ointment was applied to the eye to prevent inflammation. Injected animals were also fed with water containing sulfamethoxazole at 5 ml/500 ml concentration to avoid inflammation. After a week, GFP signal could be detected under a fluorescent microscope.

5.2.7 Injection Verification

To verify injection, GFP signal was observed through dilated pupil under fluorescent microscope in albino mice. Tissure-Tek O.C.T. (Sakura Fineteck) compound-mediated sectioning and anti-GFP staining is required to determine the success of injection for pigmented NMF137 mice. A nice GFP signal in RPE cells should be observed to verify the success of the injection.

5.2.8 Light Damage Assays for BALB/cJ

Six days after injection, mice were dark adapted for 24 hours before the light damage assay. During dark adaptation, food and water are accessible to the animal, and normal air flow was maintained in the cage. After 24 hours, mice were taken to the procedure room for light damage experiment. Inside the biological hood, four mice were dilated with 1% Tropicamide Ophthalmic Solution in both eyes. Reflective foil was wrapped around the inside of the cage to reflect light. During light exposure mice were unanesthetized to avoid developing cataract. Mice were exposed to 10,000 lux of cool white LED light in a well-ventilated hood continuously for 4 hours. The LED light was placed about 10 cm above the cage, so that no significant heating was generated during the procedure. Light damage was repeated the same way on the following day for the same cage. Food and water were accessible to the mouse during the 4 hours light exposure. A researcher was monitoring the mice behavior carefully throughout the whole experimental.

The reasons that we divide the light exposure time to two days and 4 hours each day are because: 1) The trial experiment results suggest that 8-hours light exposure is necessary to induce sufficient light damage of the retina; 2) Mice are nocturnal animals and usually rest during the day, therefore, extremely long procedure (like 8 hours) should be avoided. Severn days post light damage, mice were sacrificed for morphological analysis.

5.2.9 Eye Cup Preparation and Staining

Mice were sacrificed with overdose of Isoflurane followed by perfusion with 4% PFA. Dorsal side of the cornea was marked using an electrical burning pen. Eyes were enucleated carefully with a dissection scissor under the microscope. A hole was made on the cornea to allow PFA diffuse into the eye. Eye cups were made by dissecting away the cornea and lens followed by fixation in 4% PFA at 4 ºC overnight. Eye cups were then washed in 50 ml PBS before transferred to a tube containing pre-cooled 30% sucrose, and incubated at 4 ºC overnight. 30% sucrose was then changed to 1:1 O.C.T.: 30% sucrose mixture, and rotated at 4 ºC overnight. For fixation, eye cups were transferred to O.C.T. compound and embedded into plastic modes. Caution should be paid to make sure the dorsal side pointing to the left and the eye cups perpendicular to the bottom surface during embedding. For standard staining, O.C.T. block was sectioned at 16 μm thickness under -20 º C conditions. The blazer was adjusted so that it is perpendicular to the bottom surface of the O.C.T. block. Sections were dried for 1 hour before staining or storage at -20 ºC.

A waterproof circle was made on the section slide by a liquid-repellent slide marker pen (Daibo Sangyo Co. Ltd.). After 5 min, the sections were washed 3 times with PBS+ (1x PBS buffer with 2mM magnesium) at room temperature for 5 min each. Sections were then incubated with blocking buffer (5% normal goat serum, 0.3% Triton in PBS) at room temperature for 1 hour. After 1 hour, blocking buffer was carefully removed by suction and replaced with blocking buffer containing the primary antibody and incubated at room temperature for 1 hour. The section was washed 4 times in PBS+ followed by incubation of blocking buffer containing secondary antibodies at room temperature for 1 hour (kept in dark). The slide was washed three

times before mounted with VECTASHIELD mounting media (Vector Laboratories, Inc.). The slide was sealed with nail polish and observed under florescent microscope.

5.2.10 Statistical analysis

The mean and the standard error were calculated for each comparison group. Statistical analysis was performed using a student's t test. Statistical significant was set at $p < 0.05$.

5.3 Results

5.3.1 Light Damage Conditions

We tested different light conditions to induce retina degeneration in BALB/cJ mice. Damage effectiveness was evaluated by the thickness of ONL. Previously, we found that light, even through very strong intensity, cannot induce degeneration of the ONL on the anesthetized mice. This is likely due to the development of cataracts in mice that are anesthetized with Ketamine & Xylazine, thereby blocking light from reaching the retina. Hence we tested three light damage conditions in BALB/cJ mice under anaesthetized conditions (Chen et al., 2004). The three conditions are: condition 1, 10,000 lux light from the top with horizontal light reflected from the foil around the cage for 5 continuous hours; condition 2, 10,000 lux light from the top with horizontal light reflected from the foil around the cage for 8 hours on two days (4 hours each day); condition 3, 15,000 lux light from the top with no horizontal light for 5 continuous hours (Figs 5.1 A-C). Food and water were accessible through the damage period. The left eye of

each of the experimental mice was dilated with 1% Tropicamide Ophthalmic Solution, but not the right eye, to test the effect of the dilator.

We found that reflective foil around the cage (horizontal light) is essential in terms of inducing light damage to the retina, since condition 3 showed the weakest damaging effect among the three conditions. The dilator surprisingly, did not make any difference in retinal damage, as no difference was seen in the right and left eye. The two days 8 hours condition was much more effective in inducing significant amounts of damage than the 5 hour continuous damage (Figs 5.1 D and E). Condition 1 leads to damage only in the central retina area (near the optic nerve) but not the peripheral region. Condition 2 leads to strong degeneration throughout the retina. Therefore, condition 2 was used in this study since it gave a cleaner background.

By observing the animal behavior during the test, we also found mice gradually became less active as they acclimated to their new environment, got used to the light stimuli or simply got tired. We believe dividing the test time into two days could help resume the activity level of the mice and decrease the animal activity variability in the experiment. A variation of the degeneration is observed in the test study which was mainly due to mice's behavior.

5.3.2 Virus Titer

To deliver the genes to the mice, we cloned the two candidate genes, UBB and FSTL1, into the lentiviral vector. After cloning, we firstly determined the virus titer by serial dilution and 293T cell infection. We diluted each kind of virus from 10xe-3 to 10xe-8 and checked the co-expression of the GFP signal in the infected cells after 48 hours. Under the fluorescent microscope, thousands of GFP positive cells were detected in the10xe-3 condition. A decreasing number of GFP positive cells were observed in the diluted conditions. The titer of the LV-CIG-

CT virus was determined to be 10xe7, as three GFP positive cells were observed in the 10xe-7 condition, and more than 20 GFP-positive cells were observed in the 10xe-6 condition (Fig 5.2). The titers of the LV-CIG-His-HA-hUBB and LV-CIG-mFSTL1-His-Rim virus were determined to be 10xe7 using the same method.

5.3.3 Lentivirus Infection in the 661W Cell Culture

To test the protective effect by the candidate proteins, we cloned and tested the two factors in mouse models. Before injecting mice with the virus, we first tested if the lentivirus could infect the 661W cell line, which is a cone-like cell line derived from mice. His-HA-UBB and FSTL1-His-Rim constructs, used in the *in vitro* test, were cloned and inserted into the LV-CIG vector, respectively. HA-tag or Rim-tag was used to verify the protein secretion. Two days after infection, we stained the cells with anti-HA and anti-GFP antibodies. The anti-HA staining was used to detect the expression of UBB. In Fig 5.3, infected cells were detected as both GFP (green) and HA (red) positive. This result demonstrated that mouse 661W cells were successfully infected by LV-CIG-His-HA-UBB virus and expressing HA-tagged UBB protein. The same result was observed for LV-CIG-FSTL1-His-Rim.

5.3.4 Verification of the Subretinal Injection

Subretinal injection was performed on post natal day 2-5 NMF137 mice to deliver the lentivirus to the subretinal area. The NMF137 is a rapid retina degeneration mouse model, in which extensive degeneration of the outer nuclear layer of retina was seen at 3-weeks of age and has no rod or cone responses at eight weeks. The thickness of the ONL was measured on day 20 to evaluate the protective effect on rods. The number of cones was quantified at the same time.

Albino BALB/cJ mice were injected at 2-months of age. One week after the injection, obvious GFP signal was detected under fluorescent microscope without dilating the eyes. According to published data, CMV promoter driven lentivirus mainly infects the RPE cells of the retina (Hashimoto et al., 2007). The injection method has been indicated in Fig 5.4 A. The correct injection spot was indicated in Fig 5.4 B. The injection was considered to have failed if the virus was delivered to the intravitreal area or other parts of the eye other than the subretinal area between the retina and RPE cell layer. One week after injection, BALB/cJ mice were sacrificed for histological analysis. In Fig 5.4 D, a strong GFP signal lining adjacent to the retina was detected which indicated a successful injection, while no GFP signal was seen in Fig 5.4 C which indicated a failed injection. Injection success rate in this study was above 50%.

5.3.5 UBB Delays ONL Thinning in the Light Damage Model

Six days after subretinal injection, the mice were dark adapted for 24 hours before the light damage experiment. We performed light damage for each group of mice on two consecutive days for 4 hours each day. Morphological analysis was performed a week after the light damage.

To analyze the results, we divided the mice into three groups: 1. LV-CIG-CT virus injected group; 2. LV-CIG-UBB injected but GFP negative group; and 3. LV-CIG-UBB GFP positive group. LV-CIG-UBB GFP negative eyes are considered as the control because no viral infection happened in the RPE cells of these retinas, and hence no UBB expression in these eyes. We found that the thickness of the ONL had significantly thinned in the two control groups but not in the LV-CIG-UBB-GFP+ retinas by DAPI staining. Low magnification pictures in Figs 5.5

A-C illustrate the overall morphology of the retina in each group. High magnification pictures were taken by con-focal microscope in Figs 5.5 D-F.

A variation was observed in light-induced retinal degeneration in the trial experiment. A higher magnification picture was captured at a similar region in each retina section (near the optic never region). Three random places were measured in length in each retina. The average ONL thickness was calculated based on these measurements and was used for statistical analysis. Student's t test showed a significant difference of the ONL between the UBB-GPF positive retina and the ONL of the two control groups (Fig 5.5 G). With the presence of UBB protein, the ONL was much thicker (more than twice) than that of the control groups. LV-CIG-CT and LV-CIG-UBB-no GFP were combined as a control group and the comparison is shown in Fig 5.5 H. The success of the injection was verified by both anti-GFP staining on sectioned retinas as well as by GFP signal detected under the fluorescent microscope. Despite the variation of the retina degeneration in the control animals, no obvious thinning of ONL was detected in any GFP positive LV-CIG-UBB injected eyes, which strongly supports the protective effect of UBB protein. Extra caution was taken during the eye cup preparation, as the dorsal side was marked on the cornea, optic nerve was preserved, and the eye cup was perpendicular to the bottom surface of the model in the O.C.T. fixation to ensure a fair comparison among different retinas.

Last but not least, no significant protection by LV-CIG-FSTL1 on rods was seen in this study. More investigation will be needed on the protective effect by LV-CIG-FSTL1 on cone photoreceptors *in vivo.*

5.3.6 UBB Preserves Both Rods and Cones in the Light Damage Model

The UBB-GFP positive retinas and the control retinas were stained with DAPI (nuclei), peanut agglutinin (PNA, cone marker) and ABCA (rod marker) antibodies to examine the cell body of the photoreceptors, cone outer segments, and the rod outer segments after light damage. The differences in the thickness of the outer segments were clearly seen in the retinas of the two animals in Fig 5.6. In addition, very few of the PNA positive cone photoreceptors were seen in the control retinas (Figs5.6 B and D). None were seen in the UBB-GFP positive retinas with UBB expression (Figs 5.6 A and C). The morphology of the cones in Figs 5.6 B and D was much better than that of the control groups. Therefore, expression of UBB not only delays photoreceptor degeneration as shown in the previous session, but also preserves the outer segment of both rods and cones.

5.3.7 UBB Delays Retinal Degeneration in NMF137 Mouse Model

To test if the newly identified factors prevent retinal degeneration in genetic retinal degeneration mouse model, we performed the subretinal injection of the LV-CIG-UBB, LV-CIG-FSTL1 and LV-CIG-CT virus in the NMF137 mice. The NMF137 mouse model is a rapid retina degeneration mouse model, in which retina degeneration starts on postnatal day 1 and then rapidly progresses to a single layer of ONL at the age of three-weeks. In this study, the injection was performed on day 2 and retinas were harvested on day 20. Since it takes 72 hours for viral infection and gene expression, the UBB protein was expressed at its earliest on day 5. A weak but reproducible difference in ONL thickness was detected in the LV-CIG-UBB-GFP positive eyes compared to LV-CIG-CT eyes and LV-CIG-UBB GFP negative eyes (Fig 5.7). Protection by FSTL1 was not observed in this model.

5.4 Discussion

In this study, we have successfully cloned the UBB and FSTL1 genes into the lentiviral vector and infected the mouse RPE cells through subretinal injection. Strong expression of GFP signal was detected in RPE cells of the injected animals to confirm the expression of the gene. The expression of UBB significantly delayed the light-induced retinal degeneration in albino mice as demonstrated by the measurement of the ONL thickness. Furthermore, the expression of UBB preserves the morphology of the outer segment of both rods and cones. Since the outer segment of photoreceptors are mainly responsible for light sensing and visual phototransduction, this morphological rescue indicates a functional rescue of the photoreceptors upon light damage.

These results are consistent with the *in vitro* results that we demonstrated the factors protected primary chicken cones and 661W cells against retinal-mediated light damage. In the *in vivo* study, we have shown that the factor UBB, but not FSTL1, was capable of protecting both rods and cones against light damage. Moreover, we reproducibly observed that UBB delayed retina degeneration in the NMF137 mouse model, which is a genetic mutation-caused retinal degeneration model mimicing retinitis pigmentosa in human patients.

Innovation and Significance

Retina degeneration characterized by the progressive loss of photoreceptor cells are the common final stage for many kinds of eye diseases including RP and AMD (Gaillard and Sauve, 2007). So far, no effective treatment is available for RP or AMD and one of the key goals of new therapies are to prevent the loss of cones. With this purpose in mind, we started to search for novel neurotrophic factors that naturally exist in the IPM and protect cones. We have tested several previously claimed cone rescue factors in the cone culture system, such as RdCVF,

RdCVFL (Leveillard et al., 2004) and prosaposin (O'Brien et al., 1995). However, none of them showed a protective effect in our primary cone culture system. In contrast, the newly identified UBB and FSTL1 could effectively protect cones against light damage and oxidative damage *in vitro*. Furthermore, UBB has shown a very strong protective effect on both rods and cones against light damage *in vivo*. There have been numerous hypotheses regarding how the loss of rod photoreceptors leads to secondary cone death. Agreement has been reached however in that cone degeneration starts after rods die (Punzo et al., 2009). Therefore, the protection of rods translates into the preservation of cones.

Light Damage Condition

Light has been known as a cause of photooxidative damage in photoreceptors and RPE cells for more than five decades (Noell et al., 1966). Light damage induced oxidative stress and inflammation play key roles in retinal degeneration models. Light damage has long been used in rodents as a retinal degeneration model (Noell et al., 1966). In this model, photoreceptors die through apoptosis (Portera-Cailliau et al., 1994). In the albino BALB/cJ strain, it is known that their photoreceptors are vulnerable to light damage and are widely used by many research groups for studying light damage in rodents (Chen et al., 2004; Zhao et al., 2014; Zhu et al., 2010). In the beginning of this study, we tested the light damage conditions following some published results, however, we were never able to achieve sufficient damage using 5000 lux or even much stronger light for 2 hours under cold white light in our mice (O'Driscoll et al., 2011). Since research shows that the severity of retinal phototoxicity in rodents depends on the previous light exposure, rearing conditions and dark adaptation period (Montalban-Soler et al., 2012), the most obvious difference in our study compared to some published studies was the raising conditions of

the mice. In the O'Droscoll et al. study, the mice were raised at no more than 10 lux dim light condition after birth until 6 weeks of age for the light damage assay. Similar conditions were seen in Zhu et al., 2010, in which mice were raised at 5 lux dim light. Moreover, according to Zhu et al., 300 lux light for 2 days is strong enough to cause preconditioning in BALB/cJ and to prevent light damage from happening. We believe the light preconditioning is the leading factor contributing to the need of a much stronger light condition in our case. Specifically, a couple of factors are illustrated: first, our mouse facility has an average lighting condition of over 300 lux; second, our mice were purchased at two-months of age from Jackson Lab, and the light conditions were unknown before they arrived at UCLA; third, there is an unavoidable high intensity light exposure during the subretinal injection due to the nature of this operation. In summary, retinal degeneration by mild light could not be achieved in our study. A much stronger light condition was used in this study with stronger light intensity and a longer light exposure period (Chen et al., 2004). We have performed the light damage condition test for every batch of mice to ensure a sufficient amount of light damage.

Retina Degeneration Mouse Model

Jackson lab has published their retina degeneration mouse models regarding the genotype, disease progression, and affected cell types (Chang et al., 2002). Among all the choices, we selected NMF137 mice for our first study. Numerous mutations in β subunit of the human gene PDE6 have been found in retinitis pigmentosa patients (arRP; OMIM 180072) (Chang et al., 2008; Portera-Cailliau et al., 1994; Sakamoto et al., 2009). Hence, mouse strains harboring *Pde6b* mutant alleles are considered RP animal models. Mice homozygous for the NMF137 mutation show an early onset severe retinal degeneration through apoptosis due to a murine viral

insert and a second nonsense mutation in exon 7 of the *Pde6b* gene (Chang et al., 2002; Chang et al., 2007).

We chose this model due to the reason that a prominent protective effect by UBB and FSTL1 has been detected in the *in vitro* chicken cone culture system. We selected this rapid degeneration mouse model to study the protective effect on cones. However, in the light damage model, we surprisingly found that UBB could delay photoreceptors degeneration, regardless of whether they were rods or cones. This demonstrates that UBB protects rods against light-induced damage. Given the protective effect of UBB on rods, we decided to test other slow retina degeneration mouse models, such as *rds* and *rd10*, to examine the protective effect of UBB on rods in our next study.

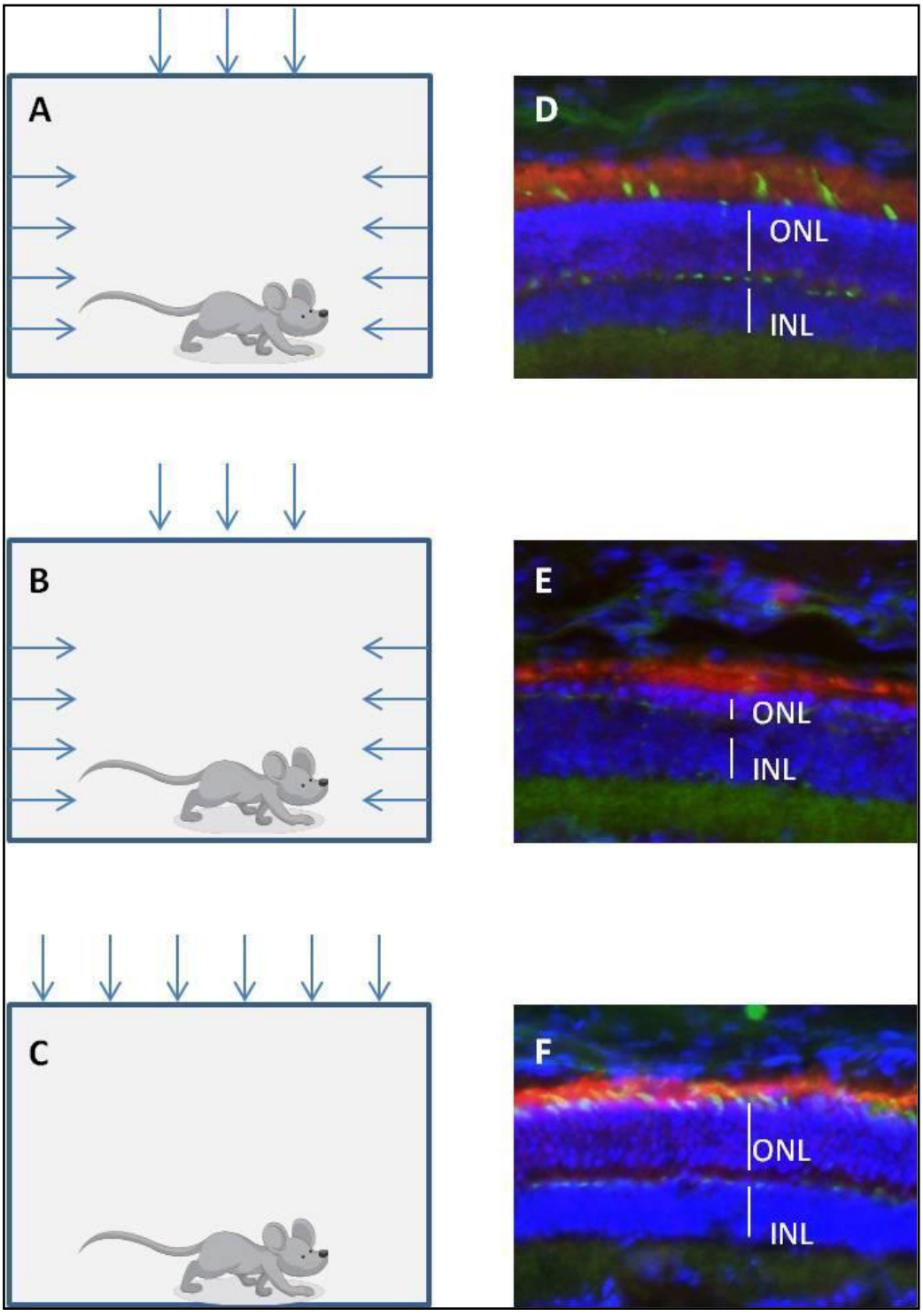
A
B
C
D
ONL
INL
E
ONL
INL
F
ONL
INL

Figure 5.1 Light Damage Conditions and Results

Three light damage conditions are tested in this study. A. Condition 1: 10,000 lux light from the top with horizontal light reflected from the foil around the cage for 5 continuous hours. B, Condition 2: 10,000 lux light from the top with horizontal light reflected from the foil around the cage for 8 hours on two days (4 hours each day). C. Condition 3: 15,000 lux light from the top with no horizontal light for 5 continuous hours. D) Damage is observed in the center of the retina, but decreased on the peripheral area of the retina in four eyes of condition 1. E) Strong damage was observed throughout the retina in condition 2, as indicated by 2-3 layers of the ONL and no OS of the rods and cones. F) Almost no damage was observed in the whole retina in condition 3. The ONL and OS of the retinas are stained by DAPI for nuclei, PNA for cones and ABCA antibody for rods.

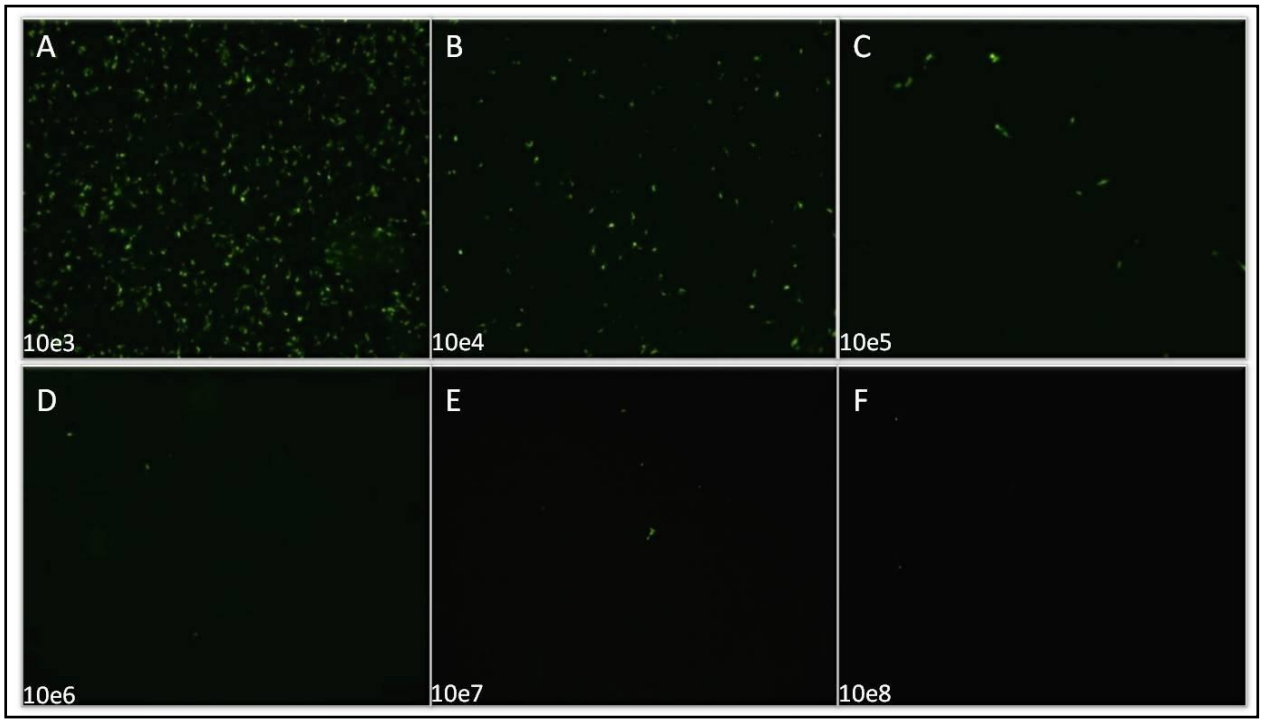

Figure 5.2 Lentivirus Titer

Virus titer was determined by serial dilution and infection of the 293T cell culture. A-F. Viruses are serially diluted from10 xe-3 to 10 xe-8. Green fluorescence of anti-GFP staining was detected by fluorescent microscope. A couple of GFP-positive cells were observed in 10 xe-7 dilution condition, suggestion the virus titer is 10 xe7.

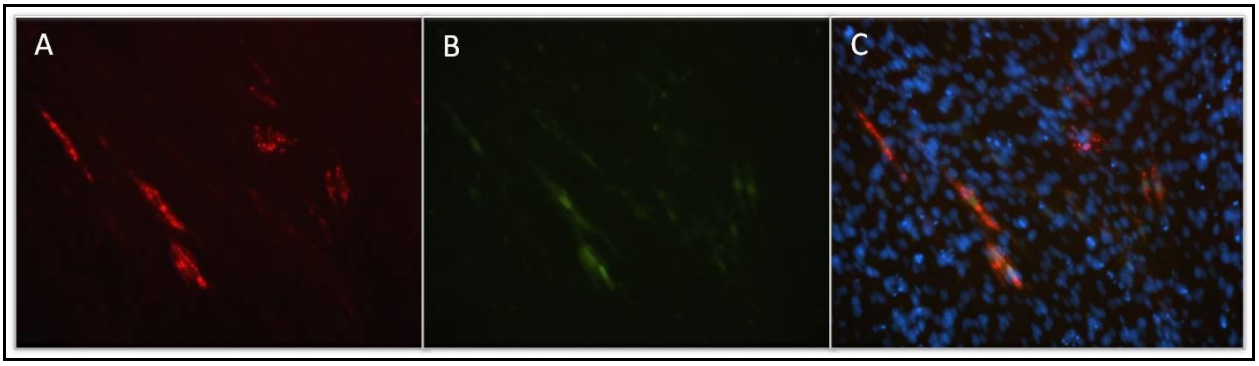

Figure 5.3 Lentiviral Infection of 661W Cells

Infected cells were fixed and stained with anti-HA antibody and anti-GFP antibody. A. A portion of the cells were determined to be HA positive. B. The same cells were GFP positive. C. Merged picture of the HA and GFP signal showing these cells were infected by the virus and expressing HA-tagged-UBB protein. Blue, DAPI nuclei staining; Green, anti-GFP staining; Red, anti-HA staining.

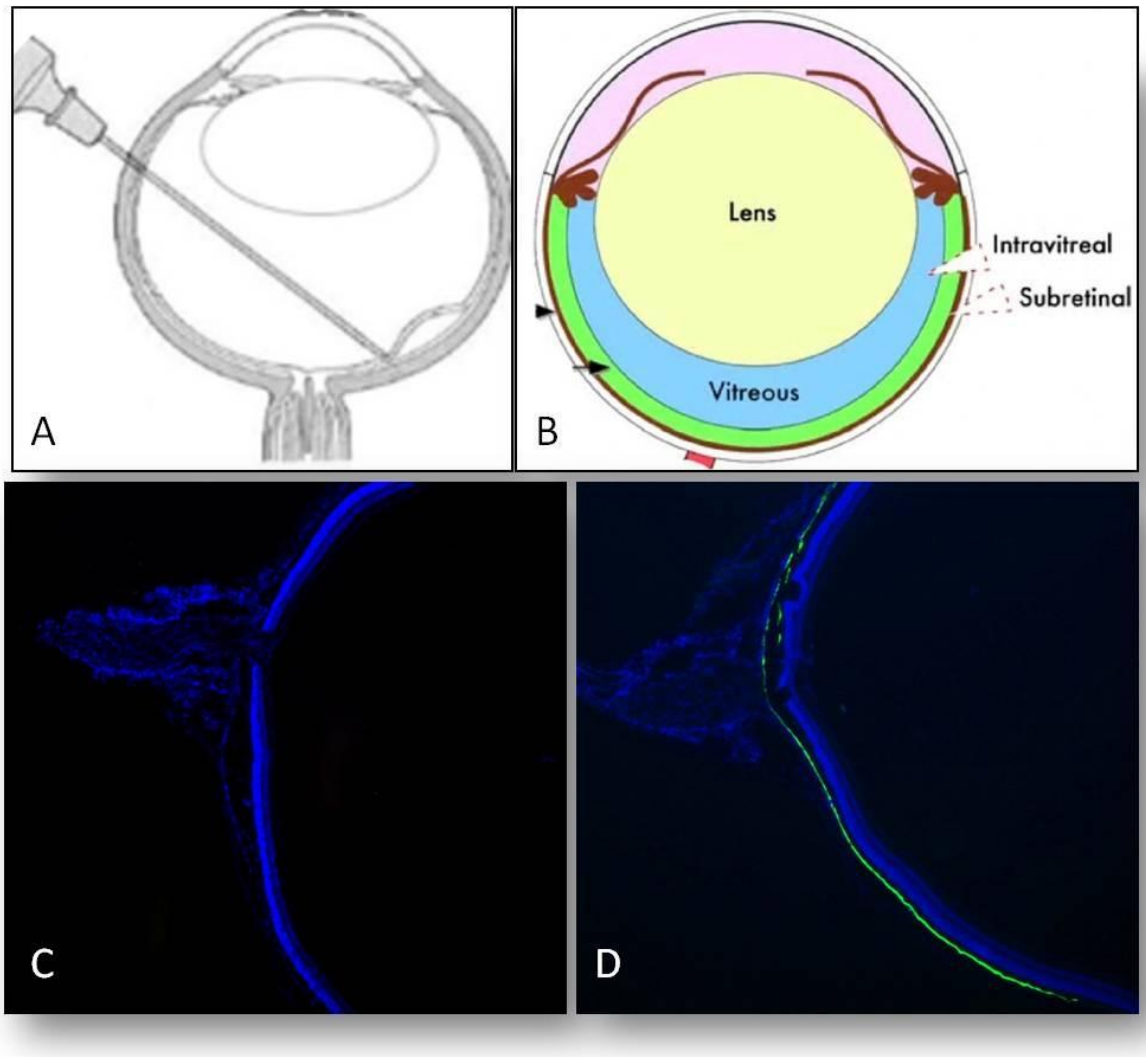

Figure 5.4 Subretinal Injection Method and Results

A. The method of subretinal injection used in both Balb/cJ and NMF137 across different ages. B. Illustrative picture showing the correct injection position, between the retina and RPE layer. C. No GFP signal detected in a Balb/cJ eye cup shows a failed injection. D. GFP positive RPE shows a successful viral injection. Blue, DAPI nuclei; Green, GFP.

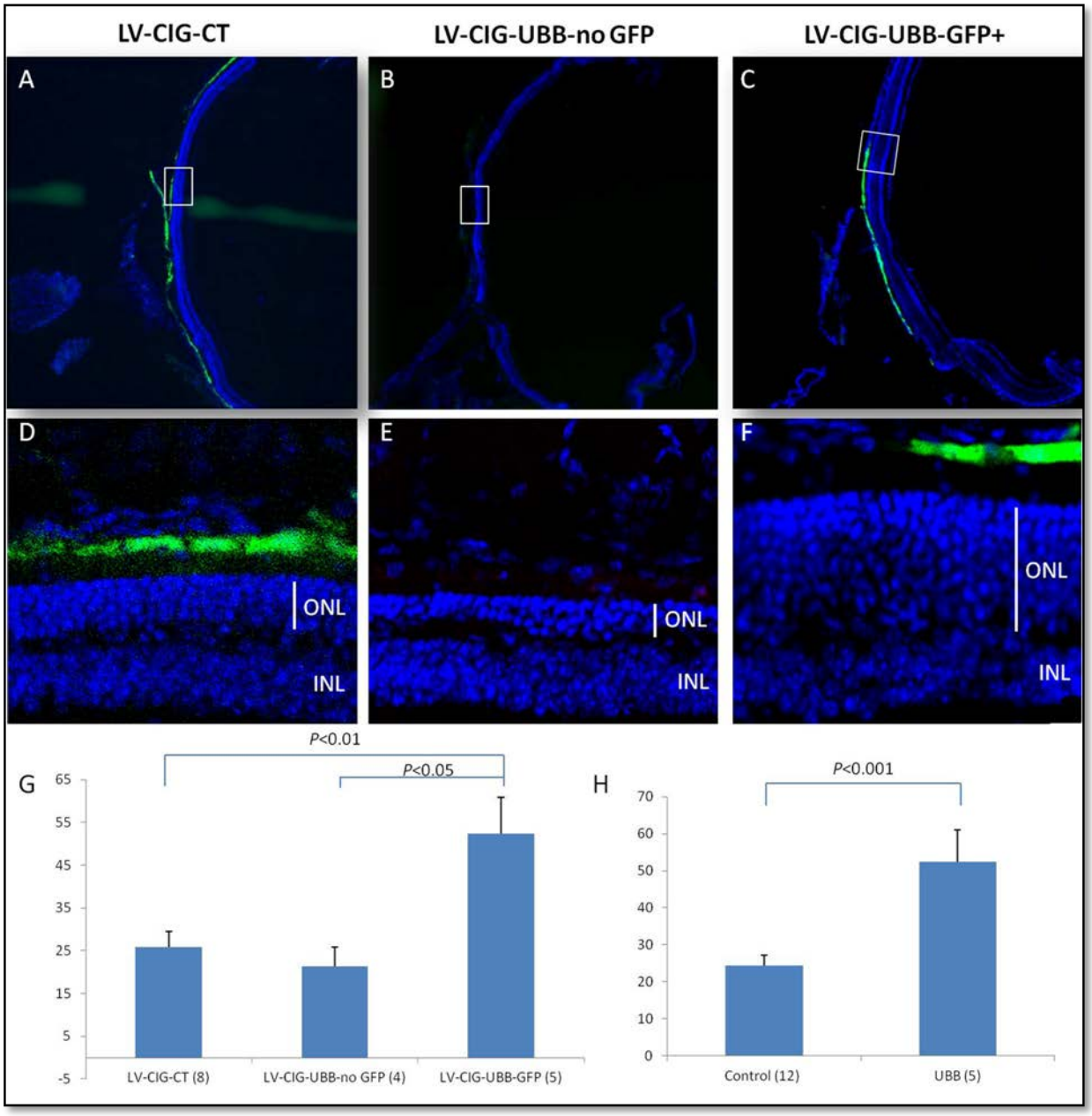
LV-CIG-CT
LV-CIG-UBB-no GFP
LV-CIG-UBB-GFP+
A
B
C
D
E
F
ONL
INL
ONL
INL
ONL
INL
G
P<0.01
P<0.05
65
55
45
35
25
15
5
-5
LV-CIG-CT (8)
LV-CIG-UBB-no GFP (4)
LV-CIG-UBB-GFP (5)
H
P<0.001
70
60
50
40
30
20
10
0
Control (12)
UBB (5)

Figure 5.5 UBB Delays ONL Thinning in the Light Damage Model *in vivo*

The analysis of the thickness of the ONL in the LV-CIG-CT, LV-CIG-UBB- GFP (-) and LV-CIG-UBB-GFP(+) eyes by immunohistochemistry staining. A-C, Fluorescent picture showing the overall retina thickness in the LV-CIG-CT-GFP (+), LV-CIG-UBB-GFP (-) and LV-CIG-UBB-GFP (+) retinas. D-F, Fluorescent pictures at high magnification showing the ONL is much thinner in the LV-CIG-CT-GFP (+), LV-CIG-UBB-GFP (-) retinas than that in the LV-CIG-UBB-GFP (+) group. G. Statistical analysis on the ONL from LV-CIG-CT-GFP (+), LV-CIG-UBB-GFP (-) and LV-CIG-UBB-GFP (+) retinas. H. Statistical analysis on the ONL from the combined control groups and the UBB-expressing group. Blue is DAPI, Green is anti-GFP staining.

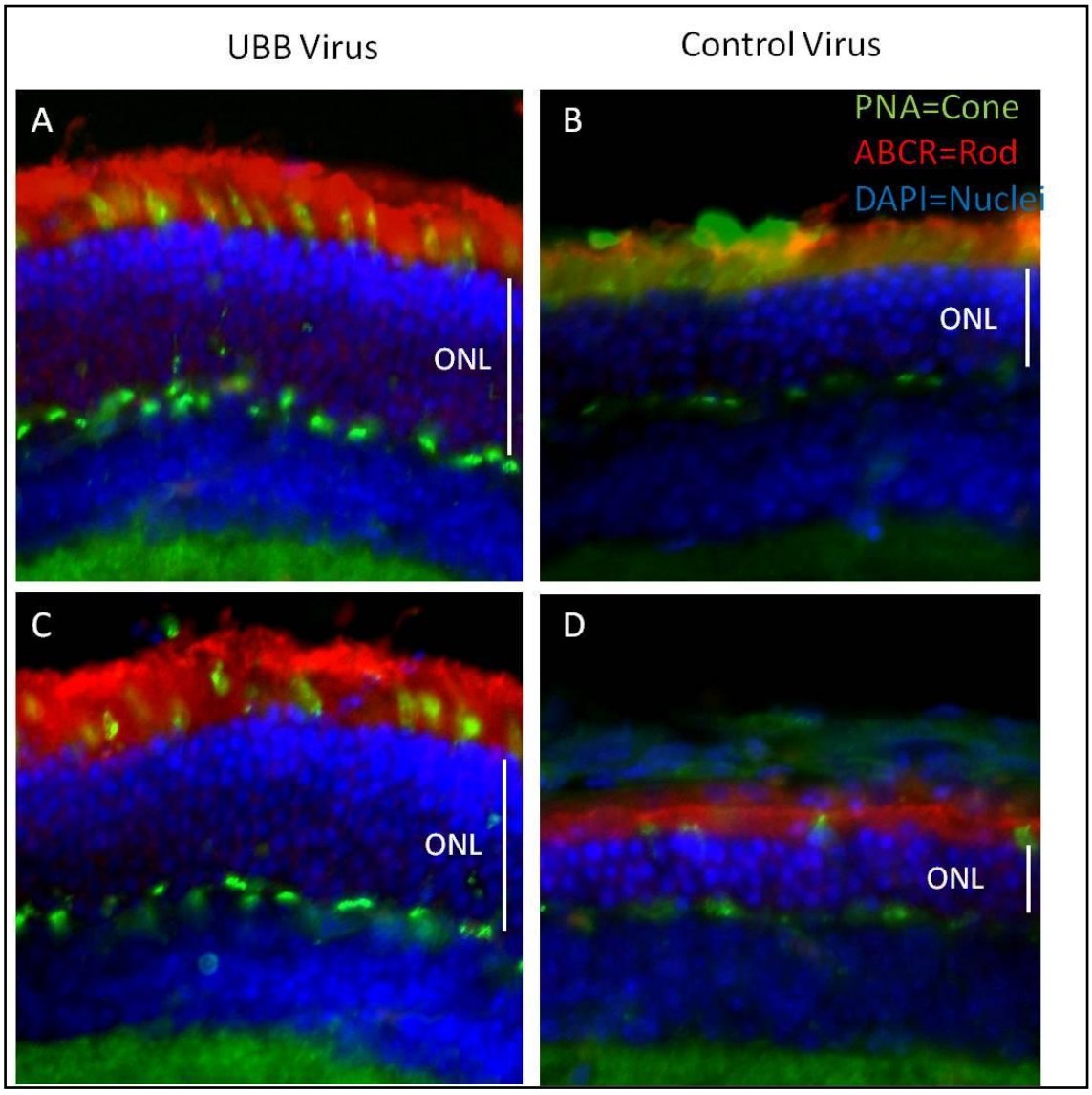

Figure 5.6 UBB Preserves Both Rods and Cones in the Light Damage Model

The thickness of the outer nuclear layer (ONL) and outer segment (OS) layer of rods and cones are shown in the UBB injected retina (A and C) and control virus injected retinas (B and D). A difference of the ONL thickness was detected among these two groups. Furthermore, the OS of rods and cones are both longer in the UBB-injected retina (A and C) than that in the control eyes (B and D). Blue, DAPI staining; Green, PNA staining; Red, anti-ABCA staining.

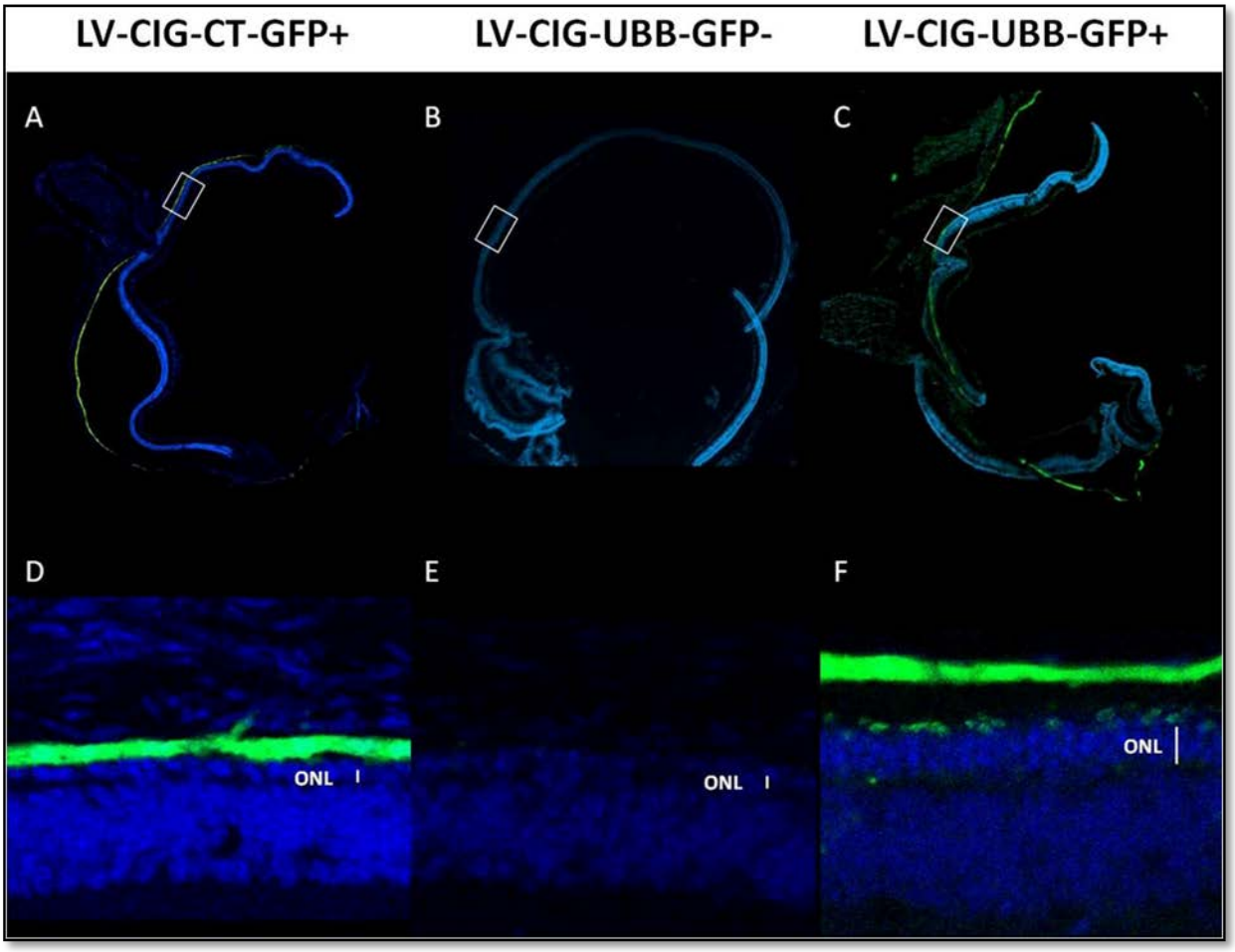

Figure 5.7 UBB Delays Retinal Degeneration in NMF137 Mouse Model

A. The overall morphology of the LV-CIG-CT-GFP positive retina, B. LV-CIG-UBB-GFP negative retina, C. LV-CIG-UBB-GFP positive retina. D, E, F, retinas examined at higher magnification for A, B, C, respectively. Blue, DAPI staining; Green, GFP signal.

Reference

Chang, B., Hawes, N.L., Hurd, R.E., Davisson, M.T., Nusinowitz, S., and Heckenlively, J.R. (2002). Retinal degeneration mutants in the mouse. Vision Res *42*, 517-525.

Chang, B., Hawes, N.L., Pardue, M.T., German, A.M., Hurd, R.E., Davisson, M.T., Nusinowitz, S., Rengarajan, K., Boyd, A.P., Sidney, S.S., et al. (2007). Two mouse retinal degenerations caused by missense mutations in the beta-subunit of rod cGMP phosphodiesterase gene. Vision Res 47, 624-633.

Elahy, M., Baindur-Hudson, S., Cruzat, V.F., Newsholme, P., and Dass, C.R. (2014). Mechanisms of PEDF-mediated protection against reactive oxygen species damage in diabetic retinopathy and neuropathy. J Endocrinol 222, R129-139.

Chang, J.Y., Bora, P.S., and Bora, N.S. (2008). Prevention of Oxidative Stress-Induced Retinal Pigment Epithelial Cell Death by the PPARgamma Agonists, 15-Deoxy-Delta 12, 14-Prostaglandin J(2). PPAR Res *2008*, 720163.

Chen, L., Wu, W., Dentchev, T., Zeng, Y., Wang, J., Tsui, I., Tobias, J.W., Bennett, J., Baldwin, D., and Dunaief, J.L. (2004). Light damage induced changes in mouse retinal gene expression. Exp Eye Res *79*, 239-247.

Gaillard, F., and Sauve, Y. (2007). Cell-based therapy for retina degeneration: the promise of a cure. Vision Res *47*, 2815-2824.

Hashimoto, T., Gibbs, D., Lillo, C., Azarian, S.M., Legacki, E., Zhang, X.M., Yang, X.J., and Williams, D.S. (2007). Lentiviral gene replacement therapy of retinas in a mouse model for Usher syndrome type 1B. Gene Ther *14*, 584-594.

Leveillard, T., Mohand-Said, S., Lorentz, O., Hicks, D., Fintz, A.C., Clerin, E., Simonutti, M., Forster, V., Cavusoglu, N., Chalmel, F., *et al.* (2004). Identification and characterization of rod-derived cone viability factor. Nat Genet *36*, 755-759.

Liang, X., Hu, Q., Li, B., McBride, D., Bian, H., Spagnoli, P., Chen, D., Tang, J., and Zhang, J.H. (2014). Follistatin-Like 1 Attenuates Apoptosis via Disco-Interacting Protein 2 Homolog A/Akt Pathway After Middle Cerebral Artery Occlusion in Rats. Stroke *45*, 3048-3054.

Marigo, V. (2007). Programmed cell death in retinal degeneration: targeting apoptosis in photoreceptors as potential therapy for retinal degeneration. Cell Cycle *6*, 652-655.

Montalban-Soler, L., Alarcon-Martinez, L., Jimenez-Lopez, M., Salinas-Navarro, M., Galindo-Romero, C., Bezerra de Sa, F., Garcia-Ayuso, D., Aviles-Trigueros, M., Vidal-Sanz, M., Agudo-Barriuso, M., *et al.* (2012). Retinal compensatory changes after light damage in albino mice. Mol Vis *18*, 675-693.

Noell, W.K., Walker, V.S., Kang, B.S., and Berman, S. (1966). Retinal damage by light in rats. Invest Ophthalmol *5*, 450-473.

O'Brien, J.S., Carson, G.S., Seo, H.C., Hiraiwa, M., Weiler, S., Tomich, J.M., Barranger, J.A., Kahn, M., Azuma, N., and Kishimoto, Y. (1995). Identification of the neurotrophic factor sequence of prosaposin. FASEB J 9, 681-685.

O'Driscoll, C., Doonan, F., Sanvicens, N., Messeguer, A., and Cotter, T.G. (2011). A novel free radical scavenger rescues retinal cells in vivo. Exp Eye Res *93*, 65-74.

Punzo, C., Kornacker, K., and Cepko, C.L. (2009). Stimulation of the insulin/mTOR pathway delays cone death in a mouse model of retinitis pigmentosa. Nat Neurosci 12, 44-52.

Portera-Cailliau, C., Sung, C.H., Nathans, J., and Adler, R. (1994). Apoptotic photoreceptor cell death in mouse models of retinitis pigmentosa. Proc Natl Acad Sci U S A *91*, 974-978.

Sakamoto, K., McCluskey, M., Wensel, T.G., Naggert, J.K., and Nishina, P.M. (2009). New mouse models for recessive retinitis pigmentosa caused by mutations in the Pde6a gene. Hum Mol Genet *18*, 178-192.

Sancho-Pelluz, J., Arango-Gonzalez, B., Kustermann, S., Romero, F.J., van Veen, T., Zrenner, E., Ekstrom, P., and Paquet-Durand, F. (2008). Photoreceptor cell death mechanisms in inherited retinal degeneration. Mol Neurobiol *38*, 253-269.

Seiler, M.J., and Aramant, R.B. (2012). Cell replacement and visual restoration by retinal sheet transplants. Prog Retin Eye Res *31*, 661-687.

Weleber, R.G. (2005). Inherited and orphan retinal diseases: phenotypes, genotypes, and probable treatment groups. Retina *25*, S4-S7.

Wood-Gush, H.G. (1989). Retinitis pigmentosa research: a review. J R Soc Med *82*, 355-358.
Zhao, L., Wang, C., Song, D., Li, Y., Song, Y., Su, G., and Dunaief, J.L. (2014). Systemic Administration of the Antioxidant/Iron Chelator alpha-Lipoic Acid Protects Against Light-Induced Photoreceptor Degeneration in the Mouse Retina. Invest Ophthalmol Vis Sci *55*, 5979-5988.

Zhu, Y., Valter, K., and Stone, J. (2010). Environmental damage to the retina and preconditioning: contrasting effects of light and hyperoxic stress. Invest Ophthalmol Vis Sci *51*, 4821-4830.